Universitat de Girona

Università degli Studi di Cagliari

PhD DEGREE

Earth and Environmental Sciences and Technologies (UniCa)

Cycle XXXIV

Water Science and Technology (UdG)

REMEDIATION OF MULTI-CONTAMINATED GROUNDWATER USING BIOELECTROCHEMICAL SYSTEMS

Scientific Disciplinary Sector

ICAR/03

PhD Student: Giulia Puggioni

Supervisors: Prof. Alessandra Carucci (UniCa)
Prof. Sebastià Puig Broch (UdG)
Dr. Stefano Milia (CNR-IGAG)

Final exam. Academic Year 2020/2021
Thesis defence: April 2022 Session

Table of contents

SUMMARY

Groundwater should be considered a complex system with several polluting inputs that may simultaneously affect its quality. Agriculture plays a key role among the various anthropogenic activities that may cause multiple groundwater contamination. It can, directly and indirectly, influence the concentrations of a large number of inorganic substances in groundwater, including nitrate.

In several geographical areas, nitrates exceed the quality standards for drinking water consumption (over 50 mgNO_3^- L^{-1}) recommended by the World Health Organisation (WHO). Reverse osmosis, electrodialysis, and ion exchange are considered the most recommended technologies for treating nitrates in groundwater. However, these conventional technologies are energy-intensive, chemicals dosage are sometimes required, and the nitrates are concentrated in a waste brine that is difficult to dispose of. Biological denitrification partly would solve this issue through harmful nitrate reduction into dinitrogen gas (N_2). However, conventional heterotrophic denitrification generates an excess of biomass and requires an electron donor (organic matter), usually not present in groundwater. The possible release of residual organic matter into the treated water would make it unusable for drinking purposes.

Bioelectrochemical systems are emerging as sustainable alternatives for treating nitrate contaminated groundwater, thanks to the autotrophic denitrifying bacteria that can use a cathode electrode as the electron donor. This process implies a negligible generation of sludge, low energy consumption and, no chemicals addition. However, the complexity of real groundwater is not only due to nitrate contamination, and can strongly influence the behaviour of BES and its scaling-up. One of the most intriguing challenges that researchers are currently facing is the application of BES to the bioremediation of multi-contaminated groundwater. This PhD thesis aims to evaluate the applicability of BES for the removal of nitrate, coupled with other typical saline groundwater contaminants. In particular, the objectives and activities of this PhD thesis are largely in line with the "SARdNAF" project, which aims to apply BES to the treatment of groundwater from the nitrate vulnerable zone of Arborea (Sardinia, Italy), characterised not only by high nitrate concentrations but also by high salinity and high calcium and manganese concentrations.

Firstly, the effect of elements typically found in groundwater (mainly calcium and manganese) was evaluated on a conventional bioelectrochemical system configuration to evaluate the effects on the denitrification process. Increasing concentrations of the selected substances (75, 100 and 150% of those found in real groundwater) were tested to evaluate their effect on denitrifying performance, microbial composition and BES constituent materials. Sensitivity tests showed a worsening of process performances as Ca^{2+} and Mn^{2+} concentrations were increased, as described and discussed in Chapter 2.

A novel 3-compartment BES configuration was developed to test a proof-of-concept for bioelectrochemical denitrification with groundwater desalination (Chapter 3). The system was operated in batch mode to study its feasibility. The possibility of exploiting the electroactive biofilm grown on the bio-cathode to remove nitrate and, at the same time, achieve electrochemically-driven desalination was successfully assessed, with a nitrate removal rate of 114±12 $mgNO_3^-$-N $m^{-2}d^{-1}$ and chloride removal rate of 66±9 mg $L^{-1}d^{-1}$. Subsequently, its performance was reinforced in terms of denitrification and desalination once continuous mode operation was applied. Different operating conditions were tested (potentiostatic mode, galvanostatic mode with or without pH control) to identify the optimal operating conditions (Chapter 4). The average nitrate removal rate achieved was 39±1 $mgNO_3^-$-N L^{-1} d^{-1}, and no intermediates (i.e., nitrite and nitrous oxide) were observed in the effluent. Groundwater salinity was considerably reduced with an average chloride removal of 63±5%. Standard limits for drinking water in terms of nitrate, nitrite, N_2O and electrical conductivity were reached. In addition, the recovery of part of the chloride removed by desalination in the form of a disinfectant (free chlorine) was successfully achieved (reaching a concentration of 26.8±3.4 $mgCl_2$ L^{-1}).

The operation with decreasing hydraulic retention times was tested to investigate the effect on overall process performance and energy consumption. This study allowed further process optimisation increasing the nitrate removal rates (up to 132 $mgNO_3^-$-N $L^{-1}d^{-1}$) and providing useful information for potential subsequent system scaling-up. The results of this research are described and discussed in Chapter 5.

Finally, an overall assessment of the studies presented and a recommendation for future research directions in this new field of bioelectrochemical systems for groundwater treatment are described in Chapter 6

The results presented in this PhD thesis support the application of the bioelectrochemical system as a potential alternative technology for the treatment of multi-contaminated groundwater.

1 GENERAL INTRODUCTION

1.1 Groundwater reservoirs

Groundwater is the water that collects or flows beneath the Earth's surface, filling the porous space in soil, sediment and rocks. When rain falls, part of it runs down the ground's surface to streams, rivers or lakes, and some moisturises the ground. The vegetation uses part of this water, while another part evaporates and returns to the atmosphere. The rest can seep into the ground, reaching the aquifers. Underground, it is possible to define two zones, the near-surface unsaturated or vadose zone and the deeper saturated or phreatic zone. The boundary between these two zones is the water table, technically defined as the surface on which the pore water pressure equals atmospheric pressure (Fitts, 2002). Figure 1.1 illustrates all these terms.

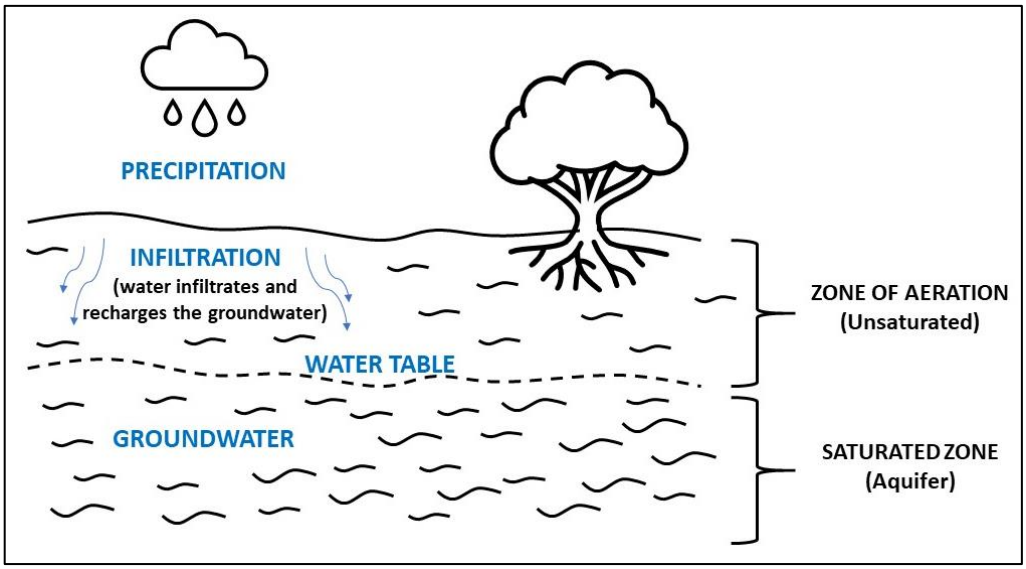

Figure 1.1 Underground diagram: unsaturated zone, water table and saturated zone.

Groundwater is naturally recharged by rainwater and snowmelt and from water that leaks through the bottom of lakes and rivers. It can also be recharged artificially when water supply systems leak and when irrigating crops with more water than necessary. The water table may be deep or shallow depending on several factors such as the physical characteristics of the region, weather conditions and recharge and exploitation rates.

Groundwater is essential for the survival of flora and fauna. When direct recharge from rainfall is low, typically during the driest months, groundwater flow becomes vital for fauna and plants.

Groundwater represents about 30% of the world's freshwater. Regarding the other 70%, nearly 69% is captured in the ice caps, mountain snow and glaciers, and merely 1% is found in rivers and lakes. Groundwater counts on average for one-third of the freshwater consumed by humans, but it is the only freshwater resource in some areas of the world (IGRAC, 2019).

Beyond the fundamental use of groundwater as drinking water, this essential natural resource has a significant role in the economy. It is the primary water source for irrigation and the food industry. Specifically, groundwater provides 43% of the global irrigation consumption (Siebert et al., 2010). Therefore, it is essential to avoid over-exploitation to maintain the right level of water in the aquifers, and the pollution of this increasingly important resource.

However, due to recent rapid technological developments and population growth, water resources such as groundwater are in danger of severe pollution worldwide (Baba and Tayfur, 2011). Groundwater contamination may be due to natural or anthropogenic sources: natural groundwater contamination is mainly due to geological formations contact with shallow groundwater, infiltration from low-quality surface water bodies, seawater intrusion, or the effect of geothermal fluids in contact with the geological formations; anthropogenic groundwater contamination is generally attributed to the use of pesticides and agricultural fertilisers, poor management of discharges from livestock and industry, mining waste, waste disposal sites and imperfect wells construction.

Arsenic is one of the most dangerous pollutants from natural sources often found in groundwater from natural sources (Lado et al., 2013; Chakraborti et al., 2010; Shrestha et al., 2003). Erosion and dissolution of arsenic minerals, water-rock interactions and geothermal processes cause groundwater to become enriched in arsenic. Fluoride is another critical issue for groundwater quality, which can be released from fluoride deposits and is easily mobilised due to its high solubility (Baba and Tayfur, 2011). The presence of formations containing salts, gypsum and anhydrite can lead their dissolution into groundwater, thus exceeding irrigation and drinking water limits for salinity and sulphates. Geothermal waters can also be a risk for

groundwater contamination, as they can contain high concentrations of boron and heavy metals such as arsenic, mercury, cadmium, lead or chromium.

Human activity has had direct and indirect effects on groundwater contamination. The direct effects are the spreading of fertilisers or chemicals and hydrological changes related to irrigation and drainage. In contrast, the indirect effects are related to changes in the reactions between water and geological formations and are caused by increased concentrations of dissolved oxidants, protons and major ions. Agriculture, intensive livestock and industrial activities can lead to groundwater contamination through the inefficient spread of fertilisers and manure on crops and the release of inadequately treated wastewater. Contamination by organic matter and nitrogen-based contaminants (mainly ammonium and nitrate) is often related to livestock farms (Kim and Kim, 2012), while petrochemical activities are usually responsible for the release of hydrocarbons (Ite et al., 2018; Baba and Tayfur, 2011). Mining activities are responsible for potential environmental problems, including groundwater contamination due to acid drainage and poor waste management. Acid mining lakes are known to contaminate water and inhibit the growth and reproduction of surrounding aquatic life due to their low pH and high content of toxic metals and elements (Baba and Tayfur, 2011; Dhakate and Singh, 2008). Also, if not adequately controlled, waste disposal sites can be a source of pollution for groundwater since a wide variety of contaminants can be released due to the leaching process.

1.2 Multi-contaminated groundwater: the "Arborea case"

Groundwater should be considered a complex system with several polluting inputs that simultaneously affect its quality. Agriculture plays a central role among the various anthropogenic activities that may cause multiple groundwater contamination. It can, directly and indirectly, influence the concentrations of a large number of inorganic substances in groundwater, including nitrate (NO_3), chloride (Cl), sulphate (SO_4), potassium (K), magnesium (Mg), calcium (Ca), iron (Fe), copper (Cu), boron (B), lead (Pb), and zinc (Zn), as well as a wide variety of pesticides and other organic compounds (Baba and Tayfur, 2011). A crystal-clear example of multi-contaminated groundwater due to inefficient agricultural activities and excessive anthropic pressure is represented by the "Nitrate Vulnerable Zone" (NVZ) of Arborea (Italy):

here, high concentrations of nitrate coexist with, among the others, calcium (Ca^{2+}), manganese (Mn^{2+}) and high salinity levels.

As for nitrate, typical sources of pollution can be divided into two main groups: nonpoint (diffuse) and point source pollution (Zhou et al., 2015). Fertiliser spreading in agriculture is the largest nonpoint source of pollution affecting groundwater quality. By definition, this form of contamination is extended over a wider area compared with point sources, which are single and identifiable sources that mainly affect localised areas. Examples of point sources include the areas of concentrated livestock confinement and areas of manure storage. In particular, point sources usually cause high nitrate concentrations in localised areas.

Nitrate is a non-toxic compound, but when reduced to nitrite, it becomes toxic to human health, causing pathological conditions such as childhood methaemoglobinaemia and gastric cancer in adults (Serio et al., 2018). The risk of specific cancers and congenital disabilities may be increased when nitrate is ingested under conditions that increase the formation of *N*-nitrous compounds. Studies have shown a possible association between ingestion of nitrate from water and colorectal cancer, thyroid disease, and central nervous system congenital disabilities (Ward et al., 2018). For these reasons, nitrate concentration values above 50 $mgNO_3^-\ L^{-1}$ limit groundwater use as a drinking water source, according to World Health Organization (WHO, 2016).

In the European Union, the Council Directive 91/676/EEC (Nitrates Directive) was adopted on December the 12th, 1991. It concerns the protection of waters against pollution caused by nitrates from agricultural sources and aims to protect water quality across Europe by promoting sound farming practices. The fundamental tools for the protection of water resources suggested by the Directive are: i) the identification of NVZ in those areas where water quality is already compromised, or there is the probability of becoming compromised due to pressing agriculture; ii) the definition of an action plan addressed to limit the use of nitrogen fertilisers and organic manure in agriculture; iii) the elaboration and the implementation of controlling and monitoring plans. In Italy, the EU directive was implemented by legislative decree (D.Lgs. 152/2006, article 92, part III), which gives Regions the task to identify the NVZs. In Sardinia, an extended area (5,500 ha) in the municipality of Arborea (province of Oristano) exceeds the limit values of nitrate concentration in groundwater provided by the legislation (50 $mg\,NO_3^-\ L^{-1}$,

D.Lgs. 152/2006, part III, All. 7A-I), and for this reason, has been designated as NVZ (Figure 1.2). The city of Arborea rises in a previous swampy area that was reclaimed during the first decades of the 20th century, and its economy was basically agricultural. Nowadays, with over 250 farms and around 33,000 heads of cattle, Arborea is one of the leading centres of agricultural and livestock production in Sardinia (municipality of Arborea, 2019). The other side of the coin of such a prosperous economy is the compromised quality of groundwater. The area of the NVZ extends in the northern sector of Campidano. It is limited on the west by the sea (Gulf of Oristano) and the ponds of Corru, S'Ittiri and Pauli Pirastu, Pond of S'Ena Arrubia, on the east by Acque Medie Channel and on the south by the Rio Mogoro and the ponds of San Giovanni and Marceddì (ARPAS, Sardinia Regional Agency for Environment Protection, 2015). In Arborea, the action plan was approved in 2006 and started in 2007 with 45 monitoring stations. Despite the slow improvement in groundwater quality documented by ARPAS in the first eight years of monitoring, the number of points that overcome the value of 50 mgNO_3^- L^{-1} is still high. Some of them have values higher than 200 mgNO_3^- L^{-1}. This occurrence could be explained by the slow movement of nitrate through the unsaturated zone of the soil, which leads to a delay in the appearance of contamination effects.

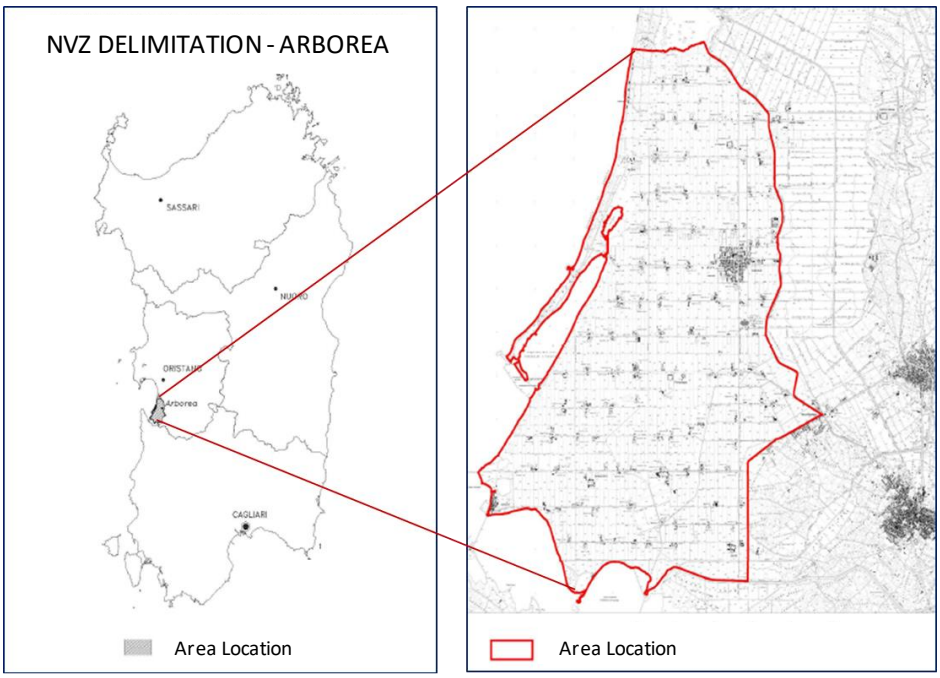

Figure 1.2. Localization and delimitation of the NVZ of Arborea (Sardinia, Italy) (Sardinia region, 2005).

As previously stated, nitrates are not the only problem found in the aquifers of the NVZ of Arborea. Calcium (Ca^{2+}), manganese (Mn^{2+}) and salinity (expressed as electrical conductivity)

have also exceeded the threshold limits for drinking water, with Ca^{2+} values concentration up to 280 mg L^{-1}, Mn^{2+} up to 2600 µg L^{-1} and electrical conductivity up to 8.0 mS cm^{-1}.

The influence of essential elements in water (e.g., Ca^{2+}, Mg^{2+}, K^{+}) on human health is not well recognised, so they are not restricted in guidelines like those issued by the WHO for drinking water. However, several studies dealing with the relationship of Ca^{2+} and Mg^{2+} in drinking water and the mortality from cardiovascular diseases report that a one-year exposure is a sufficient period to manifest into significant health effects (Rapant et al., 2017). In addition, several studies have shown that the presence of calcium can be a problem for different groundwater treatment technologies due to the formation of scale and precipitation in the various treatment sections (Matin et al., 2021; Agnihotri et al., 2020; Patrocínio et al., 2019).

Manganese (Mn^{2+}) is a metal commonly found in groundwater and, although it is an essential element for human nutrition, exposure to high concentrations has been linked to adverse health impacts. According to Iyare (2019), manganese exposure adversely affects children's cognitive, neurodevelopment and behavioural functions. The European Commission set strict threshold levels for Mn^{2+} concentration in groundwater (i.e., 50 µg L^{-1}) (Council Directive, 98/83/EEC).

The high salinity of the groundwater in the NVZ of Arborea is mainly due to the over-exploitation of groundwater pumped from wells, mainly for agricultural purposes. However, the shallow aquifer suffers from saline intrusion only around the coastal strip, while in inland areas, groundwater salinisation is primarily attributed to the use of agricultural fertilisers and their interaction with groundwater (Napoli and Vanino, 2010).

Saline groundwater is associated with several problems, especially for the economy, and risks for human health. Some studies suggest that continued consumption of water with high salinity may lead to human hypertension, as reported by Khan et al. (2008). The European Council (Council Directive 98/83/EC) established threshold limits for electrical conductivity (2.5 mS cm^{-1}) in water for human consumption. Other issues relate to agriculture and livestock breeding. Soil and water salination may reduce crop yields, limit the choice of crops to be grown in a specific area and make land semi-permanently unsuitable for other agricultural purposes. In addition, water with a high salt content can cause physiological disorders or even the death of livestock. Finally, the salinity of groundwater can reduce the life of domestic, agricultural

and industrial equipment and increase maintenance costs. Scaling due to the precipitation of dissolved salts when materials are in contact with highly saline groundwater can also lead to material damage.

These issues make it necessary to provide additional treatments (i.e., desalination) of saline groundwater for drinking water production and economic activities, leading to increased groundwater treatment costs (van Weert et al., 2009).

Therefore, the groundwater in the Arborea area is an ideal sample for developing and testing the advanced technologies proposed in this thesis and assessing their applicability to treating groundwater with multiple contaminants.

1.3 Bioelectrochemical systems applied to contaminated groundwater

1.3.1 Background knowledge

Bioelectrochemical systems (BES) are emerging technologies that couple microbiology and electrochemistry principles in a multidisciplinary approach (Figure 1.3).

Even though the first studies on microbial electrochemistry date back more than a hundred years, only in the last 15 years this area of research has been systematically investigated (Wang et al., 2020).

BES show many application niches, such as electricity generation and environmental services, including water desalination and wastewater treatment (Bajracharya et al., 2016). All bioelectrochemical technologies are based on bacterial interaction with solid electrodes, which act as electron donors or acceptors. Specifically, electro-active biomass can grow attached to the electrode (anodic or cathodic), relying on the electrons exchange through the electroconductive material.

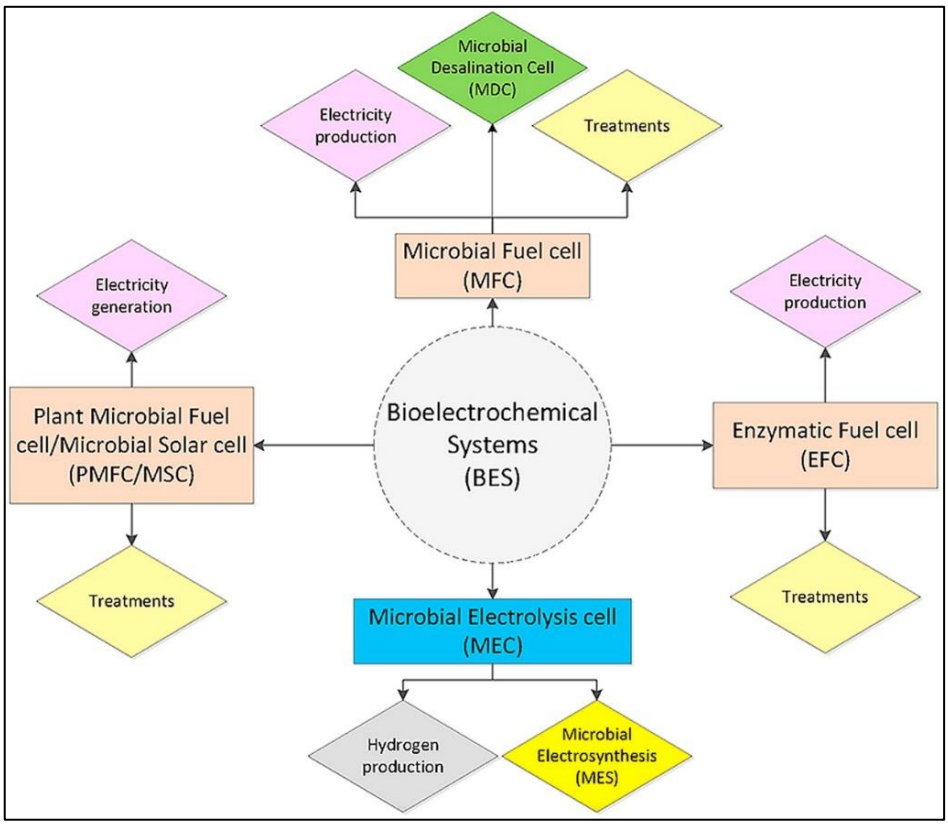

Figure 1.3. Schematic overview of various types of bioelectrochemical systems (BES) (Bajracharya et al., 2016).

Such systems can be classified as energy producers, consumers, or intermediate systems that neither produce nor require energy but need stable electrochemical conditions. Typical examples of energy-producing BES are MFC (microbial fuel cells), in which a suitable electron acceptor (e.g., oxygen) at the cathode drives current through the external circuit connecting anode and cathode. The main application of the MFC systems is to bioelectrochemically oxidise organic matter at the anode, exploiting abiotic reduction reactions at the cathode. This operational mode allows energy production from different kinds of wastewater streams, such as urban wastewater (Puig et al., 2011a), swine manure (Vilajeliu-Pons et al., 2016) and landfill leachate (Puig et al., 2011b).

In contrast, the MEC (microbial electrolysis cells) need external energy to promote specific bioelectrochemical cathodic reactions. The main application of MEC is the oxidation of organic matter at the anode with the production of hydrogen at the cathode (Logan et al., 2008; Rozendal et al., 2008).

Many different systems configurations are possible. For example, the two-compartment (anodic and cathodic) cell is widely used. It basically consists of two compartments separated by

an ion exchange membrane, which allows ions (cations, anions or only protons) to pass through, preventing the substrate or electron acceptor from passing from one compartment to the other (Figure 1.4, A). Other simple configurations are the tubular ones, often used for water treatment applications. These systems also generally have a membrane, but may feature hydraulically separated compartments or even a hydraulic connection between the two compartments (Figure 1.4, B).

However, there are also more complex configurations, depending on the particular applications studied. For example, Zhang and Angelidaki (2013) studied a two-compartments submerged system to combine several treatments in a single reactor, specifically desalination, denitrification of water and energy production (Figure 1.4, C). 3-compartments systems also generally couple several processes, and are typically exploited for water desalination and simultaneous removal of organic matter from wastewater at the anode with consequent energy production (Cao et al., 2009). However, 3-compartments systems can also be exploited in other ways, for example Koskue et al. (2021) investigates system for the 3-compartments electroconcentration for nitrogen removal and recovery from real reject water (Figure 1.4, D).

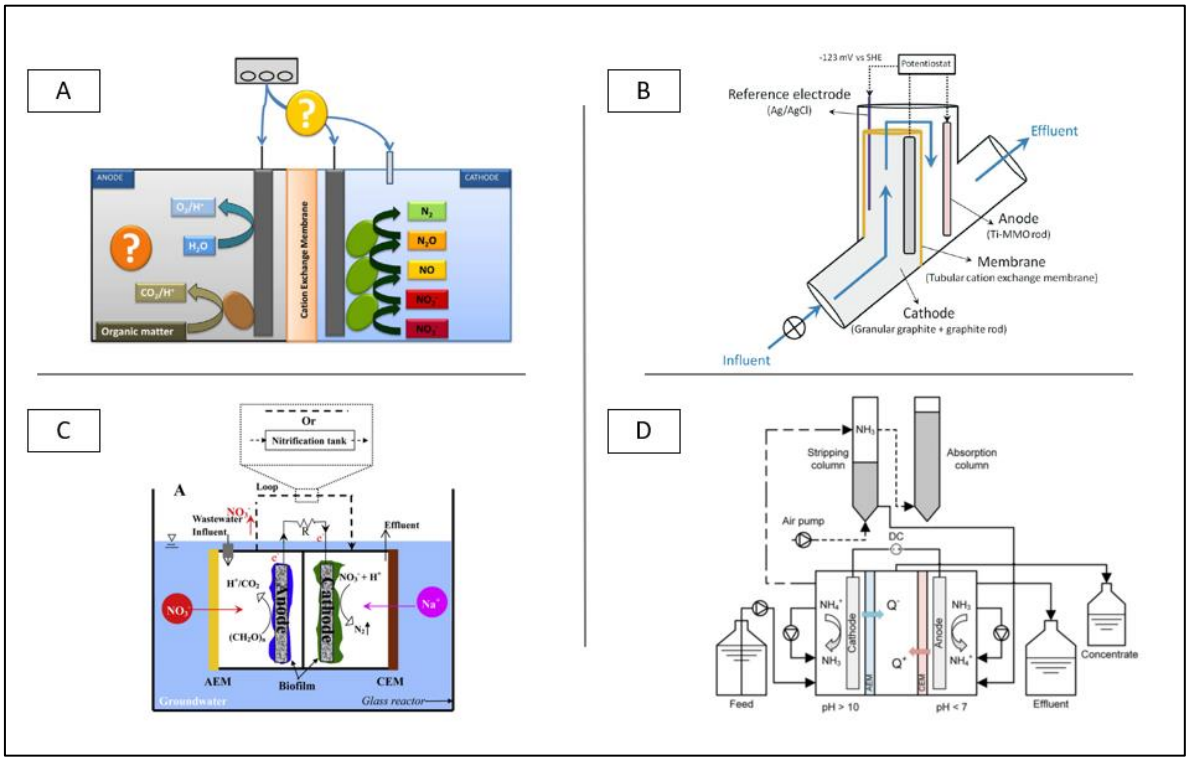

Figure 1.4. (A) Two-compartment system showing anode and bio-cathode compartments used for nitrate removal (Pous et al., 2015); (B) tubular system for groundwater treatment (Pous et al., 2017); (C) submerged microbial desalination-denitrification cell (SMDDC) to treat groundwater, produce energy, and potentially treat wastewater (Zhang and Angelidaki, 2013); (D) three-compartment electroconcentration system for nitrogen removal and recovery from reject water (Koskue et al., 2021).

Electrodes characteristics. Electrodes materials are essential factors for BES performance and they must be conductive, biocompatible, and chemically stable in the reactor solution. The most suitable electrode material is carbon, available as compact graphite plates, rods, or granules, as fibrous material (felt, cloth, paper, fibres, foam), and as glassy carbon. Conductive carbonaceous materials can also favour bacteria immobilisation on the bio-electrode (Yasri et al., 2019). Moreover, graphite plates or rods are cheap and easy to handle, and have a defined surface area. The largest surface areas are achieved with graphite felt electrodes. Also, using a compact material like reticulated vitreous carbon, which is available with different pore sizes, can increase the available area and, correspondingly, the number of biocatalytic sites. Hence the electrochemically active surface area increases. Other factors that may affect the immobilisation of microorganisms are the charge transfer resistance and electrolyte conductivity (i.e., the ion transfer through the electrolyte). Since almost all studies reported in the literature suggest that microbes use conductive minerals as conduits of electrons, a conductive anode surface can result in efficient electron transfer and better catabolism.

Membranes. Most BES designs require separating the anode and the cathode compartments by a membrane. Usually, the membranes used are either a cation exchange membrane (CEM) or an anion exchange membrane (AEM). In CEM, cations are free to exchange with other cations diffusing through the membrane or to migrate under the influence of an applied electric field (Yasri et al., 2019). Thus, the use of CEM allows the transport of H^+ and other cations such as Na^+, K^+, NH_4^+, Ca^{2+}, and Mg^{2+} toward the cathodic solution. In contrast, the AEM allows the passage of OH^-, PO^{3-}, Cl^-, SO_4^{2-}, and anionic complexes toward the anodic solution. Accordingly, the presence of membranes plays an important role in pH balancing. In fact, oxidation reactions in the anodic compartment tend to produce protons and create an acidic environment; conversely, reduction reactions at the cathode produce hydroxide ions and create an alkaline environment in the cathodic compartment. Therefore, the CEM allows the protons produced at the anode to pass to the cathode, lowering the pH in the cathodic compartment. Vice versa in the case of the presence of an AEM.

Electro-active biofilm. BES generally use microorganisms that transfer electrons to a solid electrode (exoelectrogens) or that receive electrons from the electrode (electrotrophs) (Logan et al., 2019). These microorganisms are bio-electro catalytically active species that grow in BES and are defined as extracellular electron transferors (EETs), i.e., without the need for

mediators. Donor EETs that grow on the anode are classified as anodic respiring bacteria (ARB). ARBs include various microorganisms, such as dissimilatory iron-reducing bacteria (DMRB) (e.g., *Shewanella* and *Geobacter*). ARBs oxidise soluble organics in the waste stream and donate electrons within a closed electrochemical circuit to the final electron acceptor port (Yasri et al., 2019). Microorganisms transfer electrons to the anode using a variety of methods, including direct contact of outer membrane cytochromes on the cell surface or extensions, through self-produced mediators that can transport electrons between the cell and the anode and through conducting *pili* that can achieve long-range electron transfer (Logan et al., 2019).

Many microorganisms, including bacteria and archaea, use cathode-derived electrons and various electron acceptors, including nitrate, sulphate and many metals, and grow in pure or mixed cultures (Logan et al., 2019). Microorganisms that can produce hydrogen are found in various environments and contain hydrogenases that catalyses the hydrogen production reaction (Schwartz et al., 2013). *Methanosarcina* bacteria grow on the cathode and use electrons to reduce carbon dioxide to methane (Deppenmeier, 2004). Some reduction processes are complex, and the electron transfer mechanism may not be very clear. For example, denitrification using the cathode electrode as an electron donor could be mediated by H_2 (produced by the electrochemical splitting of water), through direct electron transfer from the electrode or even by the two processes simultaneously (Pous et al., 2018). *Geobacter sp*. was shown to perform bioelectrochemical denitrification (Gregory et al., 2004). However, other studies on groundwater treatment demonstrated that other species (such as α-, β-, γ-proteobacteria and Flavobacteria) could also perform bioelectrochemical denitrification (Park et al., 2006).

1.3.2 Application to multi-contaminated groundwater: combined remediation of nitrates with other common contaminants

Among the various applications of BES, the treatment of nitrate-contaminated groundwater has been studied. Conventional technologies indicated by the Environmental Protection Agency (EPA) to reduce nitrate content below threshold limits generally consists of chemical-physical removal processes such as reverse osmosis, electrodialysis and ion exchange (EPA, 2021). However, reverse osmosis and electrodialysis imply high energy costs, and ion

exchange even requires extra costs for resin regeneration. Moreover, in these three technologies, nitrate is only separated from the groundwater and accumulates with other contaminants in the brine, which is also difficult to dispose of. Biological denitrification could overcome these drawbacks by converting nitrate into harmless dinitrogen gas (N_2). However, since groundwater is characterised by the absence (or lack) of organic matter, an organic carbon source needs to be supplied, generating an excess of sludge and increasing the treatment cost due to the dosage of chemicals.

Moreover, residual organic matter could be still present in the treated water after biological denitrification, which is prohibited according to drinking water quality standards. Bioelectrochemical systems address these criticisms by treating nitrates in an autotrophic denitrifying bio-cathode. Bio-cathodes used in BES can perform the entire denitrification process without adding organic substrates and in the presence of inorganic carbon as a carbon source.

Biological denitrification involves four reduction steps: nitrate (NO_3^-) to nitrite (NO_2^-), nitric oxide (NO), nitrous oxide (N_2O), and finally to dinitrogen gas (N_2). Therefore, the potential accumulation of denitrification intermediates such as nitrite (NO_2^-) and nitrous oxide (N_2O) must be considered. Indeed, NO_2^- in drinking water is more toxic for human health than nitrate, and N_2O is a high-impact greenhouse gas with a global warming potential 265–298 times that of CO_2 (for a 100-year timescale) (EPA, 2016).

The cathodic removal of nitrate from groundwater by BES has been successfully demonstrated since the first applications of bioelectrochemical denitrification with MFC (Clauwaert et al., 2007), although the low electrical conductivity of groundwater was found to be a limiting factor resulting in high ohmic losses and incomplete denitrification (Puig et al., 2012). Pous et al. (2015) tested a bioelectrochemical system for groundwater denitrification with different cathode potentials and different electron donors at the anode (i.e., acetate or water) in MEC. The results were surprising, showing that it is possible to achieve high performance in terms of nitrate removal with little or no accumulation of intermediates by applying a low cathode potential and without the need to add organic matter as an electron donor at the anode. The highest rate of nitrate conversion to N_2 (2.59 $mgNO_3^-N\ L^{-1}\ h^{-1}$, 93.9%) was achieved at -123 mV vs SHE using water as anode electron donor, with low energy consumption ($0.68 \cdot 10^{-2}$ kWh $g^{-1}NO_3^-N_{removed}$). Further studies focused on the identification of different operating modes

for nitrate removal using BES. For example, Wang et al. (2021) investigated the impact of intermittent current supply on denitrification in a MEC and in particular, the electron storage capacity of denitrifying electroactive biofilms on cathodes.

However, nitrate is hardly ever-present as an individual contaminant in groundwater and coexists with other contaminants of various origins due to its presence in several regions of the Earth. In this context, to meet the real need for the treatment of groundwater characterised by complex contamination, only few studies have focused on applying bioelectrochemical systems for the removal of nitrates with other contaminants.

Ceballos-Escalera et al. (2021) successfully removed nitrate and arsenic from groundwater using a tubular BES (Figure 1.5). The treatment was based on the combination of nitrate reduction to dinitrogen gas and the oxidation of arsenite to arsenate (characterised by lower toxicity, solubility and mobility) within the same reactor. In this way, the ability of BES to denitrify without being affected by arsenite and under low electrical conductivity conditions was demonstrated.

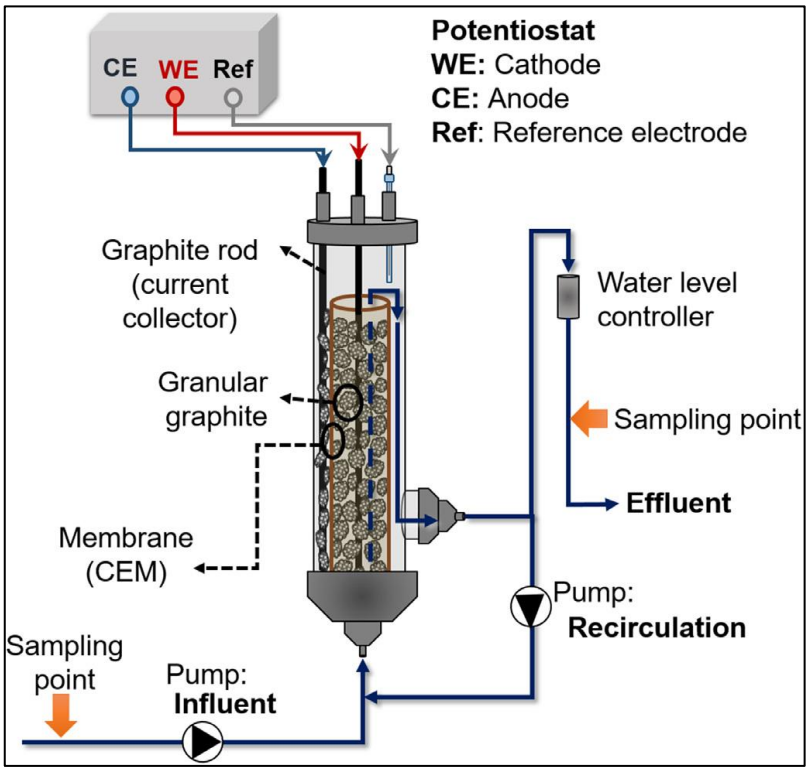

Figure 1.5. Scheme of the reactor used in the study of Ceballos-Escalera et al. (2021).

Wang et al. (2021) investigated the simultaneous removal of nitrate and perchlorate from groundwater with cathodic potential regulation (Figure 1.6).

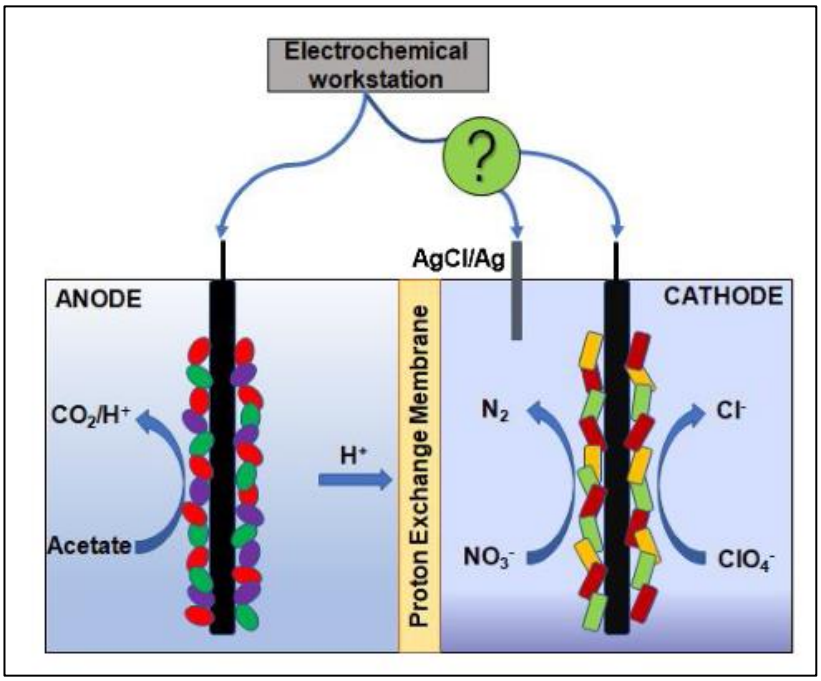

Figure 1.6. Schematic diagram of BES used in the study of Wang et al. (2021).

However, as previously demonstrated also by Sevda et al. (2018), high nitrate concentration inhibited perchlorate reduction. In addition, the supply of electrons involved the oxidation of organic matter in the anodic compartment. Therefore, the system required the addition of external organic matter, which is generally not present in groundwater.

Lai et al. (2015) investigated for the first time the bioelectrochemically-assisted reductive dechlorination (RD) of cis-dichloroethylene (cis-DCE) in real groundwater with high nitrate and sulphate concentrations (Figure 1.7).

The system did not require an external source of organic carbon, nor any inoculum other than the indigenous microbial consortia in the real groundwater. The nitrate reduction was quick and complete at all investigated potentials (between -550 and -750 mV vs SHE), whereas the sulphate reduction and cis-DCE RD rate were more affected by the cathodic potential and increased as the potential became more negative. Methanogenesis was almost absent at the less reducing potential but became the fastest reaction at -750 mV vs SHE.

These studies thus encourages the application of BES for the treatment of multi-contaminated groundwater, and provide important information for their scale-up.

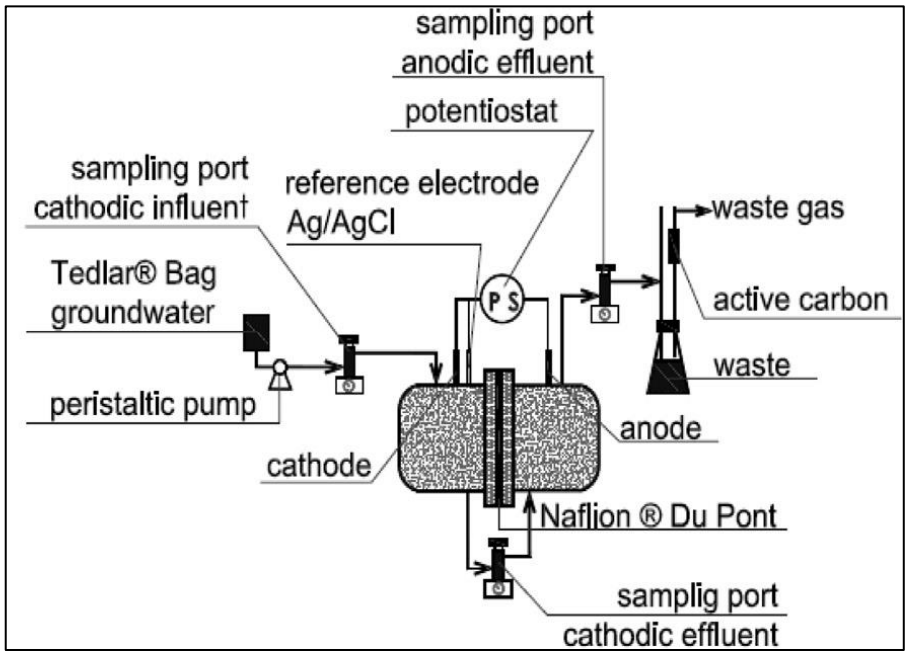

Figure 1.7. Scheme of the continuous flow BES used in the study of Lai et al. (2015).

Some of the main bioelectrochemical systems used for nitrate removal with or without other contaminants are summarised in the table 1.1.

Table 1.1. Some of the main applications of BES for nitrate removal.

Reactor type	Stream treated	Mode of operation	Nitrate removal rate [$mgNO_3^-$-N L^{-1} d^{-1}]	Other contaminants treated	Reference
Tubular MEC	softened groundwater	potentiostatic	1,269±30	NO	Ceballo-Escalera et al. (2022)
Tubular MEC	synthetic groundwater	potentiostatic	519±53	YES (Arsenic)	Ceballo-Escalera et al. (2021)
2-compartment MEC	synthetic groundwater	potentiostatic	16±1	YES (perchlorate)	Wang et al. (2021)
2- compartment MEC	synthetic groundwater	Periodic polarisation	205	NO	X. Wang et al. (2021)
Tubular MEC	synthetic groundwater	potentiostatic	849	NO	Pous et al. (2017)
2- compartment MEC	real groundwater	potentiostatic	98.2	NO	Pous et al. (2015)
2- compartment MEC	modified groundwater	potentiostatic	n.m.	YES (cis-dichloroeth-ylene and sul-fate)	Lai et al. (2015)
SMDD*	synthetic groundwater	o electrical contr	17	YES (salnitiy)	Zhang and An-gelidaki (2013)

* (Submerged Microbial Desalination Denitrification Cell); n.m. = not mentioned.

1.4 Scope and outline of this thesis

The main objective of this thesis was to develop and optimise bioelectrochemical systems for the treatment of saline groundwater from the nitrate vulnerable zone of Arborea (Sardegna, Italy). As already mentioned in paragraph 1.2, the groundwater in this area is characterised by high nitrate concentration, no or negligible organic matter content, and other contaminants such as calcium and manganese, as well as by high salinity. This PhD Thesis will reach its goals through the following specific objectives:

- To evaluate the effects of high calcium and manganese concentrations on the bioelectrochemical denitrification process (Chapter 2);
- To test a proof-of-concept based on 3-compartment BES for the simultaneous removal of nitrate and salinity from groundwater, and study the mechanisms involved in a batch mode operation (Chapter 3);
- To test different operating conditions, potentiostatic and galvanostatic modes, in continuous operation. During this step, the possibility of combining a further process, i.e., converting chloride into free chlorine and thus producing a value-added product, was also evaluated (Chapter 4);
- To investigate the effect of the progressive reduction of the hydraulic retention time on overall process performance and energy consumption in the 3-compartment BES, in the perspective of the possible pilot- and full-scale application of the technology (Chapter 5).

References

Agnihotri, B., Sharma, A., Gupta, A.B., 2020. Characterization and analysis of inorganic foulants in RO membranes for groundwater treatment. Desalination 491, 114567. https://doi.org/10.1016/j.desal.2020.114567

Baba, A., Tayfur, G., 2011. Groundwater contamination and its effect on health in Turkey. Environ. Monit. Assess. 183, 77–94. https://doi.org/10.1007/s10661-011-1907-z

Bajracharya, S., Sharma, M., Mohanakrishna, G., Dominguez Benneton, X., Strik, D.P.B.T.B., Sarma, P.M., Pant, D., 2016. An overview on emerging bioelectrochemical systems (BESs): Technology for sustainable electricity, waste remediation, resource recovery, chemical production and beyond. Renew. Energy 98, 153–170. https://doi.org/10.1016/j.renene.2016.03.002

Cao, X., Huang, X., Liang, P., Xiao, K., Zhou, Y., Zhang, X., Logan, B.E., 2009. A New Method for Water Desalination Using Microbial Desalination Cells. Environ. Sci. Technol. 43, 7148–7152. https://doi.org/10.1021/es901950j

Ceballos-Escalera, A., Pous, N., Chiluiza-Ramos, P., Korth, B., Harnisch, F., Bañeras, L., Balaguer, M.D., Puig, S., 2021. Electro-bioremediation of nitrate and arsenite polluted groundwater. Water Res. 190, 116748. https://doi.org/10.1016/j.watres.2020.116748

Chakraborti, D., Rahman, M.M., Das, B., Murrill, M., Dey, S., Chandra Mukherjee, S., Dhar, R.K., Biswas, B.K., Chowdhury, U.K., Roy, S., Sorif, S., Selim, M., Rahman, M., Quamruzzaman, Q., 2010. Status of groundwater arsenic contamination in Bangladesh: A 14-year study report. Water Res. 44, 5789–5802. https://doi.org/10.1016/j.watres.2010.06.051

Clauwaert, P., Rabaey, K., Aelterman, P., De Schamphelaire, L., Pham, T.H., Boeckx, P., Boon, N., Verstraete, W., 2007. Biological Denitrification in Microbial Fuel Cells. Environ. Sci. Technol. 41, 3354–3360. https://doi.org/10.1021/es062580r

Clímaco Patrocínio, D., Neves Kunrath, C.C., Siqueira Rodrigues, M.A., Benvenuti, T., Dani Rico Amado, F., 2019. Concentration effect and operational parameters on electrodialysis reversal efficiency applied for fluoride removal in groundwater. J. Environ. Chem. Eng. 7, 103491. https://doi.org/10.1016/j.jece.2019.103491

Deppenmeier, U., 2004. The Membrane-Bound Electron Transport System of Methanosarcina Species. J. Bioenerg. Biomembr. 36, 55–64. https://doi.org/10.1023/B:JOBB.0000019598.64642.97

Dhakate, R., Singh, V.S., n.d. Heavy metal contamination in groundwater due to mining activities in Sukinda valley, Orissa - A case study 10.

E. Ite, A., A. Harry, T., O. Obadimu, C., R. Asuaiko, E., J. Inim, I., 2018. Petroleum Hydrocarbons Contamination of Surface Water and Groundwater in the Niger Delta Region of Nigeria. J. Environ. Pollut. Hum. Health 6, 51–61. https://doi.org/10.12691/jephh-6-2-2

EPA, 2021. addressing_nitrates_with_the_dwsrf-final.pdf [WWW Document]. URL https://www.epa.gov/sites/default/files/2021-06/documents/addressing_nitrates_with_the_dwsrf-final.pdf (accessed 12.10.21).

Fitts, C.R., 2002. Groundwater Science. Elsevier.

Gregory, K.B., Bond, D.R., Lovley, D.R., 2004. Graphite electrodes as electron donors for anaerobic respiration. Environ. Microbiol. 6, 596–604. https://doi.org/10.1111/j.1462-2920.2004.00593.x

Iyare, P.U., 2019. The effects of manganese exposure from drinking water on school-age children: A systematic review. NeuroToxicology 73, 1–7. https://doi.org/10.1016/j.neuro.2019.02.013

Khan, A., Mojumder, S.K., Kovats, S., Vineis, P., 2008. Saline contamination of drinking water in Bangladesh. The Lancet 371, 385. https://doi.org/10.1016/S0140-6736(08)60197-X

Kim, H., Kim, K., 2012. Microbial and chemical contamination of groundwater around livestock mortality burial sites in Korea — a review. Geosci. J. 16, 479–489. https://doi.org/10.1007/s12303-012-0036-1

Koskue, V., Freguia, S., Ledezma, P., Kokko, M., 2021. Efficient nitrogen removal and recovery from real digested sewage sludge reject water through electroconcentration. J. Environ. Chem. Eng. 9, 106286. https://doi.org/10.1016/j.jece.2021.106286

Lado, L., Sun, G., Berg, M., Zhang, Q., Xue, H., Zheng, Q., Johnson, C., 2013. Groundwater Arsenic Contamination Throughout China. Science 341, 866–8. https://doi.org/10.1126/science.1237484

Lai, A., Verdini, R., Aulenta, F., Majone, M., 2015. Influence of nitrate and sulfate reduction in the bioelectrochemically assisted dechlorination of cis-DCE. Chemosphere 125, 147–154. https://doi.org/10.1016/j.chemosphere.2014.12.023

Logan, B.E., Call, D., Cheng, S., Hamelers, H.V.M., Sleutels, T.H.J.A., Jeremiasse, A.W., Rozendal, R.A., 2008. Microbial Electrolysis Cells for High Yield Hydrogen Gas Production from Organic Matter. Environ. Sci. Technol. 42, 8630–8640. https://doi.org/10.1021/es801553z

Logan, B.E., Rossi, R., Ragab, A., Saikaly, P.E., 2019. Electroactive microorganisms in bioelectrochemical systems. Nat. Rev. Microbiol. 17, 307–319. https://doi.org/10.1038/s41579-019-0173-x

Matin, A., Laoui, T., Falath, W., Farooque, M., 2021. Fouling control in reverse osmosis for water desalination & reuse: Current practices & emerging environment-friendly technologies. Sci. Total Environ. 765, 142721. https://doi.org/10.1016/j.scitotenv.2020.142721

Park, H.I., Kim, J.S., Kim, D.K., Choi, Y.-J., Pak, D., 2006. Nitrate-reducing bacterial community in a biofilm-electrode reactor. Enzyme Microb. Technol. 39, 453–458. https://doi.org/10.1016/j.enzmictec.2005.11.028

Pous, N., Balaguer, M.D., Colprim, J., Puig, S., 2018. Opportunities for groundwater microbial electro-remediation. Microb. Biotechnol. 11, 119–135. https://doi.org/10.1111/1751-7915.12866

Pous, N., Puig, S., Dolors Balaguer, M., Colprim, J., 2015. Cathode potential and anode electron donor evaluation for a suitable treatment of nitrate-contaminated groundwater in bioelectrochemical systems. Chem. Eng. J. 263, 151–159. https://doi.org/10.1016/j.cej.2014.11.002

Puig, S., Coma, M., Desloover, J., Boon, N., Colprim, J., Balaguer, M.D., 2012. Autotrophic Denitrification in Microbial Fuel Cells Treating Low Ionic Strength Waters. Environ. Sci. Technol. 46, 2309–2315. https://doi.org/10.1021/es2030609

Puig, S., Serra, M., Coma, M., Balaguer, M.D., Colprim, J., 2011a. Simultaneous domestic wastewater treatment and renewable energy production using microbial fuel cells (MFCs). Water Sci. Technol. J. Int. Assoc. Water Pollut. Res. 64, 904–909. https://doi.org/10.2166/wst.2011.401

Puig, S., Serra, M., Coma, M., Cabré, M., Dolors Balaguer, M., Colprim, J., 2011. Microbial fuel cell application in landfill leachate treatment. J. Hazard. Mater. 185, 763–767. https://doi.org/10.1016/j.jhazmat.2010.09.086

Rapant, S., Cvečková, V., Fajčíková, K., Sedláková, D., Stehlíková, B., 2017. Impact of Calcium and Magnesium in Groundwater and Drinking Water on the Health of Inhabitants of the Slovak Republic. Int. J. Environ. Res. Public. Health 14, 278. https://doi.org/10.3390/ijerph14030278

Rozendal, R.A., Jeremiasse, A.W., Hamelers, H.V.M., Buisman, C.J.N., 2008. Hydrogen Production with a Microbial Biocathode. Environ. Sci. Technol. 42, 629–634. https://doi.org/10.1021/es071720+

Schwartz, E., Fritsch, J., Friedrich, B., 2013. H2-Metabolizing Prokaryotes, in: Rosenberg, E., DeLong, E.F., Lory, S., Stackebrandt, E., Thompson, F. (Eds.), The Prokaryotes. Springer Berlin Heidelberg, Berlin, Heidelberg, pp. 119–199. https://doi.org/10.1007/978-3-642-30141-4_65

Serio, F., Miglietta, P.P., Lamastra, L., Ficocelli, S., Intini, F., De Leo, F., De Donno, A., 2018. Groundwater nitrate contamination and agricultural land use: A grey water footprint perspective in Southern Apulia Region (Italy). Sci. Total Environ. 645, 1425–1431. https://doi.org/10.1016/j.scitotenv.2018.07.241

Sevda, S., Sreekishnan, T.R., Pous, N., Puig, S., Pant, D., 2018. Bioelectroremediation of perchlorate and nitrate contaminated water: A review. Bioresour. Technol. 255, 331–339. https://doi.org/10.1016/j.biortech.2018.02.005

Shrestha, R.R., Shrestha, M.P., Upadhyay, N.P., Pradhan, R., Khadka, R., Maskey, A., Maharjan, M., Tuladhar, S., Dahal, B.M., Shrestha, K., 2003. Groundwater Arsenic Contamination, Its Health Impact and Mitigation Program in Nepal. J. Environ. Sci. Health Part A 38, 185–200. https://doi.org/10.1081/ESE-120016888

Siebert, S., Burke, J., Faures, J.M., Frenken, K., Hoogeveen, J., Döll, P., Portmann, F.T., 2010. Groundwater use for irrigation – a global inventory. Hydrol. Earth Syst. Sci. 14, 1863–1880. https://doi.org/10.5194/hess-14-1863-2010

US EPA, O., 2016. Understanding Global Warming Potentials [WWW Document]. URL https://www.epa.gov/ghgemissions/understanding-global-warming-potentials (accessed 12.22.21).

van Weert, F., n.d. Global Overview of Saline Groundwater Occurrence and Genesis 107.

Vilajeliu-Pons, A., Bañeras, L., Puig, S., Molognoni, D., Vilà-Rovira, A., Amo, E.H., Balaguer, M.D., Colprim, J., 2016. External Resistances Applied to MFC Affect Core Microbiome and Swine Manure Treatment Efficiencies. PLOS ONE 11, e0164044. https://doi.org/10.1371/journal.pone.0164044

Wang, C., Dong, J., Hu, W., Li, Y., 2021. Enhanced simultaneous removal of nitrate and perchlorate from groundwater by bioelectrochemical systems (BESs) with cathodic potential regulation. Biochem. Eng. J. 173, 108068. https://doi.org/10.1016/j.bej.2021.108068

Wang, X., Aulenta, F., Puig, S., Esteve-Núñez, A., He, Y., Mu, Y., Rabaey, K., 2020. Microbial electrochemistry for bioremediation. Environ. Sci. Ecotechnology 1, 100013. https://doi.org/10.1016/j.ese.2020.100013

Wang, X., Prévoteau, A., Rabaey, K., 2021. Impact of Periodic Polarization on Groundwater Denitrification in Bioelectrochemical Systems. Environ. Sci. Technol. 55, 15371–15379. https://doi.org/10.1021/acs.est.1c03586

Ward, M., Jones, R., Brender, J., de Kok, T., Weyer, P., Nolan, B., Villanueva, C., van Breda, S., 2018. Drinking Water Nitrate and Human Health: An Updated Review. Int. J. Environ. Res. Public. Health 15, 1557. https://doi.org/10.3390/ijerph15071557

What is Groundwater? | International Groundwater Resources Assessment Centre [WWW Document], n.d. URL https://www.un-igrac.org/what-groundwater (accessed 4.16.21).

Yasri, N., Roberts, E.P.L., Gunasekaran, S., 2019. The electrochemical perspective of bioelectrocatalytic activities in microbial electrolysis and microbial fuel cells. Energy Rep. 5, 1116–1136. https://doi.org/10.1016/j.egyr.2019.08.007

Zhang, Y., Angelidaki, I., 2013. A new method for in situ nitrate removal from groundwater using submerged microbial desalination–denitrification cell (SMDDC). Water Res. 47, 1827–1836. https://doi.org/10.1016/j.watres.2013.01.005

Zhou, Z., Ansems, N., Torfs, P., n.d. A Global Assessment of Nitrate Contamination in Groundwater 27.

2 EFFECT OF CALCIUM AND MANGANESE ON BIOELECTRO-CHEMICAL DENITRIFICATION[1]

Abstract

Groundwater constitutes one of the main sources of drinking water supplies, and its full exploitation is hindered by the progressive accumulation of nitrates mainly deriving from inefficient agricultural practices. Bioelectrochemical systems (BES) represent a promising option for treating nitrate-contaminated groundwater. They combine microbiology and electrochemistry principles to achieve low-cost nitrate reduction to dinitrogen gas without adding an external carbon source. This study presents the application of a resilient and sustainable bio-electricity-driven technology to treat saline groundwater contaminated by nitrates. The 2-compartment bioelectrochemical cell was fed continuously with synthetic groundwater simulating that of the nitrate vulnerable zone of Arborea (Sardinia, Italy), which is characterised by high nitrate concentration (> 20-25 $mgNO_3^-$-N L^{-1}) and electrical conductivity (> 2.5 mS cm^{-1}), as well as by the presence of other inorganic compounds such as calcium (Ca^{2+}) and manganese (Mn^{2+}). At a nitrogen loading rate of 44.7±2.4 $mgNO_3^-$-N $L^{-1}d^{-1}$, the observed nitrate removal rate stabilised at 22 $mgNO_3^-$-N $L^{-1}d^{-1}$, and no nitrite was observed in the effluent. At steady-state, specific energy consumption (SEC) was $0.9{\cdot}10^{-2}$±$0.09{\cdot}10^{-2}$ kWh $g^{-1}NO_3^-$-$N_{removed}$, which is lower than that of well-established technologies (i.e., electrodialysis) and comparable with previous BES studies. Sensitivity tests provided useful information about calcium and manganese possible effects on denitrification performance, which decreased as their concentration increased. High concentrations of Ca^{2+} (up to 172.5 mg L^{-1}) and Mn^{2+} (up to 0.525 mg L^{-1}) caused early deterioration of the electrode and membrane, affecting the performance of the bioelectrochemical cell. The change in the microbiological composition of the electroactive biofilm was also evaluated during the overall process. The genus *Thiobacillus* in the Burkholderiales and the genus *Shinella* in Rhizobiales were identified. The study provided useful information for the application of these innovative technologies to the treatment of real groundwater characterised by complex matrixes.

[1]Part of the work included in this chapter was presented at the conference: XI International symposium on environmental engineering (SIDISA-2021), 29/06-02/07/2021 July, Turin (Italy).

2.1 Introduction

Groundwater constitutes the largest drinking water reservoir, but the accumulation of anthropogenic nitrate (NO_3^-) represents one of the main concerns about its possible use for human consumption (Janža, 2022). Nitrate concentration in groundwater has been strictly regulated by the European Commission, which set a threshold level of 50 $mgNO_3^-L^{-1}$ (i.e., 11.3 $mgNO_3^-$-NL^{-1}) for drinking water (Council Directive 91/676/EEC). Conventional treatments of nitrate-contaminated groundwater consist of separation techniques (e.g., electrodialysis, ion exchange, and reverse osmosis), which have high energy requirements (1.03-2.56 kWh $m^{-3}_{treated}$) and produce highly contaminated waste brine challenging to manage (Aliaskari and Schäfer, 2021; Ceballos-Escalera et al., 2021), or biological processes (e.g., heterotrophic denitrification), which present additional treatment costs due to the requirement of an external source of organic carbon. Bioelectrochemical systems (BES) have been gaining importance for treating nitrate-contaminated water (Pous et al., 2015). In these systems, redox reactions are driven by electroactive biomass, which can develop by establishing specific conditions. When nitrate is the target pollutant in groundwater, autotrophic denitrification can occur using only the cathode as electron donor and inorganic carbon as a carbon source (Ceballos-Escalera et al., 2021). Compared to conventional technologies, BES are characterised by lower operational costs, reagents dosage and sludge production, thus representing a potential sustainable and cost-effective alternative (Pous et al., 2015; 2017).

Due to anthropogenic activities and site geochemistry, nitrate may not be the only substance of concern in groundwater, like heavy metals and other elements may also be present simultaneously, thus affecting groundwater quality and salinity and decreasing the effectiveness of groundwater remediation technologies. However, only a few studies have focused on nitrate removal from groundwater combined with other contaminants using BES (Ceballos-Escalera et al., 2021; Wang et al., 2021; Lai et al., 2015). Calcium (Ca^{2+}) has been reported as the main cause of precipitation phenomena and deactivation of bio-cathode due to the reducing environment that occurs during BES operation in the cathodic compartment (Santini et al., 2017). Thus, the effects of calcium presence on process performance and cell component (e.g., electrodes and membranes) durability need further investigation. Also, the presence of

manganese (Mn^{2+}) in water reservoirs is of particular concern due to its adverse effects on the cognitive ability and neurodevelopment of school-aged children exposed to drinking water (Iyare, 2019). The European Commission set strict threshold levels for Mn^{2+} concentration in groundwater (i.e., 50 µg L^{-1}) (Council Directive, 98/83/EEC). Moreover, the fate of manganese and its role in the autotrophic denitrification of nitrate-contaminated groundwater need further investigation, as its presence could contribute to the denitrification process (Su et al., 2016). Within this framework, our study evaluated the performance of a 2-compartment BES operated as a microbial electrolysis cell (MEC) to remove nitrate from simulated saline groundwater. The effects of calcium (Ca^{2+}) and manganese (Mn^{2+}) on the overall cell performances, components durability and composition of the bacterial communities of the cathode biomass were assessed. A comprehensive set of information was gathered, and results may be useful for the development of the efficient and cost-effective treatment of real multi-contaminated groundwater by BES.

2.2 Materials and methods

2.2.1 Configuration and set-up of the MEC

The MEC consisted of two plexiglass frames (i.e., the abiotic anodic compartment and the bio-cathodic compartment, 8x8x2 cm^3 each) separated by a Cation Exchange Membrane (CEM, 64 cm^2, CMI7000-S, Membrane International Inc., USA). Carbon felt (64 cm^2, degree of purity 99.9%, AlfaAesar, Germany) was used as the cathode and connected to a stainless-steel mesh (i.e., the current collector). A titanium mesh coated with mixed metals oxide (Ti-MMO, 15 cm^2) was used as anode (NMT-Electrodes, South Africa) and connected to a titanium wire (thickness 0.75 mm, degree of purity 99.98%, AlfaAesar, Germany) working as the current collector. A reference electrode (Ag/AgCl, mod. MF2052, BioAnalytical Systems, USA) was placed in the bio-cathodic compartment. The electrodes were connected to a multichannel potentiostat (Ivium-N-stat, Ivium technologies, NL), which was used to set a potential of -0.500 V vs Ag/AgCl (-0.303 V vs SHE) at the bio-cathode (Pous et al., 2015). Figure 2.1 shows the MEC connected to the potentiostat.

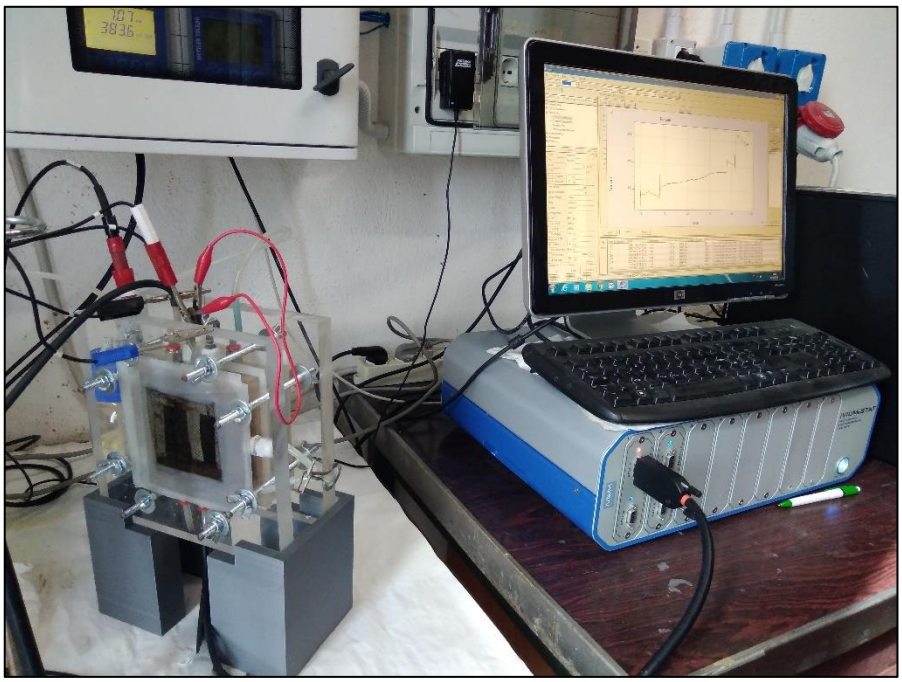

Figure 2.1. MEC connected to the potentiostat.

Experiments were conducted at room temperature (25±2 °C). The different compartments containing the electrodes used are shown in Figure AI-1, in Appendix I.

2.2.2 Operational phases

The supernatant of activated sludge liquor drawn from the municipal wastewater treatment plant of Cagliari (Italy) was used as inoculum. The bio-cathodic compartment was initially filled with Medium A and inoculum (60:40 ratio, v:v), and operated in batch mode. Medium A contained 216.6 mg L^{-1} KNO_3 (corresponding to 30.0 mgNO_3^--N L^{-1}), 10.0 mg L^{-1} NH_4Cl (corresponding to 2.6 mgNH_4^+-N L^{-1}), 4.6 mg L^{-1} KH_2PO_4, 11.5 mg L^{-1} K_2HPO_4, 350.0 mg L^{-1} $NaHCO_3$, 2,000 mg L^{-1} NaCl, and 100 µL L^{-1} of a trace element solution (Patil et al., 2010).

Once stable conditions were achieved, the bio-cathodic compartment was switched to continuous mode (Phase 1) (Figure 2.2). The hydraulic retention time (HRT) and nitrogen loading rate (NLR) were 18.5 h and 44.7±2.4 mgNO_3^--N $L^{-1}d^{-1}$, respectively.

During Phase 2, sensitivity tests were carried out to investigate the effects of calcium (Ca^{2+}) and manganese (Mn^{2+}) on the overall cell performances. Before starting Phase 2, the real groundwater from the nitrate vulnerable zone of Arborea (Sardinia, Italy) was sampled (thanks to the support of the technical staff of the Sardinian Regional Agency for Environmental

Protection) from 3 wells located in the area and characterised, resulting in high electrical conductivity (2.0-2.5 mS cm^{-1}), significant amounts of calcium (up to 115 mgCa L^{-1}) and manganese (up to 350 µgMn L^{-1}).

During Phase 2, calcium and manganese were added to Medium A in order to simulate 75% (Phase 2A), 100% (Phase 2B) and 150% (Phase 2C) of the real groundwater concentration (Table 2.1).

Before addition to the bio-cathodic compartment, the solutions were always pre-flushed with N_2 gas for 15 minutes to avoid any presence of oxygen.

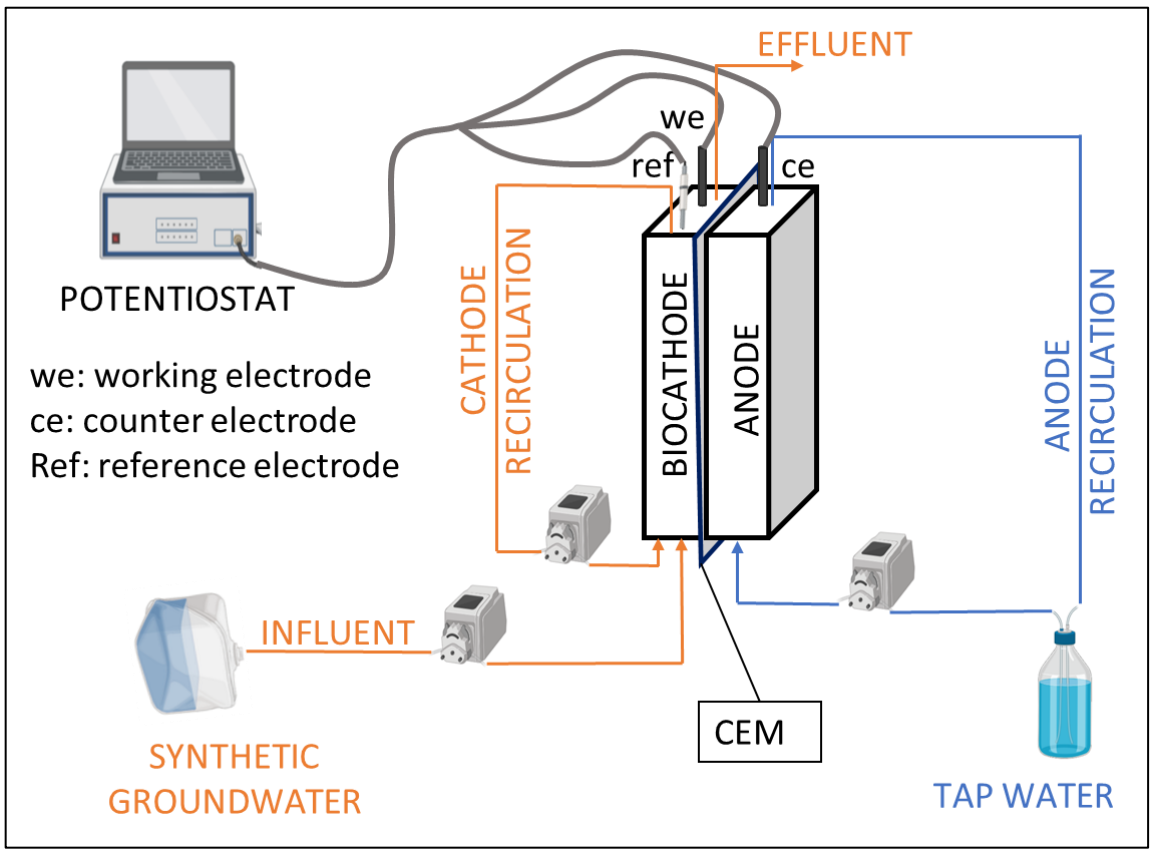

Figure 2.2. Schematic process flow diagram.

Table 2.1. Operational phases.

Phase	Phase Duration (d)	NLR ($mgNO_3^-$-N $L^{-1}d^{-1}$)	Influent Ca^{2+} conc. ($mg\ L^{-1}$)	Influent Mn^{2+} conc. ($mg\ L^{-1}$)
1	30	48.9±1.2	-	-
2A	43	44.8±1.2	86.3	0.262
2B	45	44.3±0.8	115.0	0.350
2C	45	42.3±0.4	172.5	0.525

The anodic compartment was filled with tap water and kept in batch mode for the entire duration of the experimentation, replacing water when pH dropped below 3.

At the end of the experiment, an abiotic test was run in batch mode in a twin cell, recirculating Medium A with the same Ca^{2+} and Mn^{2+} concentrations as test 2C (Table 2.1) in the cathodic compartment, and tap water in the anodic compartment. The abiotic test was performed as control, to investigate the possible electrochemical reactions occurring at the cathode, without biomass.

2.2.3 Analytical methods

Liquid samples were collected from the influent (once per week) and effluent (three times per week) of the bio-cathodic compartment as well as from the anodic compartment (three times per week). Samples were analysed for anions quantification, namely chloride (Cl^-), nitrite (NO_2^--N), nitrate (NO_3^--N), phosphate (PO_4^{3-}), and sulphate (SO_4^{2-}), using an ion chromatograph (ICS-90, Dionex-Thermofisher, USA) equipped with an AS14A Ion-PAC 5 µm column. Samples were filtered (acetate membrane filter, 0.45 µm porosity) and properly diluted using grade II water. The influent and effluent concentrations of the main cations considered for the sensitivity tests, namely calcium (Ca^{2+}) and manganese (Mn^{2+}), were determined using an ICP/OES (Optima 7000, PerkinElmer, USA): samples were filtered (acetate membrane filter, 0.45 µm porosity), acidified with 1% (v/v) nitric acid and diluted using grade I water. pH and electrical conductivity were measured using a benchtop meter (HI5522, Hanna Instruments, Italy). The effluent samples were also characterised in terms of NH_4^+ concentration by spectrophotometric analysis (DR2800, Hach Lange, Germany).

SEM images of cations exchange membranes, which were extracted from the cell at the end of each experimentation phase, were captured using an FEI Quanta 200 SEM microscope. The membranes did not undergo any preparation, and they were fixed on the stub using a double-sided graphite adhesive. The analyses were performed in low vacuum mode (i.e., residual pressure in the experimental chamber in the range of 0.3-0.9 Torr) to minimise electrostatic charge effects or high vacuum (pressure below 10^{-4} Torr). Images were collected in either secondary electrons or backscattered electrons.

2.2.4 Analysis of bacterial communities by NGS of 16S rRNA gene

In a preliminary analysis, the heterogenicity of the cathodic biomass was investigated. Three replicates of the microbial biomass were collected in three different cathode points during Phase 1 of the operational process, separately stored at -20°C before DNA extraction, and subjected to independent analysis of bacterial communities.

Then, the shift in the composition of the bacterial communities from the inoculum to the cathodic biomass was investigated. Samples of the biofilms formed on the cathode were axenically collected at the end of Phase 1 (End1) and Phase 2C (End2C) as defined in Table 2.1. At each sampling time, five cathode points were sampled, and the biomass pooled in order to mitigate the effects of microscale heterogeneity on the cathode. Biomass samples were stored at -20°C before DNA extraction. Aliquots of the activated sludge supernatant, used as inoculum of the bio-cathodic compartment, were centrifuged at 6,000 rpm for 15 min. Then, the liquid was removed, and the biomass was collected as a pellet (Inoculum).

Genomic DNA was extracted from biomass samples (250 mg wet weight) using the DNeasy PowerSoil Pro Kit (QIAGEN) and DNA was subsequently purified using the DNeasy PowerClean Cleanup Kit (QIAGEN). The DNA quality and concentration were determined on agarose gel using a DNA quantitation standard. DNA samples were submitted to Bio-Fab Research srl (Rome, Italy) for sequencing of the V3-V4 region of the bacterial 16S rRNA gene on an Illumina Miseq platform (Illumina, San Diego, CA) using 2 × 300 bp paired-end reads.

For data processing, raw sequences were demultiplexed by the sequencing facility. Illumina sequencing reads will be submitted at the European Nucleotide Archive. Reads were trimmed to remove primer sequences using the CutAdapt version 3.5. Sequences were imported into Quantitative Insights into Microbial Ecology (QIIME 2) version 2020-11 (Bolyen et al., 2019). Using the DADA2 pipeline (Callahan et al., 2016), reads with ambiguous and poor-quality bases were discarded, good quality reads were dereplicated and denoised, and the paired reads were merged. Chimeras and singletons were identified and removed from the dataset. DADA2 was used to produce alternative sequence variants (ASVs), thus obtaining a filtered ASV-abundance table. For each ASV, a representative sequence was used for taxonomy assignment against the Silva database release 138 (Quast et al., 2013). The indices of diversity (richness as

the number of observed ASV, Shannon with an e log base) and evenness (Pielou's) were used to assess the alpha-diversity by using the vegan R package (Oksanen et al., 2019). Read count data were normalised by Cumulative Sum Scaling (CSS) transformation, using the metagenomeSeq package (Paulson et al., 2013). The Bray-Curtis similarity index between samples was calculated.

2.3 Results and discussion

2.3.1 Performances of the bioelectrochemical cell

The performances of the bioelectrochemical cell were evaluated in terms of denitrification in the bio-cathodic compartment. Figure 2.3 shows the nitrate loading, removal rate and removal efficiency trends during the different experimental phases.

During Phase 1, characterised by the absence of calcium and manganese in the influent, nitrate removal rates (NRR) of 22.3±5.5 $mgNO_3^-$-N $L^{-1}d^{-1}$ were achieved, corresponding to removal efficiencies of 49.4±2.6%. The nitrate concentration in the effluent was 16.2±3 $mgNO_3^-$-N L^{-1}, thus close to the threshold limit of 11.3 $mgNO_3^-$-N L^{-1}. The average coulombic efficiency was > 60%, and no nitrites were observed in the effluent. The observed denitrification rates were lower than those reported in previous studies: Ceballos-Escalera et al. (2021) observed NRR up to 519 $mgNO_3^-$-N $L^{-1}d^{-1}$ in a tubular BES treating nitrate-contaminated groundwater (synthetic), using granular graphite as bio-cathode. However, direct comparisons are difficult since BES configurations may be significantly different in set-up, size, and materials. For instance, if the bio-cathode surface is considered, the resulting NRR observed in our study would be comparable to that observed by Ceballos-Escalera et al. (2021) (i.e., approx. 314 vs 305 $mgNO_3^-$-N $m^{-2}d^{-1}$) since the carbon felt used as cathode had a much lower area compared to granular graphite (i.e., $0.64 \cdot 10^{-2}$ m^2 vs 0.51 m^2). A smaller surface area available for biofilm growth likely resulted in lower active denitrifying biomass with lower volumetric NRR. The specific energy consumption (SEC) during Phase 1 was $0.9 \cdot 10^{-2} \pm 0.09 \cdot 10^{-2}$ kWh gNO_3^--$N^{-1}_{removed}$, which is comparable to other BES applied to nitrate removal ($0.7 \cdot 10^{-2}$ kWh gNO_3^--$N^{-1}_{removed}$, Pous et al., 2015).

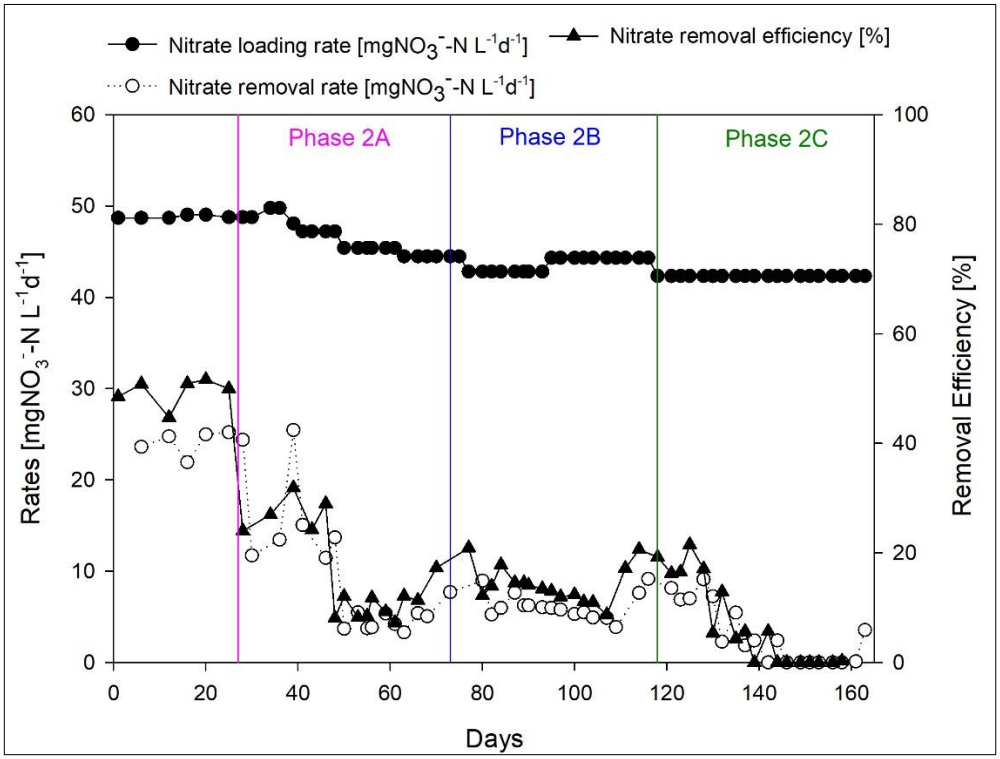

Figure 2.3. Trends of nitrate loading, removal rate and removal efficiency, during the different experimental phases.

2.3.2 Effect of Calcium and Manganese on BES performance

Sensitivity tests showed a worsening of process performances as Ca^{2+} and Mn^{2+} concentrations were increased. Table 2.2 shows a summary of the results of the removal of the different contaminants during the experimental phases. NRR during Phase 2A was 8.9±6.5 $mgNO_3^-$-N $L^{-1}d^{-1}$ and decreased slightly during Phase 2B to 6.2±1.5 $mgNO_3^-$-N $L^{-1}d^{-1}$ (with a removal efficiency of about 15 % in both phases). Coulombic efficiency also decreased during the first two Phases of sensitivity tests (i.e., 2A and 2B), stabilising at values near 30%. Although previous studies have shown that low coulombic efficiencies may be linked to the production of intermediates (Puig et al., 2011; Virdis et al., 2009), no nitrite accumulation was observed in the effluent in the present study.

Table 2.2. Summary of nitrate removal rates and nitrate, calcium and manganese removal efficiencies observed during the different experimental phases.

Phase	NRR ($mgNO_3^-$-N $L^{-1}d^{-1}$)	NO_3^--N removal efficiency (%)	Ca^{2+} removal efficiency (%)	Mn^{2+} removal efficiency (%)
1	22.3±5.5	49±3	-	-
2A	8.9±6.5	14±8	33±7	80±9
2B	6.2±1.5	14±3	15±9	45±13
2C	3.0±3.2	7±8	20±8	30±6

During Phase 2C, a steep reduction in NRR and removal efficiencies was observed from day 128, and complete inhibition of denitrifying activity at the bio-cathode was observed from day 140 onward. Such inhibition was likely due to progressive Ca^{2+} deposition (i.e., scale) on the bio-cathode surface. High Ca^{2+} concentrations and basic conditions on the bio-cathode electrode (due to the reductive nature of the cathode and the low buffering capacity of groundwater) can promote Ca^{2+} precipitation and electrodeposition on the electrode. Santini et al. (2017) reported that this induces cathode electrode blockage, leading to cell deactivation. The electrodeposition of Ca^{2+} on the bio-cathode electrode was confirmed by the reduction of effluent Ca^{2+} concentrations (i.e., -26±13 mgCa L^{-1} corresponding to a percentage removal of about 22% during the different phases of sensitivity test) as shown in Figure 2.4(A).

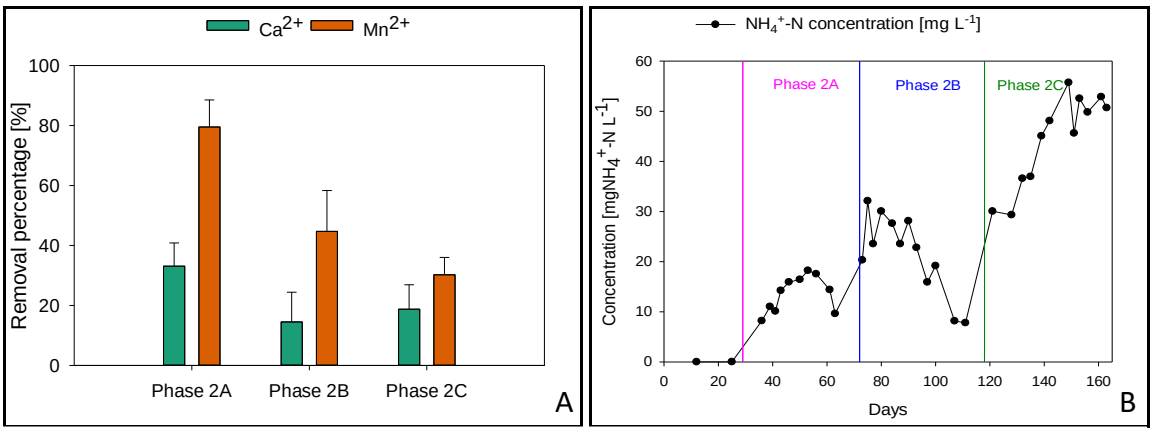

Figure 2.4. Trends of average calcium and manganese removal during sensitivity tests (A) and trend of ammonium concentration in the effluent during the different experimental phases (B).

Another possible cause of the worsening of denitrification performance may be related to biomass stress induced by the new operating conditions, as suggested by the occurrence of ammonium in the effluent. From Phase 2A, a progressive increase in effluent NH_4^+-N concentration was observed, which peaked at 50 mgNH_4^+-N L^{-1} at the end of Phase 2C (Figure 2.4(B)).

This increase could be due to cell lysis of the biomass and the occurrence of dissimilatory reduction of nitrate to ammonium. Sander et al. (2015) demonstrated that autotrophic dissimilatory reduction of NO_3^--N to NH_4^+-N in bioelectrochemical systems is possible, stating that it could be due to an incomplete biomass development or a shift in the microbial community over time. This phenomenon is confirmed by the reduction in coulombic efficiency observed (from 63% in Phase 2A to 13% in phase 2C) as the ratio of ammonium produced to nitrate removed increased (from 3.4 in Phase 2A to 16.4 in Phase 2C), consistently with results reported by Sander et al. (2015).

The results of the abiotic control test showed no production of NH_4^+-N in the cathodic compartment, thus confirming that the NH_4^+-N production observed during the sensitivity tests occurred biologically due to a stressed state of the biomass and/or its modification over time, rather than any (electro)chemical reaction.

Concerning Mn^{2+}, a reduction of the concentrations in the effluent was observed during the sensitivity tests (Figure 2.4A). Such decrease could, at first sight, suggest precipitation of Mn^{2+} in the bio-cathode compartment, but if this were the case, one should expect an increase in the amount of Mn^{2+} removed as the influent concentration increases. However, the amount of Mn^{2+} removed during the three tests was very similar (i.e., -172±42 µgMn L^{-1}), suggesting the presence of a biological process involved in Mn^{2+} removal.

Bai et al. (2021) showed that it is possible to achieve biological removal of NO_3^- and Mn^{2+} simultaneously and also that the presence of Mn^{2+} can enhance denitrifying activity. Although no improvement in denitrification performance was observed with the addition of Mn^{2+} in the present study, the results obtained are encouraging and worthy of further research, particularly to verify the possibility of developing suitable biomass for NO_3^- and Mn^{2+} removal in bioelectrochemical systems.

The effect of the sensitivity tests was also evaluated on the membrane, which was extracted from the cell at the end of each test for SEM analysis. SEM images showed the presence of concretion on the surface of the membranes (Appendix I, Figure AI-2), which could be a challenge for the durability of the exchange efficiency of the membranes, and demonstrates the importance of evaluating this aspect for the application of BES in real scale.

2.3.3 Bacterial communities at different operational phases

Heterogenicity of the bacterial community on the bio-cathode

The richness of the bacterial communities in the three biomass replicates ranged from 331 to 393 (357±32 AVSs) with a coefficient of variation (CV%) equal to 9%. The values of Shannon (H') and Pielou's evenness (J') exhibited a CV% lower than 2% (Table 2.3). The Bray-Curtis similarity index calculated in the pairwise comparison between replicate samples was 77.5±4.9%.

In the community composition, the most abundant phyla of Bacteria was Proteobacteria (28.8±0.5%) followed by Chloroflexi (19.1±2.0%), Planctomycetota (12.6±0.9%), Bacteroidota (10.0± 1.8%), Actinobacteriota (9.3±1.4%). At the order level, Burkholderiales was the most taxon (6.9±0.3%), followed by Rhizobiales (6.5±0.4%), Anaerolineales (5.9±0.8%), and Pirellulales (5.3±0.4%). All the aforementioned taxa exhibited a CV% in the relative abundances lower than 20%.

Table 2.3. Diversity (richness as the number of observed ASVs, H': Shannon with an e log base) and evenness (J': Pielou's) indices of bacterial communities in the three replicates samples of cathodic biomass collected during Phase 1.

Replicate	S	J'	H'(lodge)
1	347	0.997	5.773
2	331	0.996	5.711
3	393	0.997	5.883
mean	357	0.997	5.789
dev.st	32	0.000	0.087
CV%	9.02%	0.03%	1.51%

The shift in bacterial community diversity from the inoculum to the bio-cathodic biomass

The Bray-Curtis similarity index calculated in the pairwise comparison between the bacterial communities of the activated sludge supernatant used as inoculum to the bio-cathodic compartment and the biofilm on the cathode at the end of Phase 1 (End1) was 46%, showing a shift in community structure.

The shift in the bacterial community from the inoculum to the biomass End1 was investigated in terms of diversity and evenness indices (Table 2.4) and community composition (Figure 2.5).

The diversity indices were lower in the inoculum than in the biomass End1, demonstrating the enrichment of a more complex community on the cathode during the bioelectrochemical process.

At phylum level, the bacterial community in the inoculum was dominated by Chloroflexi (20.4%), Proteobacteria (19.7%), Actinobacteriota (14.4%), Firmicutes (10.1%), Planctomycetota (9.9%), and Bacteroidota (8.1%). The shift to the community of biomass End1 was characterised by the decrease in Firmicutes (-26%) and the increase in Planctomycetota (+24%), Chloroflexi (+13%), and Bacteroidota (+6%), while the relative abundance of Proteobacteria and Actinobacteriota were almost constant (<5%).

Table 2.4. Diversity (richness as the number of observed ASV, H': Shannon with an e log base) and evenness (J': Pielou's) indices of bacterial communities in activated sludge supernatant, used as inoculum of the bio-cathodic compartment (Inoculum), and biofilms on the cathode at the end of Phase 1 (End1) and at the end of phase 2C (End2C).

Replicate	S	J'	H'(lodge)
Inoculum	132	0,992	4,847
End1	350	0,997	5,775
End2C	328	0,996	5,702

At the order level, the most abundant taxa in the inoculum were Anaerolineales (10.5%) and Burkholderiales (6.2%), followed by Planctomycetales (4.5%), Microtrichales (4.4%), and Rhizobiales (4.3%). As compared to the inoculum, the community of biomass End1 was characterised by the increase in the relative abundances of Anaerolineales (+17%), Burkholderiales (+6%), Rhizobiales (+37%). In the class of Planctomycetes, the order Pirellulales increased (+46%) while the order Planctomycetales decreased (-99%). A reduction in the relative abundance of the order Microtrichales (-25%) was also found.

A deeper analysis of the five aforementioned orders identified 14 genera which were not detected in the inoculum community and were enriched in the community of the biomass End1. Among them, the genus *Thiobacillus* in the Burkholderiales and the genus *Shinella* in Rhizobiales were previously detected in BES biomass. The genus *Thiobacillus* has been demonstrated to contribute to bioelectrochemical denitrification (Nguyen et al., 2016b; Pous et al., 2015; Vilar-Sanz et al., 2013), while members of the genus *Shinella* have been found on cathodes in a microbial electrochemical denitrification system (Nguyen et al., 2016a).

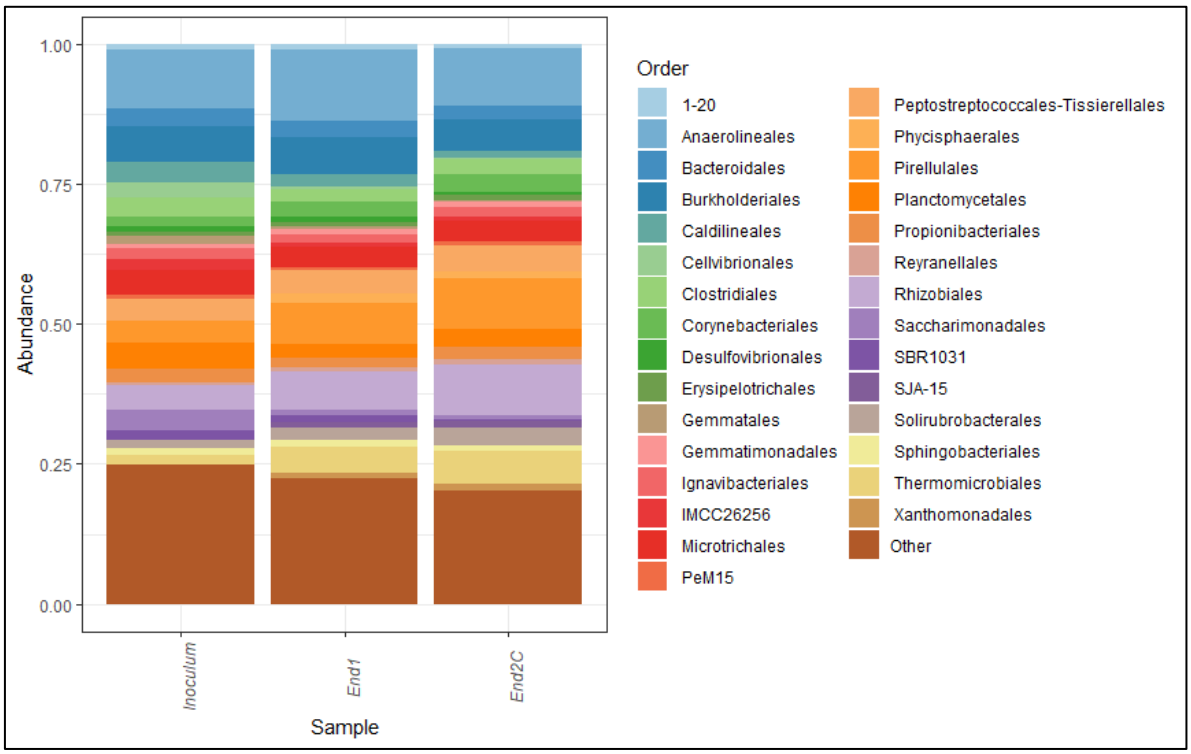

Figure 2.5. Composition of bacterial communities in activated sludge supernatant, used as inoculum of the bio-cathodic compartment (Inoculum), and biofilms formed on the cathode collected at the end of Phase 1 (End1) and at the end of phase 2C (End2C). Bar plot showing the average contribution at order level.

The Bray-Curtis similarity index calculated between the bacterial communities in bio-cathodic biomasses at the end of Phase 1 (End1) and Phase 2C (End2C) was 83.6%. Moreover, the diversity and evenness indices of the two bacterial communities were comparable. Therefore, the overall structure of the biomass community on the cathode was almost stable after the addition of Ca^{2+} and Mn^{2+}. At the order level, the most abundant taxa in biomass End2C were Anaerolineales (10.4%), Pirellulales (9.0%), Rhizobiales (8.9%), Thermomicrobiales (5.9%), and Burkholderiales (5.6%). As compared to the biomass End1, an increase in Pirellulales (+17%) and Rhizobiales (+22%) was observed, while Anaerolineales (-21%) and Burkholderiales (-17%) decreased (Figure 2.5).

2.4 Conclusions

A 2-compartment BES was tested for the electro-bioremediation of nitrate-contaminated saline groundwater. The possibility of exploiting the electroactive biofilm grown on the bio-cathode for NO_3^- removal was successfully evaluated, achieving nitrate removal comparable to other studies when normalised to the cathode surface (i.e., 340±60 mgNO_3^--N $m^{-2}d^{-1}$). In

addition, sensitivity tests showed that high Ca^{2+} concentrations (approx. 170 mg L^{-1}) have adverse effects on the durability of materials (i.e., scale on the cathode electrode and membrane) and thus on the denitrifying performance. Although Mn^{2+} removal was observed, further studies are needed to identify the processes involved. Microbiological analyses showed a more complex community enrichment on the cathode during the bioelectrochemical process (from inoculum to the end of Phase 1). The genus *Thiobacillus* in the Burkholderiales and the genus *Shinella* in Rhizobiales were identified, in agreement with previous studies concerning denitrifying BES. Moreover, the overall structure of the biomass community on the cathode was basically stable after the addition of Ca^{2+} and Mn^{2+} (end of Phase 2C). This study provides new insights into the system boundaries of electro bioremediation of nitrate contaminated groundwater.

Acknowledgement

This study was funded by Fondo di Sviluppo e Coesione 2014-2020, Patto per lo sviluppo della Regione Sardegna - Area Tematica 3 - Linea d' Azione 3.1, "Interventi di sostegno alla ricerca". Project SARdNAF "Advanced Systems for the Removal of Nitrates from Groundwater", ID: RASSR53158.

An acknowledgement is due to Prof. Elena Tamburini and Mr Riccardo Ardu (Department of Biomedical Sciences, University of Cagliari) for their support with the NGS analysis.

The Centre for Research University Services (CeSAR) of the University of Cagliari (Italy) is to be thanked for the SEM analysis.

The ARPAS technical staff are thanked for their support and cooperation in groundwater sampling.

Thanks to Dr Martina Piredda for the support with the ICP-OES analyses.

References

Aliaskari, M., Schäfer, A.I., 2021. Nitrate, arsenic and fluoride removal by electrodialysis from brackish groundwater. Water Res. 190, 116683. https://doi.org/10.1016/j.watres.2020.116683

Bai, Y., Su, J., Wen, Q., Huang, T., Chang, Q., Ali, A., 2021. Characterization and mechanism of Mn(II)-based mixotrophic denitrifying bacterium (Cupriavidus sp. HY129) in remediation of nitrate (NO3−-N) and manganese (Mn(II)) contaminated groundwater. J. Hazard. Mater. 408, 124414. https://doi.org/10.1016/j.jhazmat.2020.124414

Bolyen, E., Rideout, J. R., Dillon, M. R., Bokulich, N. A., Abnet, C. C., Al-Ghalith, G. A., … Caporaso, J. G. (2019). Reproducible, interactive, scalable and extensible microbiome data science using QIIME 2. Nature Biotechnology, 37(8), 852–857. https://doi.org/10.1038/s41587-019-0209-9

Callahan, B. J., McMurdie, P. J., Rosen, M. J., Han, A. W., Johnson, A. J. A., & Holmes, S. P. (2016). DADA2: High-resolution sample inference from Illumina amplicon data. Nature Methods, 13(7), 581–583. https://doi.org/10.1038/nmeth.3869

Ceballos-Escalera, A., Pous, N., Chiluiza-Ramos, P., Korth, B., Harnisch, F., Bañeras, L., Balaguer, M.D., Puig, S., 2021. Electro-bioremediation of nitrate and arsenite polluted groundwater. Water Res. 190, 116748. https://doi.org/10.1016/j.watres.2020.116748

Clarke, K. R., Gorely, R. N., Somerfield, P. J., and Warwick, R. M. (2014). Change in Marine Communities: An Approach to Statistical Analysis and Interpretation, 3rd edition. Plymouth: PRIMER-E.

Iyare, P.U., 2019. The effects of manganese exposure from drinking water on school-age children: A systematic review. NeuroToxicology 73, 1–7. https://doi.org/10.1016/j.neuro.2019.02.013

Janža, M., 2022. Optimization of well field management to mitigate groundwater contamination using a simulation model and evolutionary algorithm. Sci. Total Environ. 807, 150811. https://doi.org/10.1016/j.scitotenv.2021.150811

Lai, A., Verdini, R., Aulenta, F., Majone, M., 2015. Influence of nitrate and sulfate reduction in the bioelectrochemically assisted dechlorination of cis-DCE. Chemosphere 125, 147–154. https://doi.org/10.1016/j.chemosphere.2014.12.023

McMurdie, P. J., & Holmes, S. (2013). Phyloseq: An R Package for Reproducible Interactive Analysis and Graphics of Microbiome Census Data. PLoS ONE, 8(4). https://doi.org/10.1371/journal.pone.0061217

Nguyen, V.K., Park, Y., Yang, H., Yu, J., Lee, T., 2016a. Effect of the cathode potential and sulfate ions on nitrate reduction in a microbial electrochemical denitrification system. J. Ind. Microbiol. Biotechnol. 43, 783–793. https://doi.org/10.1007/s10295-016-1762-6

Nguyen, V.K., Park, Y., Yu, J., Lee, T., 2016b. Bioelectrochemical denitrification on biocathode buried in simulated aquifer saturated with nitrate-contaminated groundwater. Environ. Sci. Pollut. Res. 23, 15443–15451. https://doi.org/10.1007/s11356-016-6709-y

Oksanen, J., Blanchet, F. G., Friendly, M., Kindt, R., Legendre, P., McGlinn, D., et al. (2019). Vegan. Community Ecology Package.

Patil, S., Harnisch, F., Schröder, U., 2010. Toxicity Response of Electroactive Microbial Biofilms-A Decisive Feature for Potential Biosensor and Power Source Applications. ChemPhysChem 11, 2834–2837. https://doi.org/10.1002/cphc.201000218

Paulson, J. N., Colin Stine, O., Bravo, H. C., & Pop, M. (2013). Differential abundance analysis for microbial marker-gene surveys. Nature Methods, 10(12), 1200–1202. https://doi.org/10.1038/nmeth.2658

Pous, N., Koch, C., Vilà-Rovira, A., Balaguer, M.D., Colprim, J., Mühlenberg, J., Müller, S., Harnisch, F., Puig, S., 2015. Monitoring and engineering reactor microbiomes of denitrifying bioelectrochemical systems. RSC Adv. 5, 68326–68333. https://doi.org/10.1039/C5RA12113B

Pous, N., Puig, S., Balaguer, M.D., Colprim, J., 2017. Effect of hydraulic retention time and substrate availability in denitrifying bioelectrochemical systems. Environ. Sci. Water Res. Technol. 3, 922–929. https://doi.org/10.1039/C7EW00145B

Pous, Narcis, Puig, S., Dolors Balaguer, M., Colprim, J., 2015. Cathode potential and anode electron donor evaluation for a suitable treatment of nitrate-contaminated groundwater in bioelectrochemical systems. Chem. Eng. J. 263, 151–159. https://doi.org/10.1016/j.cej.2014.11.002

Quast, C., Pruesse, E., Yilmaz, P., Gerken, J., Schweer, T., Yarza, P., et al. (2013). The SILVA ribosomal RNA gene database project: improved data processing and web-based tools. Nucleic Acids Res. 41, 590–596. doi: 10.1093/nar/gks1219

Sander, E.M., Virdis, B., Freguia, S., 2015. Dissimilatory nitrate reduction to ammonium as an electron sink during cathodic denitrification. RSC Adv. 5, 86572–86577. https://doi.org/10.1039/C5RA19241B

Santini, M., Marzorati, S., Fest-Santini, S., Trasatti, S., Cristiani, P., 2017. Carbonate scale deactivating the biocathode in a microbial fuel cell. J. Power Sources 356, 400–407. https://doi.org/10.1016/j.jpowsour.2017.02.088

Su, J. feng, Luo, X. xin, Wei, L., Ma, F., Zheng, S. chen, Shao, S. cheng, 2016. Performance and microbial communities of Mn(II)-based autotrophic denitrification in a Moving Bed Biofilm Reactor (MBBR). Bioresour. Technol. 211, 743–750. https://doi.org/10.1016/j.biortech.2016.03.101

Vilar-Sanz, A., Puig, S., García-Lledó, A., Trias, R., Balaguer, M.D., Colprim, J., Bañeras, L., 2013. Denitrifying Bacterial Communities Affect Current Production and Nitrous Oxide Accumulation in a Microbial Fuel Cell. PLoS ONE 8, e63460. https://doi.org/10.1371/journal.pone.0063460

Wang, C., Dong, J., Hu, W., Li, Y., 2021. Enhanced simultaneous removal of nitrate and perchlorate from groundwater by bioelectrochemical systems (BESs) with cathodic potential regulation. Biochem. Eng. J. 173, 108068. https://doi.org/10.1016/j.bej.2021.108068

Appendix I

Additional figures

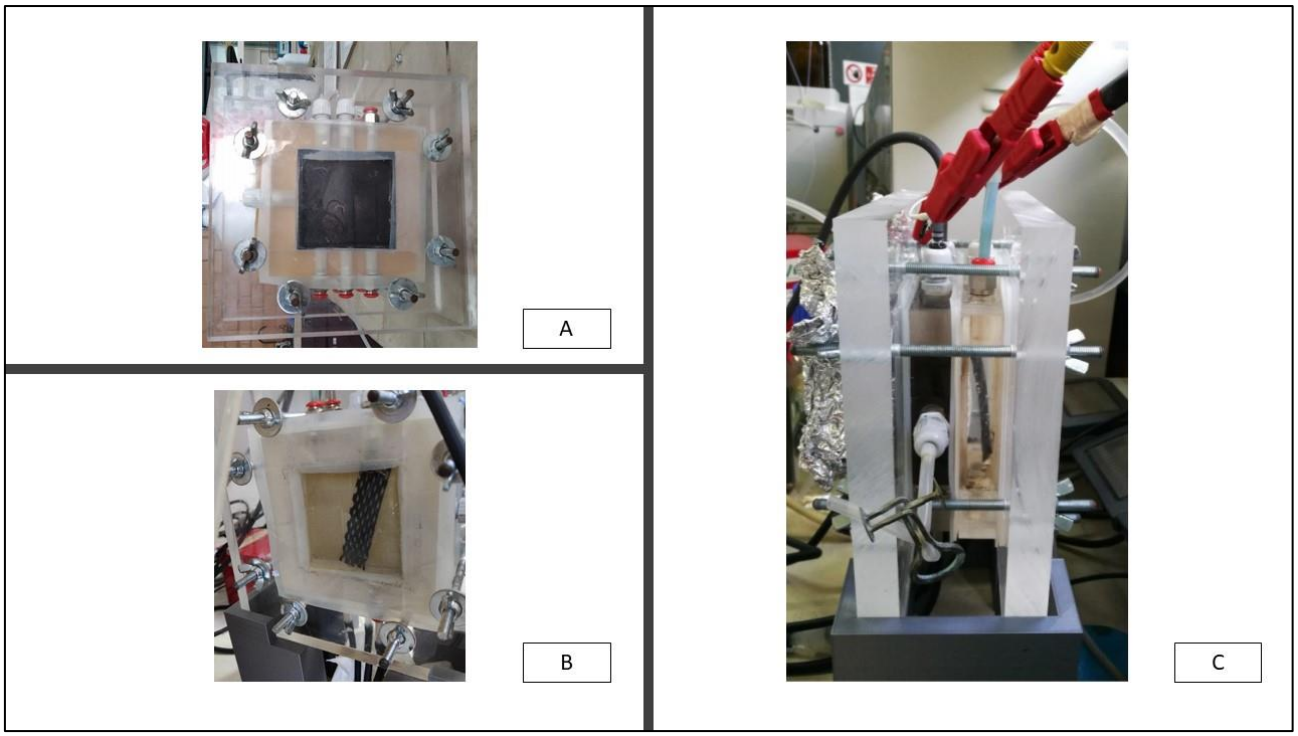

Figure AI-1. Cathode compartment (A), anode compartment (B) and side view (C) of the bioelectrochemical cell.

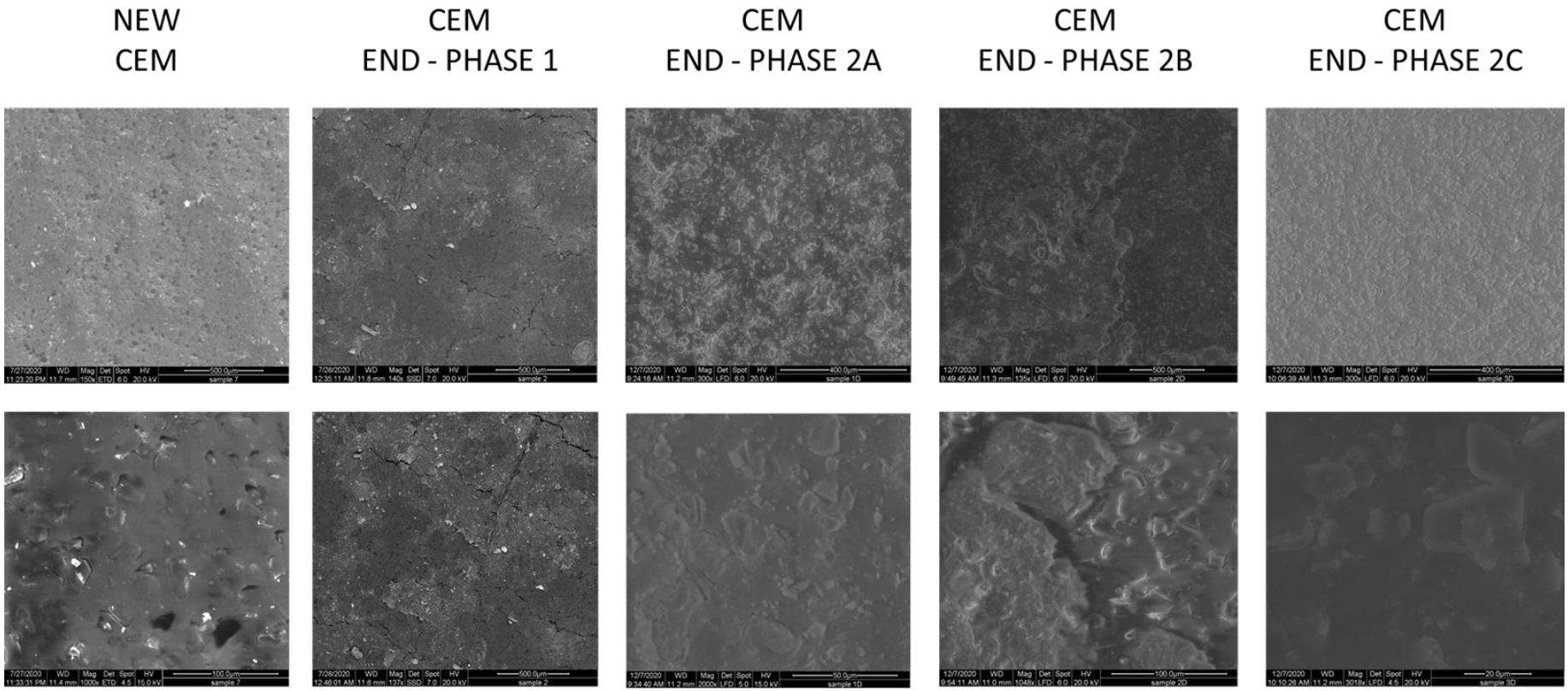

Figure AI-2. Comparison of SEM images of a new membrane (CEM) with the membrane at the end of each experimental phase.

3 START-UP OF A BIOELECTRO-CHEMICAL SYSTEM FOR THE REMEDIATION OF NITRATE CONTAMINATED SALINE GROUNDWATER[1]

Abstract

Sustainable exploitation of coastal aquifers is often hindered by the presence of contaminants and high salinity levels. This study proves the feasibility of electro-bioremediation of nitrate contaminated saline groundwater using a proof-of-concept bioelectrochemical system (BES) configuration. Two 3-compartment BES were started-up and batch-operated in potentiostatic mode for the treatment of a synthetic medium mimicking saline groundwater from the Nitrate Vulnerable Zone of Arborea (Sardinia, Italy), which is characterised by high nitrate concentrations (>25 $mgNO_3^-$-N L^{-1}) and electrical conductivity (>2.5 mS cm^{-1}). The electrochemically active microbial community grew attached to the bio-cathode's surface and achieved nitrate removal rates and efficiencies of 114±12 $mgNO_3^-$-N $m^{-2}d^{-1}$ (corresponding to 6.8±0.4 $mgNO_3^-$-N $L^{-1}d^{-1}$) and 87±2%, respectively. Groundwater electrical conductivity significantly decreased from 4.11±0.2 to 0.17±0.2 mS cm^{-1} due to the migration of ions from the central compartment to the peripheral anodic and bio-cathodic compartments. Under the applied conditions, WHO (World Health Organization) drinking water threshold limits for nitrate (11.3 $mgNO_3^-$-N L^{-1}) and electrical conductivity (2.5 mS cm^{-1}) were satisfied. Moreover, high chloride migration was observed (66±9 mg $L^{-1}d^{-1}$), suggesting its possible recovery as chlorine in the anodic compartment using a specific electrode (Ti-MMO). These results pave the way for setting up the optimal process in the perspective of achieving the simultaneous bioelectrochemically driven remediation of saline groundwater and the sustainable production of value-added chemicals (i.e., chlorine) within a circular economy-based approach.

[1] Part of the work included in this chapter was presented at the conference: 17th International Conference on Environmental Science and Technology (CEST2021), 1-4/07/2021, Athens (Greece), hybrid event.

3.1 Introduction

The World Health Organization (WHO) has predicted that half of the world's population will live in water-stressed areas by 2025 (WHO, 2019). Groundwater represents an essential resource for human life, crucial for drinking water and agriculture irrigation. It has been esteemed that 43% of the water used for irrigation has an underground origin. In this regard, it becomes a priority to preserve groundwater quality and adapt it to human consumption and use. In those areas where natural conditions and human activities have caused aquifers degradation (EEA, 2016), sustainable treatments that can lead to water reclamation must be implemented.

In many countries worldwide, groundwater quality is threatened by the simultaneous presence of high nitrate and salinity levels. This problem mainly affects coastal areas in the Mediterranean basin, East Africa, and China (Troudi et al., 2020; Alfarrah and Walraevens, 2018; Gounari et al., 2014; Hu et al., 2005). Due to activities related to agriculture, such as the spread of inorganic fertilisers and animal manure on crops, nitrate has become one of the most widespread pollutants in groundwater (Menció et al., 2016). Since nitrate consumption can cause serious health risks (Carrey et al., 2021; Ward et al., 2018; Coss, 2004), the WHO has set stringent limits for nitrate concentrations in drinking water (11.3 mgNO_3^--N L^{-1}). Groundwater salinity is also a concern as it limits the potential use of water for drinking purposes. The consumption of saline water has been associated with high blood pressure (Naser et al., 2017). The WHO has also set thresholds for electrical conductivity in drinking water (2.5 mS cm^{-1}). The salinity of groundwater depends on various factors associated with the aquifer's geology and anthropogenic impacts and is therefore highly variable. Aquifer salinisation is often related to the phenomenon of seawater intrusion into the subsoil. This phenomenon is due to the over-exploitation of groundwater in coastal areas, which leads to a significant drop in groundwater levels, causing an alteration of the hydrodynamic balance between seawater and freshwater (Liu et al., 2020). The removal of nitrate and salinity from groundwater is commonly carried out through conventional technologies using separation processes such as reverse osmosis, nanofiltration, ion exchange, and electrodialysis (Della Rocca et al., 2007). These technologies have the advantage of being very effective in achieving high removal rates in a short time. However, they also have some criticalities such as (i) the high costs for energy

and chemical consumption, (ii) the production of waste/brine difficult to dispose of, (iii) the need for regular regeneration of materials (ion exchange), (iv) and the loss of efficiency due to fouling and material deposition (electrodialysis, nanofiltration, reverse osmosis) (Aliaskari and Schäfer, 2021; Epsztein et al., 2015; Koter et al., 2015; Twomey et al., 2010; Bamforth and Singleton, 2005). It is also important to note that separation-based processes remove all ions present in the water indifferently, so they cannot selectively remove nitrates (Rezvani et al., 2019).

Bioelectrochemical systems (BES) are among the most innovative and promising technologies to remove nitrate from groundwater (Ceballos-Escalera et al., 2021; Pous et al., 2017). Their development towards full-scale application can potentially overtake traditional treatments disadvantages. To date, few studies have focused on removing nitrate from groundwater in combination with other contaminants by BES. In many cases, the aim was to identify potential competing electron donors/acceptors or inhibitory effects (Lai et al., 2015; Nguyen et al., 2016). Ceballos-Escalera et al. (2021) successfully proved the feasibility of the simultaneous bioelectrochemical removal of nitrate and arsenic from groundwater, based on the combination of nitrate reduction to dinitrogen gas and arsenite oxidation to less toxic arsenate. Concerning the simultaneous removal of nitrate and salinity from groundwater using BES, Zhang and Angelidaki (2013) tested a submerged 2-compartment desalination-denitrification cell for treating synthetic nitrate contaminated saline groundwater. In the anodic compartment, simulated municipal wastewater was fed for the oxidation of organic matter by the anodic biofilm, which allowed the transfer of electrons, and thus the passage of electric current through the external circuit.

Within this framework, our study assesses the feasibility of a proof-of-concept based on a three- compartments BES configuration specifically designed for the simultaneous removal of nitrates and salinity from a synthetic medium mimicking saline groundwater from the Nitrate Vulnerable Zone (NVZ) of Arborea (Sardinia, Italy). The experiments were carried out in batch-mode to promote electroactive biomass development and assess the fate of nitrate and salinity under the applied operating conditions. The extent of bio-electroactive nitrate removal was investigated, as well as the role played by electromigration on salinity removal. Moreover, the possibility of recovering value-added chemicals (namely chlorine, a disinfecting agent widely used for water disinfection in water treatment plants) from groundwater was also

evaluated within a circular economy-based approach. A comprehensive set of information was gathered in view of further process optimisation, aimed at maximising nitrate and salinity removal, as well as the recovery of free chlorine, thus contributing to the development of a sustainable technology that could successfully tackle an urgent environmental issue.

3.2 Materials and methods

3.2.1 Bioelectrochemical cells set-up

The experimentation was carried out in two bioelectrochemical cells made of transparent Plexiglas and divided into three compartments (Figure 3.1): the bio-cathodic compartment (8x8x2 cm^3), the anodic compartment (8x8x2 cm^3), and the central "desalination" compartment (8x8x0.5 cm^3). The thickness of the central compartment was four times smaller than that of the side compartments (Figure 3.2).

A Cation Exchange Membrane (CEM, 64 cm^2, CMI-7000, Membrane International Inc., USA) and an Anion Exchange Membrane (AEM, 64 cm^2, AMI-7001, Membranes International Inc., USA) were used to separate the central compartment from the bio-cathodic and anodic ones, respectively.

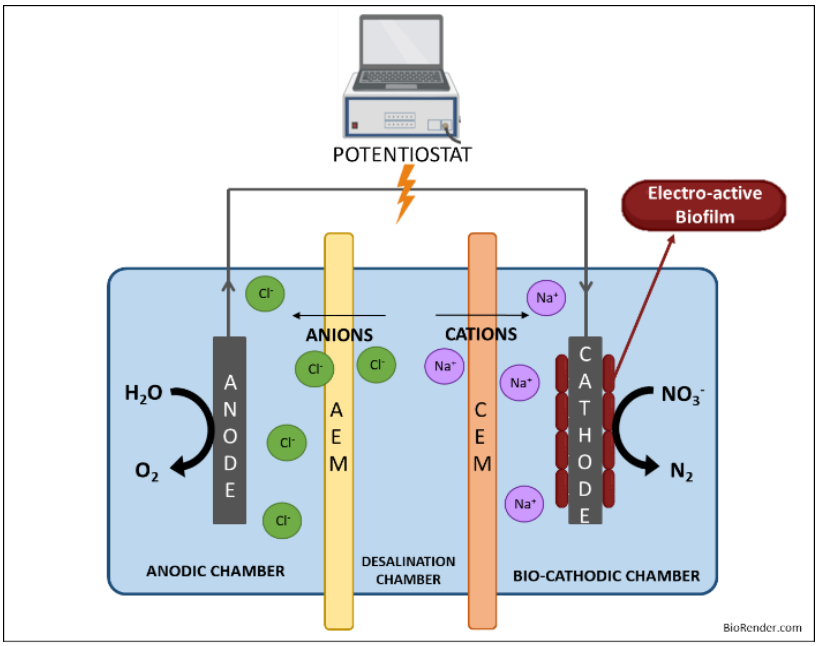

Figure 3.1. Schematic diagram of the bioelectrochemical cell.

Figure 3.2. Photo of the bioelectrochemical cell, from left to right: anodic, central and cathodic compartments.

Carbone felt (64 cm^2, degree of purity 99.9%, AlfaAesar, USA) was used as cathode and connected to a stainless-steel mesh, which worked as the current collector. A reference electrode (Ag/AgCl, mod. MF2052, BioAnalytical Systems, USA) was placed in the same compartment.

Titanium mesh coated with mixed metals oxide (Ti-MMO) was used as anode (NMT-Electrodes, South Africa) and connected to a titanium wire (thickness 0.75 mm, degree of purity 99.98%, AlfaAesar, USA), which worked as the current collector. Cathode, anode, and reference electrodes were connected to a multichannel potentiostat (Ivium-N-stat, Ivium technologies, NL). Experiments were carried out in a thermostated room (25±2 °C). A potential of -0.500 V vs Ag/AgCl (-0.303 V vs SHE) was poised at the bio-cathode using a multichannel potentiostat (Ivium-N-stat, Ivium technologies, NL), in agreement with previous studies (Pous et al., 2015). The resulting currents were recorded every five minutes.

The schematic process flow diagram and a photo of the experimental set-up are shown in Figures 3.3 and 3.4, respectively.

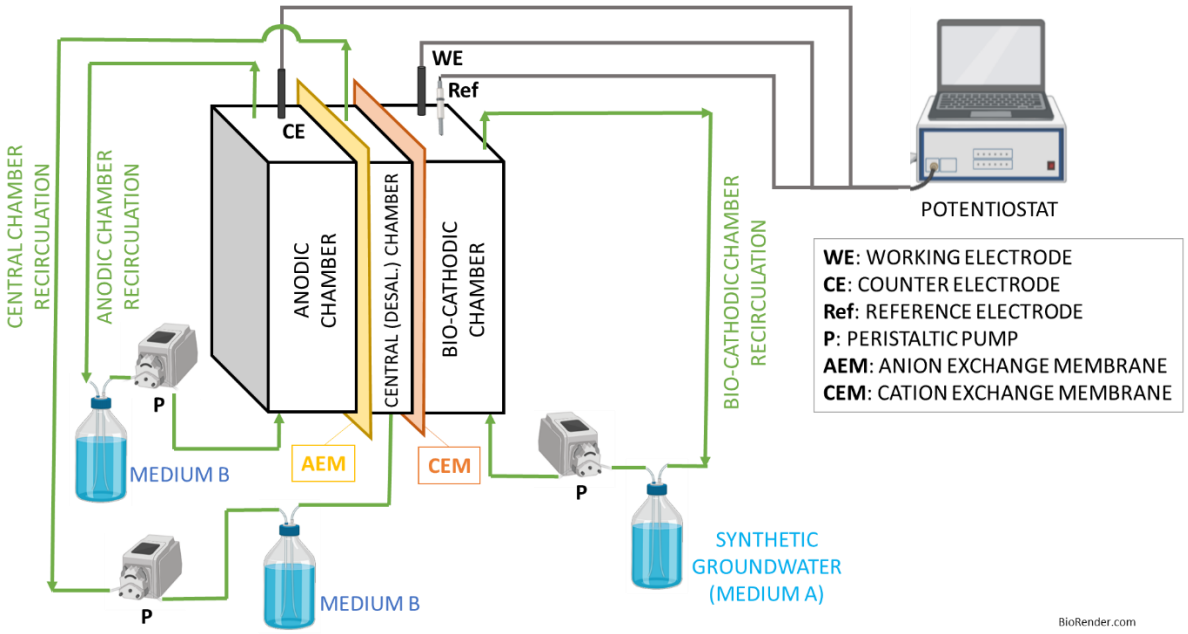

Figure 3.3. Schematic process flow diagram.

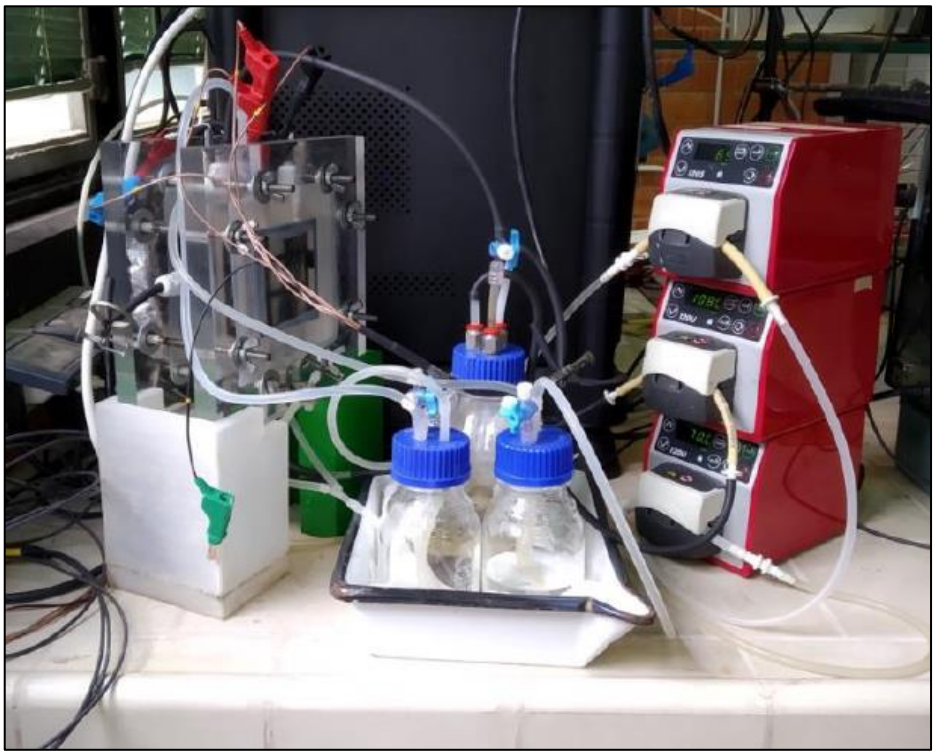

Figure 3.4. Bioelectrochemical cell set-up.

3.2.2 Inoculum and media characteristics

The bio-cathodic compartment was inoculated with a mixture (< 100 mgTSS L^{-1}) of electroactive biomass coming from a parent denitrifying BES (LEQUiA, University of Girona, Spain) and

supernatant of activated sludge liquor drawn from the municipal wastewater treatment plant of Cagliari (Italy).

The bio-cathodic compartment was fed with medium A and inoculum (50:50 ratio, v:v). Medium A contained 216.6 mg L^{-1} KNO_3 (corresponding to 30.0 mgNO_3^--N L^{-1}), 10.0 mg L^{-1} NH_4Cl (corresponding to 2.6 mgNH_4^+-N L^{-1}), 4.6 mg L^{-1} KH_2PO_4, 11.5 mg L^{-1} K_2HPO_4, 350.0 mg L^{-1} $NaHCO_3$, 2000 mg L^{-1} NaCl, and 100 µL L^{-1} of a trace element solution (Patil et al., 2010). The anodic compartment and the central desalination compartment were filled with medium B, which had the same characteristics as medium A to avoid electrical conductivity and pH gradients between the compartments, but without KNO_3 and NH_4Cl. The resulting pH and electrical conductivity of both media were 7.5±0.6 and 4.1±0.5 mS cm^{-1}, respectively. Both media were prepared using grade I water, and medium A was pre-flushed with N_2 gas for 15-20 minutes to avoid any presence of oxygen.

3.2.3 Experimental procedure

The medium in the bio-cathodic compartment was periodically supplied with nitrate by dosing a proper amount of KNO_3 solution when nitrate concentration dropped below 5 mgNO_3^--N L^{-1}, to bring it up to 30 mgNO_3^--N L^{-1} (each NO_3^--N supply corresponded to a new batch cycle in the bio-cathodic compartment).

The media in the anodic and central compartments were replaced once during the experiment (corresponding to a new batch cycle in each compartment).

The experimental procedure followed in this study is summarised in Table 3.1.

Table 3.1. Number and duration of batch cycles in each compartment of the system.

Cell compartment	**Batch cycles**	**Duration of each cycle** days (min-max)
Bio-cathodic	5	6-13
Central	2	24-30
Anodic	2	24-30

3.2.4 Control test

Abiotic tests in OCV (open circuit voltage) were performed to evaluate the contribution of diffusion on the overall migration of ions across ion-selective membranes.

The abiotic tests were carried out in a cell identical to those used for the main experiments. A solution containing 2 g L^{-1} NaCl, 216.6 mg L^{-1} KNO_3, and 10.0 mg L^{-1} NH_4Cl was recirculated in the central compartment, while a solution containing 4.88 g L^{-1} KH_2PO_4 and 0.8 g L^{-1} K_2SO_4 was recirculated in the anodic and cathodic compartments. The two solutions were prepared to avoid electrical conductivity gradients between the different compartments, and the resulting electrical conductivity was 4.3±0.05 mS cm^{-1}. The contribution of diffusion was determined by monitoring the concentration of the main anions and cations in each cell compartment for 24 hours. The ions concentrations measured were used to calculate diffusion coefficients.

3.2.5 Analytical methods

Samples from the cathodic, anodic, and central compartments were taken and analysed three times per week. Liquid samples were analysed for anions quantification, namely chloride (Cl^-), nitrite (NO_2^--N), nitrate (NO_3^--N), phosphate (PO_4^{3-}), and sulphate (SO_4^{2-}), using an ion chromatograph (ICS-90, Dionex-Thermofisher, USA) equipped with an AS14A Ion-PAC 5 µm column. Samples were filtered (acetate membrane filter, 0.45 µm porosity) and properly diluted using grade II water. The concentrations of the principal cations, i.e., sodium (Na^+) and potassium (K^+), were determined using an ICP/OES (Optima 7000, PerkinElmer, USA): samples were filtered (acetate membrane filter, 0.45 µm porosity), acidified with 1% (v/v) of nitric acid and diluted using grade I water. pH and electrical conductivity were measured using a benchtop meter (HI5522, Hanna Instruments, Italy).

SEM images of ion-selective membranes were captured using an FEI Quanta 200 SEM microscope. The membranes did not undergo any preparation, and they were fixed on the stub using a double-sided graphite adhesive. The analyses were performed in low vacuum mode (i.e., residual pressure in the experimental chamber in the range of 0.3-0.9 Torr) to minimise electrostatic charge effects or high vacuum (pressure below 10^{-4} Torr). Images were collected in either secondary electrons or backscattered electrons.

X-ray spectra were obtained using an energy-dispersive X-ray spectrometer (EDS) with multi-stage peltier-cooled silicon drift type detector (ThermoFisher Scientific UltraDry series) and analysed with a standardless semi-quantitative technique using ThermoFisher Pathfinder software, which employs a Phi-Rho-Z type algorithm.

3.2.6 Calculations

Nitrate Removal Efficiency (N-RE) and Nitrate Removal Rate (N-RR) were calculated according to equations 1 and 2, respectively:

$$\mathrm{N-RE\ [\%]} = \frac{C_{NO_3^- - N(t_0)} - C_{NO_3^- - N(t_X)}}{C_{NO_3^- - N(t_0)}} \times 100 \quad \textbf{(1)}$$

$$\mathrm{N-RR\ [mg\ N\ L^{-1}\ d^{-1}]} = \frac{C_{NO_3^- - N(t_0)} - C_{NO_3^- - N(t_X)}}{t_X} \quad \textbf{(2)}$$

Where $C_{NO_3^-N(t_0)}$ and $C_{NO_3^-N(t_x)}$ [mg L^{-1}] are nitrate concentrations in the bio-cathodic compartment at the beginning of the batch cycle (t_0, [d]) and a generic time of the batch (t_x, [d]), respectively.

The nitrate removal rate was also calculated as a function of the free electrode area available for biomass growth, as shown in equation 3:

$$\mathrm{N-RR\ [mg\ N\ m^{-2}\ d^{-1}]} = \frac{C_{NO_3^- - N(t_0)} - C_{NO_3^- - N(t_X)}}{t_X\ A_m}\ V_{NCC} \quad \textbf{(3)}$$

Where A_m [m^2] is the free electrode area available for biomass growth, and V_{NCC} [L] is the net volume of the bio-cathodic compartment.

The quality ratio (QR) for safe drinking water in terms of nitrate and nitrite was calculated according to equation 4, as Pous et al. (2015) reported:

$$QR\ [-] = \frac{C_{NO_3^- - N}}{11.29} + \frac{C_{NO_2^- - N}}{0.91} \leq 1 \quad \textbf{(4)}$$

where $C_{NO_3^-N}$ and $C_{NO_2^-N}$ [mg L^{-1}] are the nitrate and nitrite concentrations, respectively, while 11.29 and 0.91 [mg L^{-1}] are their respective guideline values for drinking water.

The desalination performance was evaluated by calculating the electrical conductivity removal efficiency (EC-RE, equation 5), the chloride removal efficiency (Cl^--RE, equation 6), and the chloride removal rate (Cl^--RR, equation 7).

$$\mathrm{EC-RE\ [\%]} = \frac{\mathrm{EC_{(t_0)} - EC_{(t_x)}}}{\mathrm{EC_{(t_0)}}} \times 100 \quad \textbf{(5)}$$

$$\mathrm{Cl^- - RE\ [\%]} = \frac{\mathrm{C_{Cl^-(t_0)} - C_{Cl^-(t_x)}}}{\mathrm{C_{Cl^-(t_0)}}} \times 100 \quad \textbf{(6)}$$

$$\mathrm{Cl^- - RR\ [mg\ L^{-1}\ d^{-1}]} = \frac{\mathrm{C_{Cl^-(t_0)} - C_{Cl^-(t_x)}}}{\mathrm{t_x}} \quad \textbf{(7)}$$

where $EC_{(t_0)}$ [mS cm^{-1}] and $C_{Cl\text{-}(t_0)}$ [mg L^{-1}] represent the electrical conductivity and chloride concentration in the central compartment at the beginning of the batch cycle (t_0), respectively. $EC_{(t_x)}$ [mS cm^{-1}] and $C_{Cl\text{-}(t_x)}$ [mg L^{-1}] represent the electrical conductivity and chloride concentration at a generic moment (t_x, [d]) of the batch cycle, respectively.

The coulombic efficiency for nitrate reduction (εNO_x) was calculated according to equation 8 (Virdis et al., 2008):

$$\mathrm{\varepsilon NO_x[\%]} = \frac{\mathrm{I}}{\mathrm{n\,\Delta C_{NO_x} Q_{in} F}} \times 100 \quad \textbf{(8)}$$

where I is the recorded current [A], n is the number of electrons that can be accepted by 1 mol of oxidised nitrogen compound present in the bio-cathode compartment assuming N_2 is the final product; ΔC_{NOx} is the difference between the nitrate concentration in the bio-cathode influent and effluent [molNO_3^--N L^{-1}]; Q_{in} is the influent flowrate [L s^{-1}], and F is Faraday's constant [96485 C mol^{-1}].

3.3 Results and discussion

3.3.1 Denitrification and desalination performances

The overall performances of the bioelectrochemical cells were evaluated by considering the denitrification in the bio-cathodic compartment and electrical conductivity reduction in the central compartment. Both systems were operated for 54 days treating synthetic groundwater containing nitrate in the bio-cathodic compartment and a saline solution in the central desalination compartment. Figure 3.5 compares the average nitrate concentrations in the bio-cathodic compartment and the electrical conductivity in the central compartment at the beginning and the end of batch cycles.

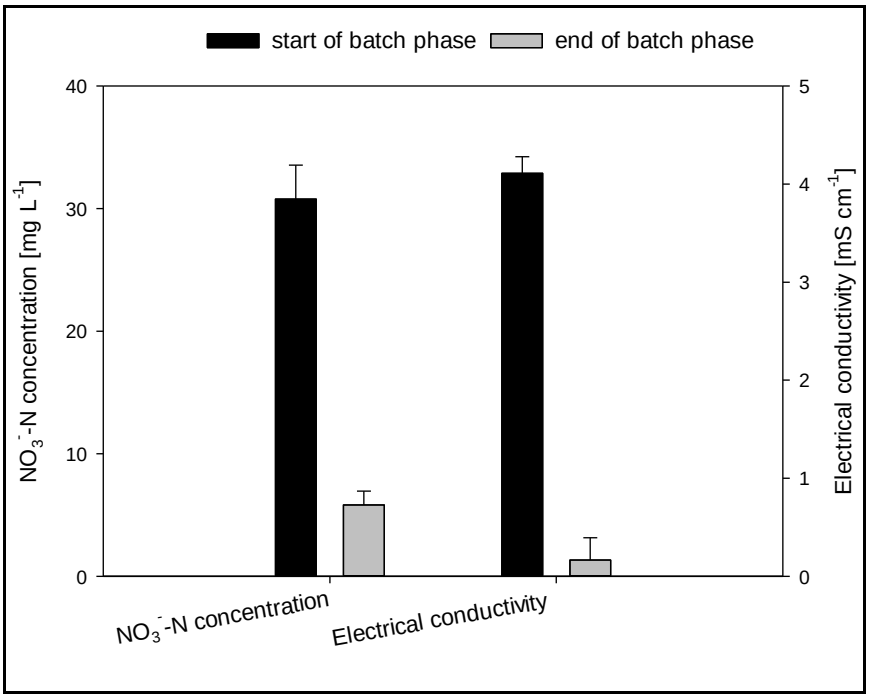

Figure 3.5. Average nitrate concentrations in the bio-cathodic compartment and electrical conductivity in the central compartment at the beginning and at the end of batch cycles.

Nitrate concentration in the bio-cathodic compartment and electrical conductivity in the central one significantly dropped between the beginning and the end of each batch cycle, from 30.8±2.8 to 5.8±1.1 mgNO_3^--N L^{-1} (nitrate removal efficiency of 87±2 %) and from 4.1±0.2 to 0.17±0.2 mS cm^{-1} (desalination efficiency of 57±12 %), respectively. These results showed that simultaneous bioelectrochemical removal of nitrate and salinity reduction could be achieved with such cell configuration.

The width of the central compartment (0.5 cm) minimised the distance between membranes, thereby reducing the internal resistance of the system and consequently promoting the migration of ions, i.e., the desalination process. Previous tests carried out using a configuration with a central compartment width equal to the side compartments (i.e., 2 cm) confirmed this observation.

Regarding nitrate, drinking water threshold limits in the bio-cathodic compartment were met after only four days in each batch cycle, corresponding to a nitrate removal rate and efficiency of 114±12 mgNO_3^--N $m^{-2}d^{-1}$ (about 7 mg L^{-1} d^{-1}) and 90%, respectively. No nitrite was observed throughout the whole experiment. These results allowed to meet the QR for safe drinking

water in terms of nitrate and nitrite, calculated according to Pous et al. (2015). To comply with the NO_3^- and NO_2^- legislation, drinking water must have a QR value ≤1.

The rates obtained were lower than those reported in previous studies concerning nitrate removal using BES (Ceballos-Escalera et al., 2021; Liu et al., 2019; Pous et al., 2015; Zhang and Angelidaki, 2013) and can probably be attributed to many causes. First of all, in the present study, we describe the system's start-up, when the biomass was still in a growth and acclimation phase and not yet at its full potential. Moreover, in the studies mentioned above, BES were mostly operated in continuous mode, which positively affects performance as the constant substrate supply may increase denitrifying activity, in contrast to batch operation. Finally, the system's configuration in our study may undergo oxygen intrusion during the start-up, slowing down the denitrification process. With this regard, values of coulombic efficiency related to nitrate removal higher than 100% were observed in our study and related to oxygen intrusion. Oxygen represents a preferential electron acceptor for the electroactive biofilm compared to nitrate, resulting in a higher current in the system and, consequently, in values of coulombic efficiency higher than 100%. Virdis et al. (2010) stated that the current produced by nitrate reduction was lower than that produced by oxygen reduction, as confirmed by polarisation curves.

The electrical conductivity in the central compartment dropped below the threshold limit of 2.5 mS cm^{-1} after 13 days in each cycle, corresponding to a desalination efficiency of about 60%. At the end of each batch cycle, the electrical conductivity in the central compartment was below 0.2 mS cm^{-1}, as confirmed by the significant reduction not only in chloride concentration (i.e., the removal efficiency was about 95%) but also in the concentration of cationic species, particularly Na^+ and K^+ (i.e., removal efficiencies of up to 95% and 70%, respectively). Figure 3.6 shows the trend of a representative batch cycle for electrical conductivity and chloride concentration in the central compartment.

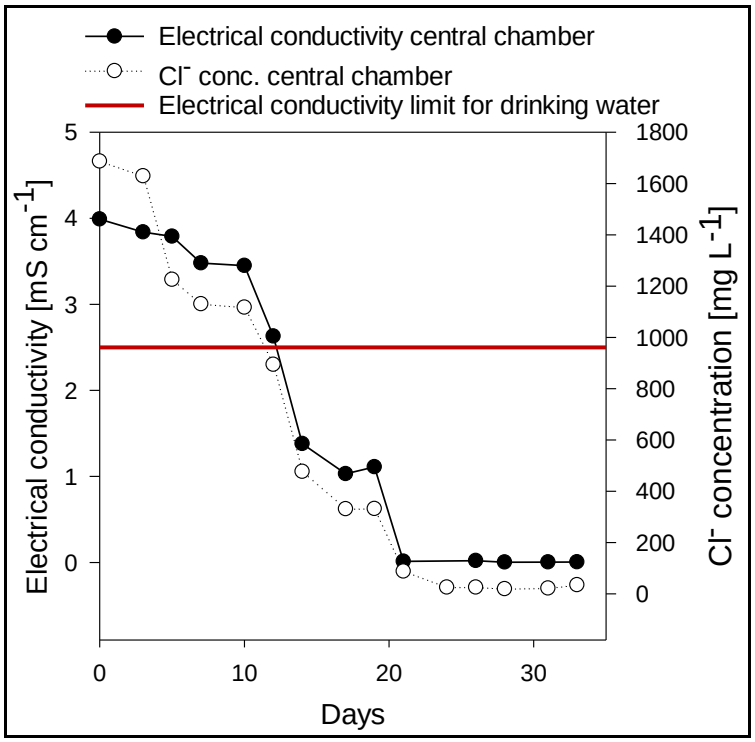

Figure 3.6. Trends of a representative batch cycle for electrical conductivity and chloride concentration in the central compartment.

Therefore, the performance achieved was comparable with the conventional technologies used for groundwater desalination, typically electrodialysis and reverse osmosis (Pirsaheb et al., 2016). If BES are considered, to the authors' knowledge, the simultaneous nitrate and salinity removal from groundwater was studied only by Zhang and Angelidaki (2013), using a submerged microbial desalination denitrification cell, achieving removal efficiencies of 94% and thus comparable to those of the present study. However, the system was significantly different and required the addition of organic matter to the anode, which is not typically present in groundwater.

Despite the observed decrease in salinity, the current density achieved during experimentation (about 0.1 A m^{-2}) was low compared to that observed in previous studies operating with systems designed explicitly for desalination, such as microbial desalination cells (MDC). Kim and Logan (2013) reported current densities for MDC ranging from 0.7 to 8.4 A m^{-2}, varying mainly according to the specific configuration, type of cathode reaction, and external resistance applied. However, systems like MDCs operate in a very different way to that proposed in this study and require the addition of organic matter to the anode compartment, so the comparison with such systems is not properly fair.

A summary of the main results achieved in our study is shown in Table 3.2.

Table 3.2. Best nitrate and salinity removal performance observed during experimentation.

Parameter	Results achieved	Days of experimentation
Bio-cathodic nitrate removal efficiency	87±2 [%]	4
Bio-cathodic nitrate removal rate	114±12 [mgNO_3^--N $m^{-2}d^{-1}$] (6.8±0.4 [mg $L^{-1}d^{-1}$])	4
Desalination efficiency of the central compartment	57±12 [%]	13
Chloride removal rate from central compartment	66±9 [mg $L^{-1}d^{-1}$]	13

Electricity-driven migration of ions across membranes was observed, resulting in the accumulation of anionic species in the anodic solution and cationic species in the cathodic solution. The accumulation of chlorides in the anodic compartment was significant, reaching end-of-batch concentrations of 2.7±0.9 gCl L^{-1} (starting from 1.5±0.3 gCl L^{-1}), with a consequent increase in electrical conductivity from 4.3±0.2 to 7.3±2.8 mS cm^{-1}). This result suggests the possibility of converting the accumulated chloride into a valuable form, such as free chlorine (Cl_2), a strong disinfectant widely used in water treatment. The potential to recover chlorine suggested by the accumulation of chlorides at the anode compartment also depends on the type of electrode used. In this study, an electrode of titanium coated with mixed metals oxide (Ti-MMO) was used because, as pointed out by Batlle-Vilanova (2019), the Ti-MMO anode electrodes promote chlorine production, thanks to the metals in the coating acting as catalysts. Anodes of this type, which consist of a Ti base metal plate as conductive substrate and one or more metal oxide coatings as active electrocatalyst, are traditionally used in the chlor-alkali industry for chlorine evolution reactions (Dong et al., 2021).

The state of the membranes was also assessed by SEM analysis. Figure 3.7 shows CEM and AEM conditions before being used and at the end of the experiment (day 54).

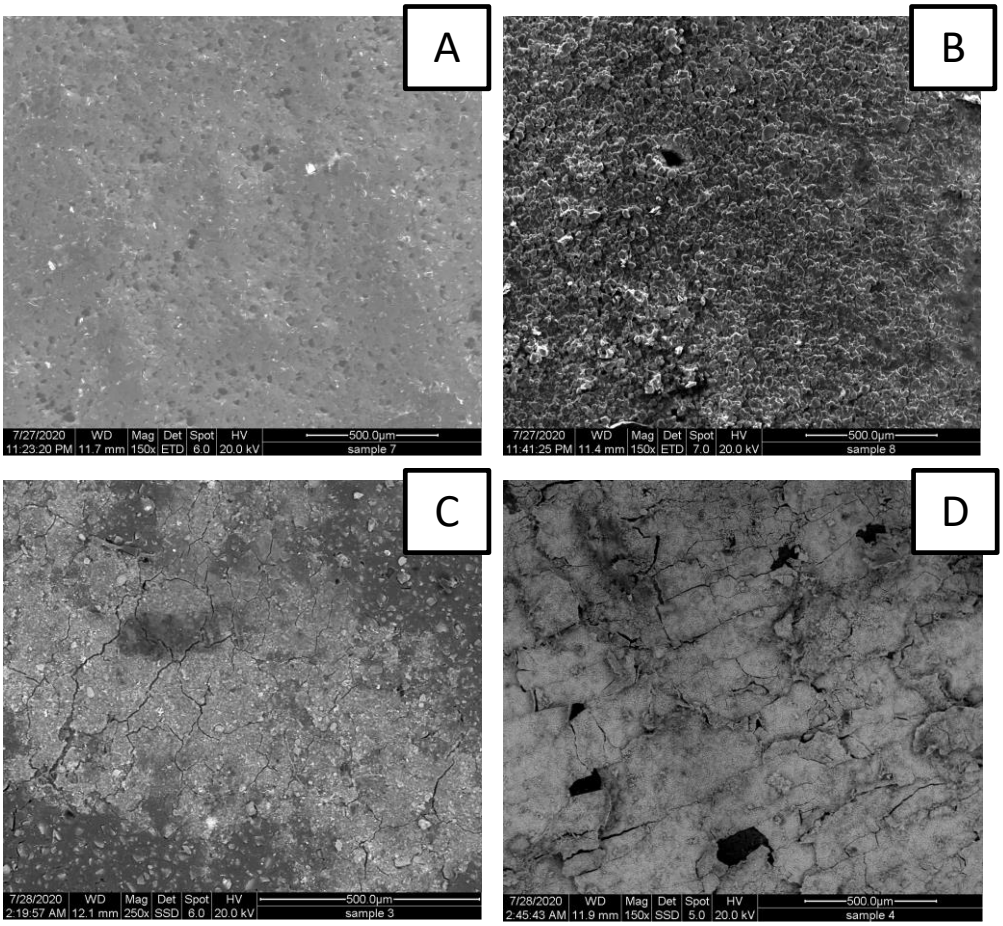

Figure 3.7. SEM images of the cation and anion exchange membranes before use (A and B, respectively) and at the end of the experiment (C and D, respectively).

In particular, concretion formation was observed on the surface of both the cation exchange and anion exchange membranes. The concretions formation and, in general, the solids deposition (clogging) on the membrane surfaces could lead to a loss of the exchange efficiency of the membranes over time, so the need to clean or replace the membranes should be assessed.

X-ray spectra revealed the presence of elements on the surfaces of used membranes that were generally not present on new membranes. The main elements detected on the surface of the new membranes were C (carbon), O (oxygen), F (fluorine), Al (aluminium), Na (sodium), and S (sulphur). On the surface of the used membrane, however, the following elements were also detected: Mg (magnesium), Si (silicon), P (phosphorus), Cl (chlorine), K (potassium), Ca (calcium), Fe (iron), Zn (zinc), Cu (copper), Mo (molybdenum), Ti (titanium) almost all of which can be traced back to the solutions treated and materials used in the systems. This result indicated that the various phenomena involved in the process could influence the durability of the membranes, leading to the accumulation of substances that may reduce the lifetime of

the membranes. Given the presence of titanium observed on the membrane surface, the lifetime of the electrodes may also be reduced.

With a view to overall performance optimisation, switching to continuous mode operation in the bio-cathode and central compartments appears particularly convenient. The continuous supply of nitrate for the electroactive biofilm could promote denitrifying activity, as confirmed by Pous et al. (2017), in which the reduction of hydraulic retention time (i.e., the increase of influent flow) led to an improvement in denitrification performance. Increasing the nitrate removal kinetics at the bio-cathode could increase current density and thus further enhance the electromigration of ionic species through the membranes, resulting in a faster reduction of electrical conductivity in the central compartment.

3.3.2 pH trend and prospects for upcoming tests

The pH is a parameter of fundamental importance for the proper functioning of the biological systems, and specifically, a neutral pH is optimal for denitrifying activity (Ceballos-Escalera et al., 2022). The pH is also one of the most important water quality parameters: the optimum pH should be in the range of 6.5–9.5 (WHO, 2003).

Figure 3.8 shows the average pH in the different cell compartments at the beginning and the end of batch cycles. During cells operation, pH increased in the bio-cathodic compartment (from 7.4±0.5 to 9.0±0.5), while a decrease occurred in the anodic compartment (from 7.4±0.1 to 2.8±1.1) and, less marked, in the central compartment (from 7.7±0.3 to 4.9±0.5).

The decrease in pH in the anodic compartment is mainly due to the production of H^+ as a result of the electrolysis reaction of the water. In the central compartment, the less pronounced pH decrease may be due to the passage of part of the protons produced in the anodic compartment through the AEM, which is possible due to the small size of the H^+ ions.

Bacteria usually require a pH close to neutral for optimal growth; however, reduction reactions on the cathode electrode result in an alkaline environment, which is a source of overpotentials (Puig et al., 2010).

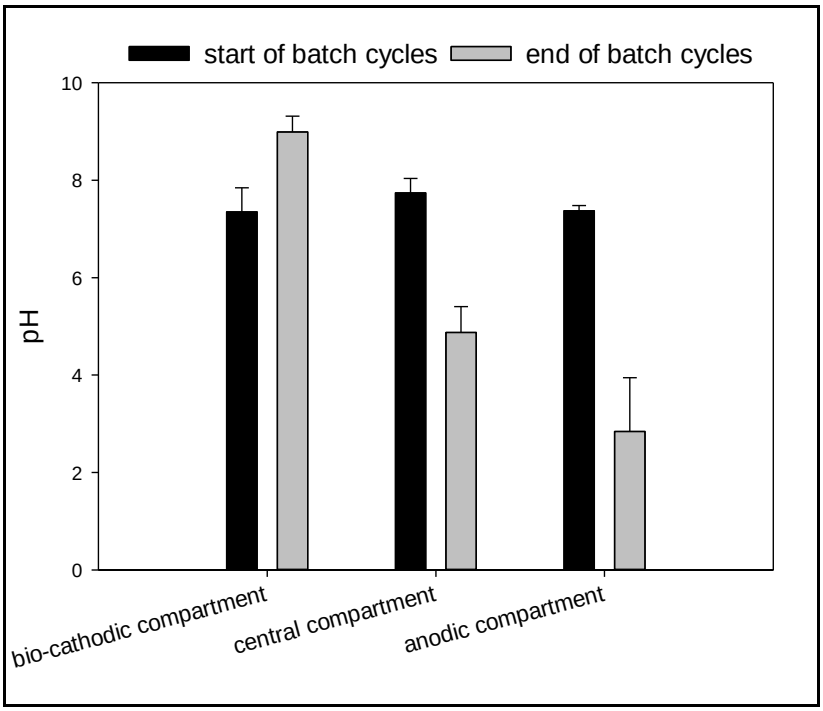

Figure 3.8. Average pH values at the beginning and the end of batch cycles.

Generally, in the 2-compartment bioelectrochemical systems for nitrate removal, the compartments are separated by a cation exchange membrane that allows protons diffusion from the anode to the cathode, which counter-balances pH variations. In our system, the flow of protons to the bio-cathodic compartment was hindered by the distance between the anode and the cathode due to the presence of the central compartment and the membranes. Therefore, since protons were not replenished through the membrane and a pH control system was not implemented, the pH increased undisturbed in the bio-cathodic compartment, as Rozendal et al. (2006) reported. In this sense, continuous feeding to the bio-cathode with "fresh" groundwater may potentially counter-balance pH increase, ensuring optimal values for denitrifying biomass activity.

It will be essential for the next step of the study (continuous mode operation) to monitor pH trends to assess whether a pH control system in the bio-cathodic compartment needs to be implemented.

3.3.3 Evaluation of the diffusive contribution to the movement of ions within the system

Abiotic and open circuit control tests were performed to assess diffusion contribution on the overall movement of ions across the membranes. Figure 3.9 shows the ions concentration trends across the different compartments of the cell during the 24-hour test.

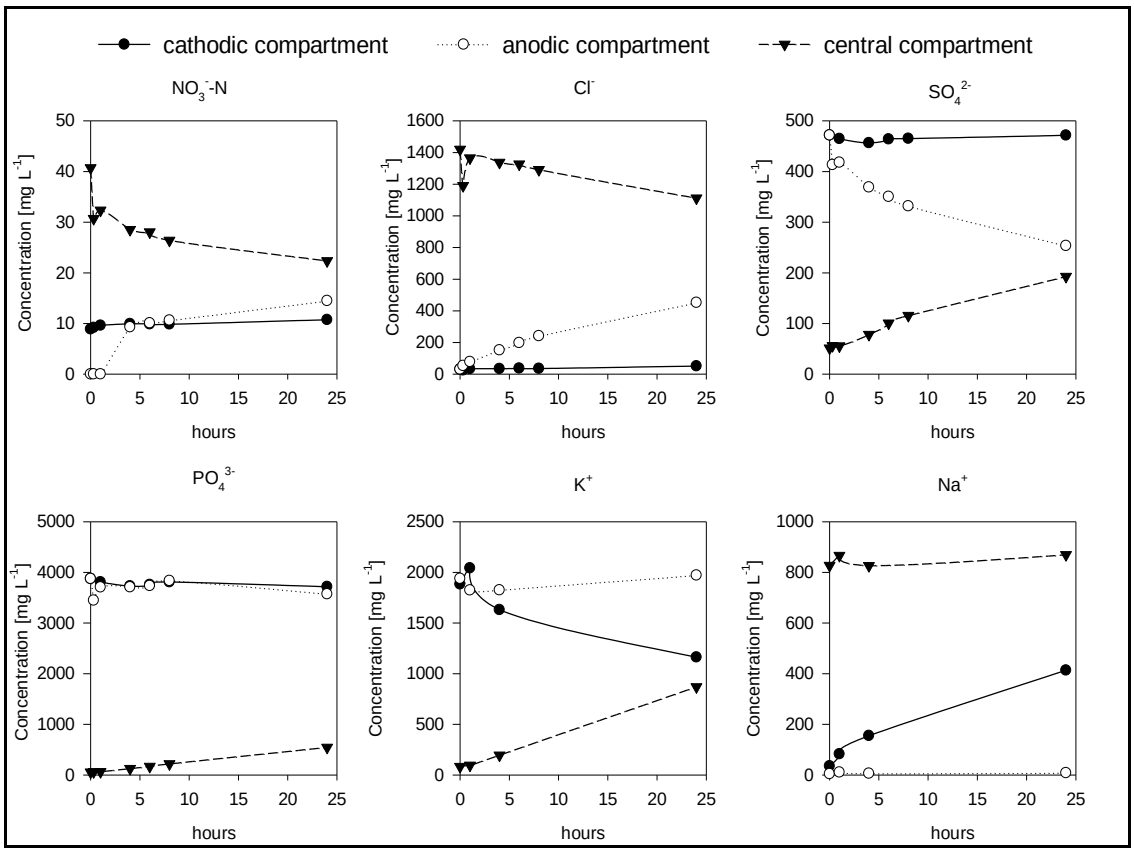

Figure 3.9. Trend of the concentrations of ions in each of the three compartments of the bioelectrochemical cell under abiotic and open circuit conditions.

The results showed a significant diffusion of ions across membranes, mainly nitrate and chloride, from the central to the anodic compartment. Under these conditions, the diffusion process can only be driven by the difference in concentration of the ions in the different solutions contained in the three compartments. A 45% decrease in nitrate concentration was observed in the central compartment, most of which (80%) passed into the anodic compartment, while 10% passed into the cathode compartment. The passage of anions towards the cathode compartment is limited by the presence of the cation exchange membrane, while it is facilitated in the anode compartment by the anion exchange membrane. This result is confirmed by the diffusion coefficient, calculated as reported by Kim et al. (2007). The diffusive coefficient for

nitrate migrating from the central compartment to the anode compartment through the AEM was $1.5 \cdot 10^{-7}$ $cm^2 s^{-1}$, an order of magnitude higher than that calculated for migration through the CEM (equal to $9.2 \cdot 10^{-8}$ $cm^2 s^{-1}$). This difference was even more evident for chloride, with a diffusion coefficient through the AEM two orders of magnitude higher than that calculated for the CEM ($1.2 \cdot 10^{-7}$ and $9.2 \cdot 10^{-9}$ $cm^2 s^{-1}$, respectively), likely due to the higher chloride concentration gradient than nitrate. A decrease of 22% was observed for chloride in the central compartment, most of which (more than 90%) passed into the anodic compartment.

The opposite trend (i.e., from the anodic compartment to the central compartment) was observed for sulphate and phosphate, as expected due to the concentration gradient between the anodic and central compartment solutions. Sulphate in the anodic compartment decreased by 46% and passed completely into the central compartment, while a less significant reduction was observed in phosphate (only 8%), which may be due to the larger size of the molecule and the consequent difficulty in passing through the AEM. The diffusion coefficients, in this case, were equal to $9.0 \cdot 10^{-7}$ $cm^2 s^{-1}$ for sulphate and $1.7 \cdot 10^{-7}$ $cm^2 s^{-1}$ for phosphate. Similar values were also obtained for diffusion through the CEM, corresponding to $8.0 \cdot 10^{-7}$ and $1.5 \cdot 10^{-7}$ $cm^2 s^{-1}$ respectively for sulphate and for phosphate, demonstrating a lower selectivity of the membrane towards these anions.

A predictable pattern was also observed for the cations across the CEM, specifically a sharp decrease in potassium concentration in the bio-cathodic compartment (-38%) with a consequent increase in the central compartment. Similar diffusion coefficient values were obtained for the passage of potassium through the two membranes (equal to approximately $1.2 \cdot 10^{-6}$ $cm^2 s^{-1}$). Sodium moved from the central to the cathode compartment (increasing from 35 to more than 400 mg L^{-1} in the latter), with a diffusion coefficient of $8.0 \cdot 10^{-7}$ $cm^2 s^{-1}$. The diffusion coefficient was equal to $2.4 \cdot 10^{-9}$ $cm^2 s^{-1}$ for the passage through the AEM.

The diffusion effect can therefore contribute to the movement of ions between membranes. In accordance with the above results, an almost constant electrical conductivity was observed in the central compartment, slightly decreasing in the cathode compartment (from 4.32 to 4.21 mS cm^{-1}), while an increase was observed in the anode compartment (from 4.32 to 5.51 mS cm^{-1}).

3.4 Conclusions

A 3-compartment BES was started up and tested for the electro-bioremediation of nitrate-contaminated saline groundwater. The possibility of exploiting the electroactive biofilm grown on the bio-cathode to remove nitrate and, at the same time, achieve electrochemically-driven desalination was successfully assessed, with a nitrate removal rate of 114±12 $mgNO_3^-$-N $m^{-2}d^{-1}$ (corresponding to 6.8±0.4 $mgNO_3^-$-N $L^{-1}d^{-1}$) and chloride removal rate of 66±9 mg $L^{-1}d^{-1}$. One of the keys to the system's effectiveness is its particular configuration, i.e., using a very thin central compartment that allows the ions to pass through the membranes (thus performing the desalination) without excessively increasing the distance between the electrodes and membranes. The WHO threshold limits for drinkable water were satisfied for both nitrate and salinity. Moreover, batch experiments showed that significant chloride accumulation occurred in the anodic compartment, which could be subsequently recovered as chlorine, a valuable disinfectant. The images obtained from SEM analysis of the membranes revealed the presence of scaling on their surface, indicating the possible deterioration of these materials over time. Abiotic tests in OCV showed a significant contribution of diffusion on the migration of ions between the different compartments of the cell. The diffusion coefficients for nitrate and chloride through the AEM ($1.5 \cdot 10^{-7}$ and $1.2 \cdot 10^{-7}$ cm^2s^{-1}, respectively), were significantly higher than those calculated for the passage through the CEM ($9.2 \cdot 10^{-8}$ and $9.2 \cdot 10^{-9}$ cm^2s^{-1}). The opposite trend was observed for sodium, with a diffusion coefficient through the CEM end AEM of $8.0 \cdot 10^{-7}$ and $2.4 \cdot 10^{-9}$ cm^2s^{-1}, respectively. Results are promising and provide helpful information for the feasibility of the process, showing the need to switch to continuous mode operation to overcome the limitation observed with the batch mode.

Acknowledgements

This study was funded by Fondo di Sviluppo e Coesione 2014-2020, Patto per lo sviluppo della Regione Sardegna - Area Tematica 3 - Linea d' Azione 3.1, "Interventi di sostegno alla ricerca". Project SARdNAF "Advanced Systems for the Removal of Nitrates from Groundwater", ID: RASSR53158. The Centre for Research University Services (CeSAR) of the University of Cagliari (Italy) is to be thanked for the SEM analysis. Thanks to Dr Martina Piredda for the support with the ICP-OES analyses.

References

Alfarrah, N., Walraevens, K., 2018. Groundwater Overexploitation and Seawater Intrusion in Coastal Areas of Arid and Semi-Arid Regions. Water 10, 143. https://doi.org/10.3390/w10020143

Aliaskari, M., Schäfer, A.I., 2021. Nitrate, arsenic and fluoride removal by electrodialysis from brackish groundwater. Water Res. 190, 116683. https://doi.org/10.1016/j.watres.2020.116683

Bamforth, S.M., Singleton, I., 2005. Bioremediation of polycyclic aromatic hydrocarbons: current knowledge and future directions. J. Chem. Technol. Biotechnol. 80, 723–736. https://doi.org/10.1002/jctb.1276

Batlle-Vilanova, P., 2019. Biogas upgrading, CO2 valorisation and economic revaluation of bioelectrochemical systems through anodic chlorine production in the framework of wastewater treatment plants. Sci. Total Environ. 9.

Carrey, R., Ballesté, E., Blanch, A.R., Lucena, F., Pons, P., López, J.M., Rull, M., Solà, J., Micola, N., Fraile, J., Garrido, T., Munné, A., Soler, A., Otero, N., 2021. Combining multi-isotopic and molecular source tracking methods to identify nitrate pollution sources in surface and groundwater. Water Res. 188, 116537. https://doi.org/10.1016/j.watres.2020.116537

Ceballos-Escalera, A., Pous, N., Balaguer, M.D., Puig, S., 2022. Electrochemical water softening as pretreatment for nitrate electro bioremediation. Sci. Total Environ. 806, 150433. https://doi.org/10.1016/j.scitotenv.2021.150433

Ceballos-Escalera, A., Pous, N., Chiluiza-Ramos, P., Korth, B., Harnisch, F., Bañeras, L., Balaguer, M.D., Puig, S., 2021. Electro-bioremediation of nitrate and arsenite polluted groundwater. Water Res. 190, 116748. https://doi.org/10.1016/j.watres.2020.116748

Christina, G., Konstantinos, S., Alexandros, G., Dimitrios, K., Aikaterini, K., 2014. Seawater Intrusion and Nitrate Pollution in Coastal Aquifer of Almyros – Nea Anchialos Basin, Central Greece 10, 13.

Coss, A., 2004. Pancreatic Cancer and Drinking Water and Dietary Sources of Nitrate and Nitrite. Am. J. Epidemiol. 159, 693–701. https://doi.org/10.1093/aje/kwh081

Della Rocca, C., Belgiorno, V., Meriç, S., 2007. Overview of in-situ applicable nitrate removal processes. Desalination 204, 46–62. https://doi.org/10.1016/j.desal.2006.04.023

Dong, H., Yu, W., Hoffmann, M.R., 2021. Mixed Metal Oxide Electrodes and the Chlorine Evolution Reaction. J. Phys. Chem. C 125, 20745–20761. https://doi.org/10.1021/acs.jpcc.1c05671

Epsztein, R., Nir, O., Lahav, O., Green, M., 2015. Selective nitrate removal from groundwater using a hybrid nanofiltration–reverse osmosis filtration scheme. Chem. Eng. J. 279, 372–378. https://doi.org/10.1016/j.cej.2015.05.010

Hu, K., Huang, Y., Li, H., Li, B., Chen, D., White, R.E., 2005. Spatial variability of shallow groundwater level, electrical conductivity and nitrate concentration, and risk assessment of nitrate contamination in North China Plain. Environ. Int., Soil Contamination and Environmental Health 31, 896–903. https://doi.org/10.1016/j.envint.2005.05.028

Kim, J.R., Cheng, S., Oh, S.-E., Logan, B.E., 2007. Power Generation Using Different Cation, Anion, and Ultrafiltration Membranes in Microbial Fuel Cells. Environ. Sci. Technol. 41, 1004–1009. https://doi.org/10.1021/es062202m

Kim, Y., Logan, B.E., 2013. Microbial desalination cells for energy production and desalination. Desalination 308, 122–130. https://doi.org/10.1016/j.desal.2012.07.022

Koter, S., Chojnowska, P., Szynkiewicz, K., Koter, I., 2015. Batch electrodialysis of ammonium nitrate and sulfate solutions. J. Membr. Sci. 496, 219–228. https://doi.org/10.1016/j.memsci.2015.08.064

Lai, A., Verdini, R., Aulenta, F., Majone, M., 2015. Influence of nitrate and sulfate reduction in the bioelectrochemically assisted dechlorination of cis-DCE. Chemosphere 125, 147–154. https://doi.org/10.1016/j.chemosphere.2014.12.023

Liu, J., Gao, Z., Wang, Z., Xu, X., Su, Q., Wang, S., Qu, W., Xing, T., 2020. Hydrogeochemical processes and suitability assessment of groundwater in the Jiaodong Peninsula, China. Environ. Monit. Assess. 192, 384. https://doi.org/10.1007/s10661-020-08356-5

Liu, R., Zheng, X., Li, M., Han, L., Liu, X., Zhang, F., Hou, X., 2019. A three chamber bioelectrochemical system appropriate for in-situ remediation of nitrate-contaminated groundwater

and its reaction mechanisms. Water Res. 158, 401–410. https://doi.org/10.1016/j.watres.2019.04.047

Menció, A., Mas-Pla, J., Otero, N., Regàs, O., Boy-Roura, M., Puig, R., Bach, J., Domènech, C., Zamorano, M., Brusi, D., Folch, A., 2016. Nitrate pollution of groundwater; all right..., but nothing else? Sci. Total Environ. 539, 241–251. https://doi.org/10.1016/j.scitotenv.2015.08.151

Naser, A.M., Rahman, M., Unicomb, L., Doza, S., Ahmed, K.M., Uddin, M.N., Selim, S., Gribble, M.O., Anand, S., Clasen, T.F., Luby, S.P., 2017. Drinking water salinity and kidney health in southwest coastal Bangladesh: baseline findings of a community-based stepped-wedge randomised trial. The Lancet, Inaugural Planetary Health/GeoHealth Annual Meeting 389, S15. https://doi.org/10.1016/S0140-6736(17)31127-3

Nguyen, V.K., Park, Y., Yang, H., Yu, J., Lee, T., 2016. Effect of the cathode potential and sulfate ions on nitrate reduction in a microbial electrochemical denitrification system. J. Ind. Microbiol. Biotechnol. 43, 783–793. https://doi.org/10.1007/s10295-016-1762-6

Patil, S., Harnisch, F., Schröder, U., 2010. Toxicity Response of Electroactive Microbial Biofilms-A Decisive Feature for Potential Biosensor and Power Source Applications. ChemPhysChem 11, 2834–2837. https://doi.org/10.1002/cphc.201000218

Pirsaheb, M., Khosravi, T., Sharafi, K., Mouradi, M., 2016. Comparing operational cost and performance evaluation of electrodialysis and reverse osmosis systems in nitrate removal from drinking water in Golshahr, Mashhad. Desalination Water Treat. 57, 5391–5397. https://doi.org/10.1080/19443994.2015.1004592

Pous, N., Puig, S., Balaguer, M.D., Colprim, J., 2017. Effect of hydraulic retention time and substrate availability in denitrifying bioelectrochemical systems. Environ. Sci. Water Res. Technol. 3, 922–929. https://doi.org/10.1039/C7EW00145B

Pous, N., Puig, S., Dolors Balaguer, M., Colprim, J., 2015. Cathode potential and anode electron donor evaluation for a suitable treatment of nitrate-contaminated groundwater in bioelectrochemical systems. Chem. Eng. J. 263, 151–159. https://doi.org/10.1016/j.cej.2014.11.002

Puig, S., Serra, M., Coma, M., Cabré, M., Balaguer, M.D., Colprim, J., 2010. Effect of pH on nutrient dynamics and electricity production using microbial fuel cells. Bioresour. Technol. 101, 9594–9599. https://doi.org/10.1016/j.biortech.2010.07.082

Rozendal, R.A., Hamelers, H.V., Buisman, C.J., 2006. Effects of membrane cation transport on pH and microbial fuel cell performance. Environ. Sci. Technol. 40, 5206–5211.

Troudi, N., Hamzaoui-Azaza, F., Tzoraki, O., Melki, F., Zammouri, M., 2020. Assessment of groundwater quality for drinking purpose with special emphasis on salinity and nitrate contamination in the shallow aquifer of Guenniche (Northern Tunisia). Environ. Monit. Assess. 192, 641. https://doi.org/10.1007/s10661-020-08584-9

Twomey, K.M., Stillwell, A.S., Webber, M.E., 2010. The unintended energy impacts of increased nitrate contamination from biofuels production. J Env. Monit 12, 218–224. https://doi.org/10.1039/B913137J

Virdis, B., Rabaey, K., Rozendal, R.A., Yuan, Z., Keller, J., 2010. Simultaneous nitrification, denitrification and carbon removal in microbial fuel cells. Water Res. 44, 2970–2980. https://doi.org/10.1016/j.watres.2010.02.022

Virdis, B., Rabaey, K., Yuan, Z., Keller, J., 2008. Microbial fuel cells for simultaneous carbon and nitrogen removal. Water Res. 42, 3013–3024. https://doi.org/10.1016/j.watres.2008.03.017

Ward, M., Jones, R., Brender, J., de Kok, T., Weyer, P., Nolan, B., Villanueva, C., van Breda, S., 2018. Drinking Water Nitrate and Human Health: An Updated Review. Int. J. Environ. Res. Public. Health 15, 1557. https://doi.org/10.3390/ijerph15071557

Zhang, Y., Angelidaki, I., 2013. A new method for in situ nitrate removal from groundwater using submerged microbial desalination–denitrification cell (SMDDC). Water Res. 47, 1827–1836. https://doi.org/10.1016/j.watres.2013.01.005

4 COMBINING ELECTRO-BIOREMEDIATION OF NITRATE IN SALINE GROUNDWATER WITH CONCOMITANT CHLORINE PRODUCTION[1]

Abstract

Groundwater pollution and salinization have increased steadily over the years. As the balance between water demand and availability has reached a critical level in many world regions, a sustainable approach for the management (including recovery) of saline water resources has become essential. A 3-compartment cell configuration was tested for a new application based on the simultaneous denitrification and desalination of nitrate-contaminated saline groundwater and the recovery of value-added chemicals (Figure AII-1, Appendix II). The cells were initially operated in potentiostatic mode to promote autotrophic denitrification at the biocathode, and then switched to galvanostatic mode to improve the desalination of groundwater in the central compartment. The average nitrate removal rate achieved was 39±1 $mgNO_3^-$-N L^{-1} d^{-1}, and no intermediates (i.e., nitrite and nitrous oxide) were observed in the effluent. Groundwater salinity was considerably reduced (average chloride removal was 63±5%). Within a circular economy approach, part of the removed chloride was recovered in the anodic compartment and converted into chlorine, which reached a concentration of 26.8±3.4 $mgCl_2$ L^{-1}. The accumulated chlorine represents a value-added product, which could also be dosed for disinfection in water treatment plants. With this cell configuration, WHO and European legislation threshold limits for nitrate (11.3 $mgNO_3^-$-N L^{-1}) and salinity (2.5 mS cm^{-1}) in drinking water were met, with low specific power consumptions (0.13±0.01 kWh $g^{-1}NO_3^-$-$N_{removed}$). These results are promising and pave the ground for successfully developing a sustainable technology to tackle an urgent environmental issue.

[1]This Chapter was published as Puggioni, G., Milia, S., Dessì, E., Unali, V., Pous, N., Balaguer, M.D., Puig, S., Carucci, A., (2021). "Combining electro-bioremediation of nitrate in saline groundwater with concomitant chlorine production". Water Research. 206, 117736.

4.1 Introduction

Groundwater represents one of the primary sources of drinking water in many countries worldwide (Zhang et al., 2017). However, this crucial water resource is threatened by multiple polluting sources, both natural and anthropogenic (Burri et al., 2019), which limit its possible exploitation for human consumption.

Nitrate is one of the most widespread pollutants, and it can accumulate in groundwater mainly due to agricultural-related activities such as the spread of inorganic fertilizers and animal manure on crops (Menció et al., 2016). The consumption of nitrate can cause severe health risks (Carrey et al., 2021; Ward et al., 2018; Coss, 2004). Besides nitrates, groundwater salinity is a matter of concern since it limits the potential use of water for drinking purposes. Saline water consumption has been associated with high blood pressure (Naser et al., 2017). Groundwater salinity is variable and depends on both the aquifer geology and anthropogenic impacts. Over-exploitation of groundwater in coastal areas leads to a significant drop in groundwater levels, causing an alteration of the hydrodynamic balance between seawater and freshwater, with the consequent seawater intrusion and salinization of the aquifer (Liu et al., 2020).

Nitrates and salinity simultaneously affect groundwater quality in many countries, especially in coastal areas of the Mediterranean Basin, East Africa, and China (Troudi et al., 2020; Alfarrah et al., 2018; Gounari et al., 2014; Hu et al., 2005). For this reason, the World Health Organization (WHO) and the European Council (Council Directive 98/83/EC) established strict threshold limits for nitrates (11.3 mg NO_3^--N L^{-1} or 50 mg NO_3^- L^{-1}) and salinity (2.5 mS cm^{-1}) in water for human consumption.

Conventional technologies for groundwater treatment used to remove both nitrate and salinity, such as reverse osmosis, nanofiltration, ion exchange, and electrodialysis, are mainly based on separation processes (Della Rocca et al., 2007). Besides being effective, these technologies are characterized by: i) high costs for energy and chemicals consumptions, ii) the production of wastes/brines that are difficult to be disposed of, iii) the need for regular rejuvenation of materials (ion exchange), and iv) the loss of efficiency due to scaling and fouling (electrodialysis, nanofiltration, reverse osmosis) (Aliaskari et al., 2021; Epsztein et al., 2015;

Koter et al., 2015; Twomey et al., 2010; Bamforth et al., 2005). It must also be considered that separation-based processes remove all the ions present in water, so they cannot selectively remove nitrate (Rezvani et al., 2019).

Among biological treatment processes, autotrophic denitrification represents the key metabolism for remediation of nitrate-contaminated groundwater, usually characterized by low organic carbon concentrations (Regan et al., 2017).

Bioelectrochemical systems (BES) proved to be a promising sustainable and efficient alternative for nitrate removal from groundwater (Li et al., 2019; Pous et al., 2018). In such systems, the electrochemical redox processes are enhanced by electroactive bacteria, which can use a solid electrode as the electron donor or acceptor (Rabaey et al., 2009). Previous studies have demonstrated the possibility of achieving complete nitrate conversion into dinitrogen gas in BES via autotrophic denitrification at the bio-cathode, with no nitrite or nitrous oxide production (Ceballos-Escalera et al. 2021; Puig et al. 2011; Desloover et al., 2011).

Several studies were also carried out with bioelectrochemical technologies applied to desalination, i.e., Microbial Desalination Cells (MDC), which exploit the oxidation of organic matter in wastewater as a source of energy for desalination. The electric potential gradient created by the exoelectrogenic bacteria desalinates water by driving ion transport through a series of ion exchange membranes (IEM) (Ramírez-Moreno et al., 2019; Sevda et al., 2015; Kim et al., 2013).

However, to our knowledge, there is only one study concerning the simultaneous removal of nitrate and salinity from groundwater using BES. Zhang et al. (2013) tested a submerged 2-compartment desalination-denitrification cell for treating synthetic groundwater affected by high salinity and nitrate concentrations, using simulated municipal wastewater as the source of electrons. A higher nitrate removal (99%) was achieved at high ionic strength compared to low ionic strength conditions (91%), even though salinity removal was lower (60% versus 95%). In this regard, it must be considered that groundwater is usually characterized by low electrical conductivity (<1 mS cm^{-1}), which would lead to more ohmic and transport losses and higher pH gradients (Logan et al., 2006) thus hindering BES treatment performances. In this sense, high salinity groundwater could be more suitable for BES treatment since nitrate removal efficiency should not be limited by low electrical conductivity.

Within this framework, a proof-of-concept based on a 3-compartment BES configuration was designed and tested to treat saline groundwater contaminated by nitrates. The main objective of the study was to investigate the feasibility of coupling bioelectrochemical nitrate removal with salinity reduction in a single bioelectrochemical cell. Moreover, the possibility to sustainably produce value-added chemicals in the same reactor was assessed within a circular economy-based approach. Specifically, the conversion of chlorides into free chlorine was investigated, a disinfecting agent widely used for water disinfection in water treatment plants. The 3-compartment cell was tested under different operating modes (e.g., potentiostatic and galvanostatic mode) and conditions (e.g., with and without pH control) to find the optimal balance where the three processes (i.e., denitrification, desalination, and chlorine recovery) can coexist.

4.2 Materials and methods

4.2.1 Reactor set-up

Two identical 3-compartment bioelectrochemical cells made of transparent Plexiglass were used in this study. Each cell consisted of a bio-cathodic compartment (8x8x2 cm^3, net volume 110 mL), an anodic compartment (8x8x2 cm^3, net volume 130 mL), and a central "desalination" compartment (8x8x0.5 cm^3, net volume 30 mL).

The cathodic and the central compartments were separated by a cation exchange membrane (CEM 7000-S, Membrane International Inc., USA) with a surface of 64 cm^2. Carbon felt (thickness 1.12 cm, degree of purity 99.9%, AlfaAesar, Germany) with a surface of 64 cm^2 was used as the bio-cathode (working electrode) and connected to a stainless steel mesh which worked as the current collector. A reference electrode (Ag/AgCl, +0.197 V vs SHE, mod. MF2052, Bio-Analytical Systems, USA) was also placed in this compartment. The anodic and the central compartments were separated by an anion exchange membrane (AEM 7001-CR, Membranes International Inc., USA) with a surface of 64 cm^2. Titanium coated with mixed metals oxide (Ti-MMO, 15 cm^2, NMT-Electrodes, South Africa) was used as anode (counter electrode) and connected to a titanium wire (thickness 0.75 mm, degree of purity 99.98%, AlfaAesar, Germany), which worked as the current collector. Cathode, anode, and reference electrodes were

connected to a multichannel potentiostat (Ivium Technologies, Ivium-N-stat, NL). A schematic representation of the final setup is shown in Figure 4.1.

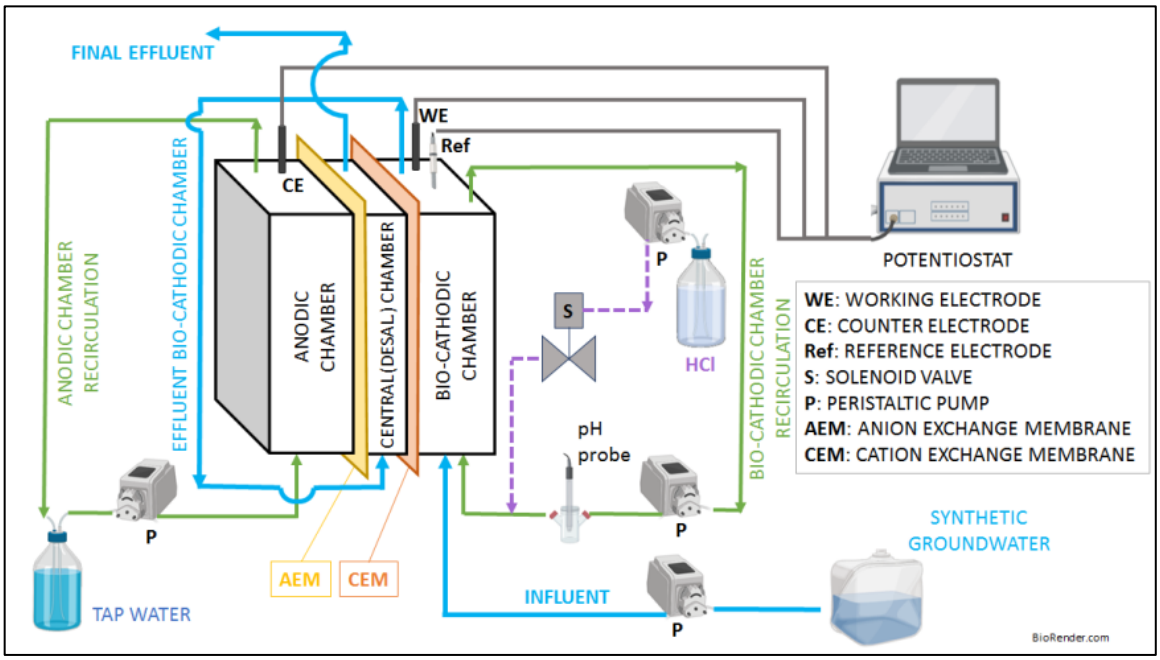

Figure 4.1. Schematic process flow diagram.

4.2.2 Synthetic groundwater and media composition

A synthetic medium mimicking nitrate concentration and salinity of groundwater from the nitrate vulnerable zone of Arborea (Sardinia, Italy) was fed to the bio-cathodic compartment (Medium A): 216.6 mg L^{-1} KNO_3 (corresponding to 30.0 mgNO_3^--N L^{-1}); 10 mg L^{-1} NH_4Cl (corresponding to 2.6 mgNH_4^+-N L^{-1}), 4.64 mg L^{-1} KH_2PO_4; 11.52 mg L^{-1} K_2HPO_4; 350 mg L^{-1} $NaHCO_3$; 2000 mg L^{-1} NaCl and 100 µL L^{-1} of trace elements solution (Patil et al., 2010). The resulting electrical conductivity and pH were 3.3±0.3 mS cm^{-1} and 8.2±0.2, respectively. Medium B (same composition as Medium A, but without KNO_3 and NH_4Cl) was used to fill the anodic and central compartments during batch mode operation to avoid electrical conductivity and pH gradients during biofilm development and enrichment. All media were prepared using distilled water, and Medium A was pre-flushed with N_2 gas for 15 minutes to avoid any presence of oxygen.

4.2.3 Experimental procedure

Table 4.1 summarizes the experimental procedure followed in this study. Both cells were started up in batch mode (Phase 1) (Figure AII-2, Appendix II). The supernatant of activated

sludge liquor drawn from the municipal wastewater treatment plant of Cagliari (Italy) and the effluent from a parent electro-denitrifying system were mixed in a 60:40 ratio (v:v) and used as inoculum. The bio-cathodic compartment was initially filled with synthetic groundwater (Medium A) and inoculum (<100 mgTSS L^{-1}) in a 50:50 ratio (v:v). A proper amount of KNO_3 solution (0.2 M) was periodically added when nitrate concentration measured inside the bio-cathodic compartment dropped below 3.5 mgNO_3^--N L^{-1} to bring nitrate concentration up to 30 mgNO_3^--N L^{-1}.

Table 4.1. Experimental procedure: number and duration of batch cycles in each compartment of the system.

Phases	Days of experimentation [d]	Hydraulic operation	Hydraulic retention time [h]	Electrical operation	Controlled parameter	pH control
1	30	Batch mode (inoculation)	-	Potentiostatic	Cathode potential: -0.500V vs Ag/AgCl	NO
2	40	Continuous mode	18	Potentiostatic	Cathode potential: -0.500V vs Ag/AgCl	NO
3a	7	Continuous mode	24	Galvanostatic	Applied current: 2 mA	NO
3b	5	Continuous mode	24	Galvanostatic	Applied current: 5 mA	NO
3c	5	Continuous mode	24	Galvanostatic	Applied current: 10 mA	NO
4	30	Continuous mode	18	Galvanostatic	Applied current: 10 mA	YES

The anodic and central compartments were filled with Medium B, which was periodically replaced when pH dropped below 3 in the anodic compartment, or salinity was below 2 mS cm^{-1} in the desalination compartment. Three peristaltic pumps were used to recirculate the solutions in each compartment with a flow rate of 50 mL min^{-1}, thus providing thorough mixing of the media. The working, reference, and counter electrodes were connected to a potentiostat set in potentiostatic mode (Ivium Technologies, Ivium-N-Stat, NL). Bio-cathode was poised at

-0.500 V vs Ag/AgCl (-0.303 V vs SHE), a potential suitable for nitrate removal (Pous et al., 2015). During Phase 2, the bio-cathodic compartment was continuously fed with Medium A, and the effluent was sent into the central compartment to achieve desalination (Figure AII-3, Appendix II). Tap water was batch-fed and recirculated in the anodic compartment instead of Medium B. The potentiostat was kept in potentiostatic mode, and the electrical parameters remained the same as in Phase 1.

During Phase 3, the potentiostat was switched to galvanostatic mode, and three different currents were applied, namely 2, 5, and 10 mA.

In the last experimental phase (Phase 4), pH control was introduced to keep the pH below 7.5 by dosing HCl (1 M) in the cathode recirculation line (Figure 4.1). The probe for continuous pH measurement was connected to a transmitter (Mettler Toledo, mod. M300, USA), which recorded data every 10 minutes. During Phase 4, the cells were operated in galvanostatic mode with a fixed current of 10 mA.

4.2.4 Control tests

Abiotic tests were performed in duplicate to evaluate the different contributions to nitrate removal during operation in galvanostatic mode.

The abiotic tests were carried out in a cell identical to those used for the main experiments, in open circuit and galvanostatic mode, with an applied current of 10 mA. Synthetic groundwater was continuously fed to the cathodic compartment, then transferred into the central compartment before discharge. Tap water was batch-fed and recirculated into the anodic compartment. The different contributions were obtained by monitoring the nitrate concentration in each compartment of the cell. All tests lasted 24 hours.

4.2.5 Analytical methods

Samples were periodically taken from influent (once per week), effluent (three times per week), cathodic, and anodic compartments (three times per week) to evaluate overall cells performances. Liquid samples were analyzed for quantification of anions, i.e., chloride (Cl^-), nitrite (NO_2^--N), nitrate (NO_3^--N), phosphate (PO_4^{3-}), and sulfate (SO_4^{2-}), using an ion chromatograph (ICS-90, Dionex-Thermofisher, USA) equipped with an AS14A Ion-PAC 5 µm column.

Samples were filtered (acetate membrane filter, 0.45 µm porosity) and properly diluted with distilled water. The concentrations of the main cations, i.e., potassium (K^+) and sodium (Na^+), were determined using an ICP/OES (Optima 7000, PerkinElmer, USA): samples were filtered (acetate membrane filter, 0.45 µm porosity), acidified (1% v:v of nitric acid) and diluted with grade I water.

Electrical conductivity and pH were measured using a benchtop meter (HI5522, Hanna Instruments, Italy).

The free chlorine concentration was analyzed using a spectrophotometer (DR1900, Hach Lange, Germany) according to the DPD free chlorine method (DPD free chlorine reagent powder pillows, Hach Lange, Germany).

Nitrous oxide (N_2O) was measured using an N_2O liquid-phase microsensor (Unisense, Denmark) located in the effluent line of the reactors, thanks to a dedicated glass measuring cell.

The resulting currents and potentials were recorded every five minutes during Phase s 1-2 and Phases 3-4, respectively, through potentiostat. Cell potential was periodically checked using a multimeter (K2M, mod. KDM-600C, Italy).

SEM images of ion-selective membranes were captured using an FEI Quanta 200 SEM microscope. The membranes did not undergo any preparation, and they were fixed on the stub using a double-sided graphite adhesive. The analyses were performed in low vacuum mode (i.e., residual pressure in the experimental chamber in the range of 0.3-0.9 Torr) to minimize electrostatic charge effects, or high vacuum (pressure below 10^{-4} Torr). Images were collected in either secondary electrons or backscattered electrons.

4.2.6 Calculations

Nitrate Removal Efficiency (N-RE) and Nitrate Removal Rate (N-RR) were calculated according to equations 1 and 2, respectively:

$$\mathrm{N-RE}\,[\%] = \frac{C_{NO_3^- - N(inf)} - C_{NO_3^- - N(eff)}}{C_{NO_3^- - N(inf)}} \times 100 \quad \textbf{(1)}$$

$$\mathrm{N-RR}\,[\mathrm{mg\ N\ L^{-1}\ d^{-1}}] = \frac{C_{NO_3^- - N(inf)} - C_{NO_3^- - N(eff)}}{HRT} \quad \textbf{(2)}$$

Where $C_{NO_3^-N(inf)}$ and $C_{NO_3^-N(eff)}$ [mg L^{-1}] are nitrate concentrations in the influent and the effluent, respectively, while HRT [d] is the hydraulic retention time considering the cathodic and central compartments volumes.

The desalination performance was evaluated by calculating the electrical conductivity removal efficiency (EC-RE, equation 3), the chloride removal efficiency (Cl^--RE, equation 4), and the chloride removal rate (Cl^--RR, equation 5).

$$\mathrm{EC-RE\ [\%]} = \frac{EC_{(inf)} - EC_{(eff)}}{EC_{(inf)}} \times 100 \quad \textbf{(3)}$$

$$\mathrm{Cl^- - RE\ [\%]} = \frac{C_{Cl^-(inf)} - C_{Cl^-(eff)}}{C_{Cl^-(inf)}} \times 100 \quad \textbf{(4)}$$

$$\mathrm{Cl^- - RR\ [mg\ L^{-1}\ d^{-1}]} = \frac{C_{Cl^-(inf)} - C_{Cl^-(eff)}}{HRT} \quad \textbf{(5)}$$

where $EC_{(eff)}$ [mS cm^{-1}] and $C_{Cl-(eff)}$ [mg L^{-1}] represent the effluent electrical conductivity and chloride concentration, respectively. $EC_{(inf)}$ [mS cm^{-1}] and $C_{Cl-(inf)}$ [mg L^{-1}] represent the influent electrical conductivity and chloride concentration for Phases 1-3, respectively. Instead, during Phase 4, $EC_{(inf)}$ and $C_{Cl-(inf)}$ corresponded to the electrical conductivity and chloride concentration of the solution in the bio-cathodic compartment (i.e., the influent to the central compartment), respectively, to consider the chloride input due to the acid dosage in the cathodic compartment. The HRT [d] is the hydraulic retention time of the central compartment.

The coulombic efficiency for nitrate reduction (εNO_x) was calculated according to equation 6 (Virdis et al., 2008):

$$\varepsilon NO_x[\%] = \frac{I}{n\,\Delta C_{NO_x} Q_{in} F} \times 100 \quad \textbf{(6)}$$

where I is the current [A]; n is the number of electrons that can be accepted by 1 mol of oxidized nitrogen compound present in the bio-cathodic compartment assuming N_2 is the final product; ΔC_{NOx} is the difference between the nitrate concentration in the cathodic influent and effluent [molNO_3^--N L^{-1}]; Q_{in} is the influent flow rate [L s^{-1}]; F is Faraday's constant [96485 Ce^-mol^{-1}].

The current efficiency (CE) was expressed as the percentage of the charge associated with the chloride removed from the central compartment to the amount of electric charge transferred

(ECT) across the membranes (Ramírez-Moreno et al., 2019). CE [%] and ECT [C m^{-3}] were calculated using equations 7 and 8, respectively:

$$\mathrm{CE}\ [\%] = \frac{\mathrm{v\ z\ F}\left(\mathrm{C_{Cl^-(inf)}} - \mathrm{C_{Cl^-(eff)}}\right)}{\mathrm{ECT}} \times 100 \quad \textbf{(7)}$$

$$\mathrm{ECT}\ [\mathrm{C\ m^{-3}}] = \frac{\int \mathrm{I\,dt}}{\mathrm{V}} \quad \textbf{(8)}$$

where v and z represent the stoichiometric coefficient and the valence of the chloride ion, respectively; V [m^{-3}] is the volume of water treated; dt is the time [s].

The specific energy consumption (SEC) was calculated according to equation 9 for potentiostatic mode (Ben Sik Ali et al., 2010), and according to equation 10 for galvanostatic mode (Djouadi Belkada et al., 2018):

$$\mathrm{SEC_{pot.}}\ [\mathrm{kWh\ m^{-3}}] = \frac{\mathrm{E} \int \mathrm{I\,dt}}{\mathrm{V}} \quad \textbf{(9)}$$

$$\mathrm{SEC_{gal.}}\ [\mathrm{kWh\ m^{-3}}] = \frac{\mathrm{I} \int \mathrm{E\,dt}}{\mathrm{V}} \textbf{(10)}$$

where E is the cell potential [V].

Energy losses were calculated as reported by Sleutels et al. (2009). Precisely, the cathode overpotential (η_{cat}) was calculated using the theoretical cathode potential ($E_{NO_3^-/N_2}$) and the measured cathode potential, while the anode overpotential (η_{an}) was calculated using the theoretical anode potential (E_{O_2/H_2O}) and the measured anode potential. pH gradient losses ($\mathrm{E_{\Delta pH}}$) were determined using the Nernst equation, with a potential loss of −0.059 V per pH unit. Ionic losses (E_{ionic}) were calculated at each side of the membranes, considering the distance between the anode and the AEM for the anodic compartment (1 cm), the AEM and the CEM for the central compartment (0.5 cm), and the cathode and the CEM for the bio-cathodic compartment (1 cm).

4.3 Results and discussion

4.3.1 Cells performances in potentiostatic mode

The two cells worked as duplicates during the whole experiment, which started with the inoculation period in batch mode (Phase 1). Denitrification took place in the bio-cathodic compartment, while the electro-migration of ions through the membranes and therefore the desalination, occurred in the central compartment. During Phase 1, an average nitrate removal rate of 6.8±0.4 $mgNO_3^-$-N L^{-1} d^{-1} was achieved, and a significant reduction in electrical conductivity was also observed in the central compartment, from 4.11±0.2 to 0.17±0.2 mS cm^{-1}.

Once stable conditions were achieved, the reactors were switched to continuous mode (Phase 2), with an HRT of 18 h. This new operation mode resulted in increased nitrate removal compared to Phase 1. The average nitrate removal rate and removal efficiency were 10±5 $mgNO_3^-$-N L^{-1} d^{-1} and 23±11%, respectively. Although no nitrite and nitrous oxide were detected in the effluent, the highest value of coulombic efficiency obtained during this period was about 50%, which could indicate the occurrence of side reactions (e.g., oxygen oxidation).

The current density was close to 0.03 A $m^{-2}_{membrane}$, suggesting a limited electrons demand at the bio-cathode, likely due to the high internal system resistance. As reported by Cao et al. (2009) for MDCs, the lower the electrical conductivity of the central compartment, the higher the ohmic resistance of the system. In our cell configuration, the presence of the two membranes between the compartments hindered the transfer of protons from the anodic to the bio-cathodic compartment. An efficient transfer is indeed necessary for the successful denitrification reaction as the four steps of nitrate reduction require protons (Nguyen et al., 2015). In addition, an increase in the pH gradient between the anodic and bio-cathodic compartment also causes an increase in the internal resistance of the system (Puig et al., 2012). However, according to calculations reported by Sleutels et al. (2009), energy losses due to pH gradient between the compartments were only 1.6% of the total energy loss (corresponding to -0.1 V), while the highest energy losses are attributable to cathode overpotential, ionic and transport losses, amounting respectively to 14.9% (-0.96 V), 11.8% (-0.76 V), and 59.5% (-3.86 V).

Even though nitrate removal was observed in potentiostatic mode, a low chloride removal efficiency was achieved (4±3%). Again, the current density (0.03 A $m^{-2}_{membrane}$) was too low

and not sufficient to promote electro-migration of ions: at such current density, the theoretical maximum chloride removal would be about 220 mg L^{-1} d^{-1}, corresponding to a removal efficiency of 2%. Coherently, no significant electro-migration of ions across the membranes with consequent electrical conductivity reduction in the effluent was observed. Electro-migration is directly related to the applied (or generated) current, together with the 2 perm-selectivities imposed by the membranes (Dykstra et al., 2021). Kim et al. (2013) reported that the maximum current densities for microbial desalination cells range from 0.7 to more than 8.4 A $m^{-2}_{membrane}$. Since currents measured in the 3-compartment BES during Phase 2 were too low to sustain significant desalination, the operation of the cells was switched from potentiostatic to galvanostatic mode working at higher current conditions to maximise both nitrate and salinity removals.

4.3.2 Cells performances in galvanostatic mode

Bes operation without pH control

During Phase 3, the operation of the reactors was switched to galvanostatic mode, and three different currents were tested (Table 4.2).

Table 4.2. Operating conditions and main results obtained during tests in galvanostatic mode with different applied currents.

Phase	Applied current [mA]	Nitrate removal rate [$mgNO_3^-$-N $L^{-1}d^{-1}$]	Nitrate removal efficiency [%]	Effluent nitrate concentration [$mgNO_3^-$-N L^{-1}]	Chloride removal efficiency [%]	Effluent electrical conductivity [mS cm^{-1}]
3a	2	6.5±1.7	30±7	26.5±2.6	0	5.4±0.4
3b	5	12.1±4.9	65±37	11.7±6.9	68±37	3.6±4.0
3c	10	19.6±1.1	89±3	3.4±0.1	97±2	0.2±0.1

The best results in terms of nitrate and salinity removal were obtained during Phase 3c when 10 mA was applied (current density of 1.6 A $m^{-2}_{membrane}$): average nitrate removal efficiency was 89±3% (corresponding to an effluent nitrate concentration of 3.4±0.1 $mgNO_3^-$-N L^{-1}), and

desalination efficiency was 97±2% (corresponding to an effluent electrical conductivity of 0.2±0.1 mS cm^{-1}).

The short duration of Phases 3a, 3b, and 3c (Table 1) due to rapid membranes deterioration (as it will be explained below) did not allow to observe the migration of the major cations (K^+ and Na^+) through the CEM, and their possible accumulation in the bio-cathodic compartment.

During these operating phases, the cathodic potential was lower than -0.9 V vs Ag/AgCl. Such values were demonstrated to be favourable to enhance hydrogen production, which in turn can improve nitrate reduction by contributing through hydrogenotrophic denitrification (Nguyen et al., 2016).

The coulombic efficiency (εNO_x) related to nitrate reduction was always greater than 100%, with increasing values as the applied current increased. This was likely due to side reactions occurring in the bio-cathodic compartment. The current efficiency (CE) related to chlorides removal from the central compartment was zero (desalination was negligible), 83±73%, and 28±1% during Phases 3a, b, and c, respectively. Although the highest CE was achieved during Phase 3b, it must be noticed that the process was highly unstable.

Abiotic tests were carried out to highlight the different contributions (i.e., bioelectrochemical, electrochemical, and migration across AEM) to nitrate removal. The denitrifying performance of the biological cell in galvanostatic operation (10 mA) was compared with that of the abiotic cell in galvanostatic (10 mA) and open circuit (OCV) operation (Figure 4.2).

Recent studies have shown that electrochemical technologies, including electroreduction (ER), effectively remove nitrates in wastewater due to their high reactivity (Xu et al., 2018). The reaction mechanism depends strongly on the type of cathode material, cathode potential, and solution pH. To the authors' knowledge, there are no specific studies on electroreduction applied with carbon felt cathodes, but the conditions established in the cathodic compartment in galvanostatic mode may be favorable for nitrate electroreduction, as clearly indicated by the abiotic test. However, the results proved that the bioelectrochemical contribution significantly improved nitrate removal, which was 16% higher than that obtained electrochemically in the abiotic cell.

Although significant nitrate and salinity removal was achieved with the galvanostatic operation, the high reaction rate caused an uncontrolled increase in pH (>10) in the bio-cathodic compartment, resulting in membranes damage and subsequent decline in the overall process performance, including denitrification capacity. Even though the optimal pH working range of both AEM and CEM is between 0 and 10 pH, the worst deterioration was observed in the anion exchange membrane (Figure AII-4, in Appendix II), which resulted in being particularly sensitive to high pH values.

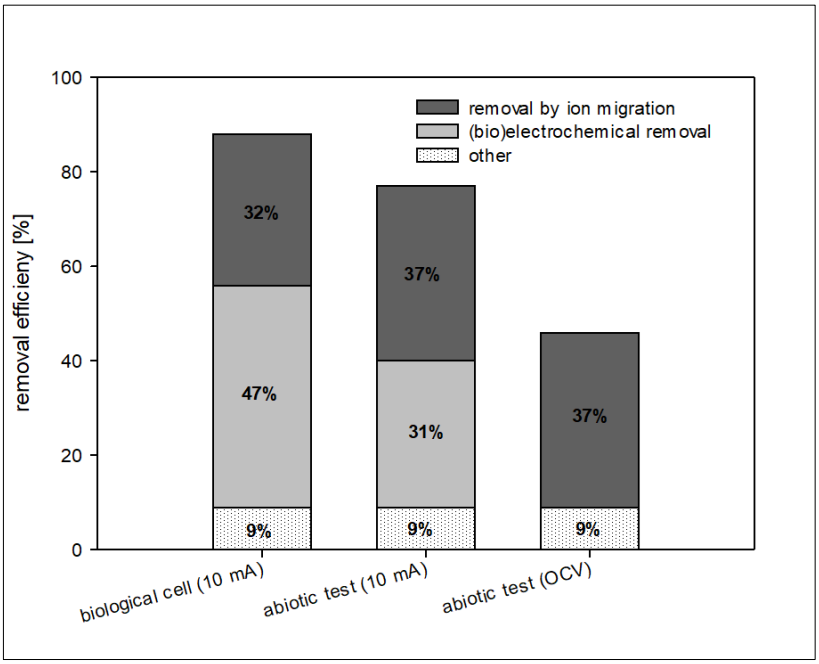

Figure 4.2. Different contributions to nitrate removal (i.e., bioelectrochemical, electrochemical, and migration of nitrate ions through the AEM) determined with biotic and abiotic tests.

Effect of pH control on BES performance

To improve the stability of the process and the lifetime of the membranes, several tests were carried out, which included the on/off operation of the potentiostat and the periodic washing of the bio-cathodic compartment. However, no improvements were observed in terms of performance and process stability (data not shown). Implementing pH control (<7.5) based on acid dosage in the recirculation line of the bio-cathodic compartment significantly improved process stability (Phase 4). The average nitrate removal rate was 39±1 mgNO_3^--N L^{-1} d^{-1} (corresponding to a nitrate removal efficiency of 69±2%), while the chloride removal rate was

13±2 $gCl^{-} L^{-1} d^{-1}$ (corresponding to a chloride removal efficiency of 63±5%). A decrease in electrical conductivity between the inflow and outflow of the central compartment was observed, from about 6 to 2 mS cm^{-1}, corresponding to an EC removal efficiency of 59±13%. The current efficiency related to chloride migration was 104±16%, indicating that all the applied current was used for chloride migration.

During Phase 4, a significant accumulation of major cations (K^{+} and Na^{+}) was observed in the bio-cathodic compartment (Figure AII-5, in Appendix II). This result was consistent with the trend of anions, particularly chlorides, and confirmed that it was possible to promote the electro-migration of ions from the central compartment to the anodic and bio-cathodic compartments in such conditions. Besides, the concentrations of cations in the effluent showed a constantly increasing trend over time, and they equalled the influent concentrations after 25 days of experiments (Figure AII-6, Appendix II). Despite such an increase in cations concentration, no precipitates or deposits on the electrode were observed at the end of Phase 4.

Figure 4.3 compares reactors' performances, in terms of denitrification and desalination, obtained during the potentiostatic (Phase 2) and galvanostatic (Phase 4) operating modes. The galvanostatic mode with pH control significantly enhanced desalination (as expected), and a significant improvement in denitrification rates was also observed. Energy losses in Phase 4 were significantly higher than those in Phase 2, and mainly associated with ionic and transport losses, corresponding to 33% and 54% of the total energy losses, respectively.

During galvanostatic operation with pH control, nitrate concentration and electrical conductivity in the effluent (11.4±0.5 $mgNO_3^{-}$-N L^{-1} and 2.2±0.3 mS cm^{-1}, respectively) were close to WHO and European legislation threshold limits for drinking water, corresponding to 11.3 $mgNO_3^{-}$-N L^{-1} (91/767/EU) and 2.5 mS cm^{-1} (98/83/CE), respectively.

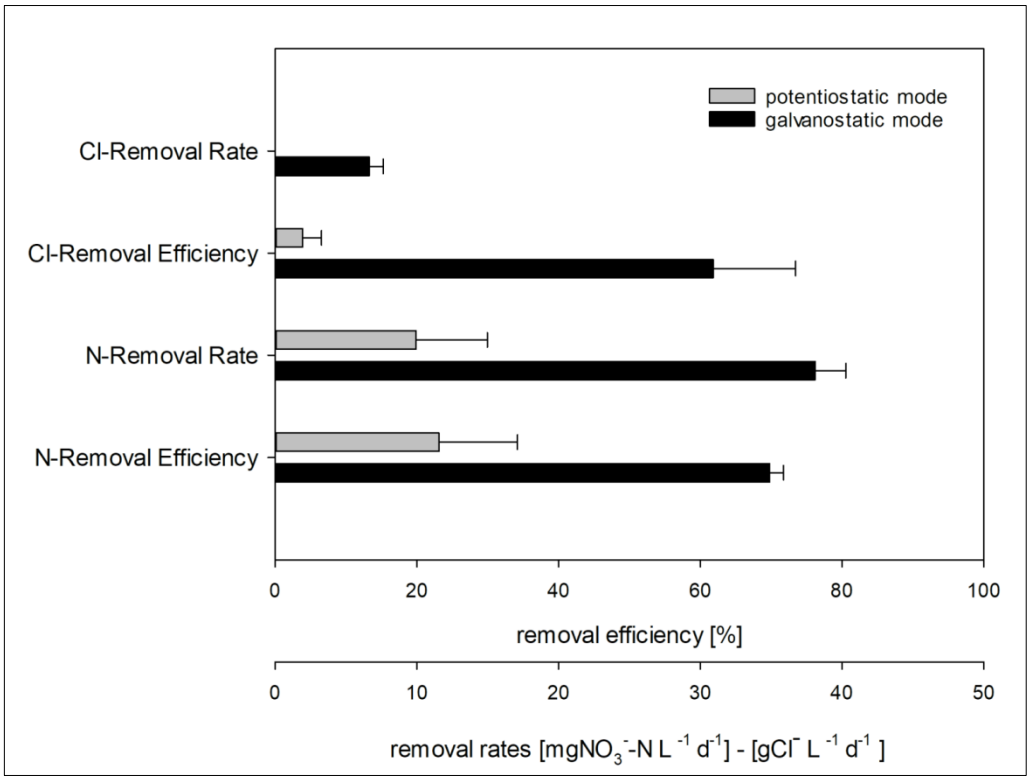

Figure 4.3. Comparison of overall performance observed during the reactors' potentiostatic (Phase 2) and galvanostatic operation (Phase 4).

During Phase 4, the specific energy consumption (SEC) was 0.13±0.01 kWh $g^{-1}NO_3^-$-$N_{removed}$, comparable with those previously reported in the literature concerning bioelectrochemical reactors operated with similar conditions. Zhou et al. (2009) reported an SEC of 0.07 kWh $g^{-1}NO_3^-$-$N_{removed}$ in a bioelectrochemical reactor (BER) fed with real nitrate-contaminated groundwater and operated in galvanostatic mode. Although Pous et al. (2015) achieved lower SEC in bioelectrochemical systems operated in potentiostatic mode (0.7 10^{-2} kWh $g^{-1}NO_3^-$-$N_{removed}$), it should be noticed that the energy provided in our system was used not only for nitrate removal but also to promote ions electro-migration and achieve a reduction in salinity of the treated water. In this sense, a direct comparison of SEC may be misleading. The average SEC (per unit volume of treated water) was 3.48 ± 0.13 kWh $m^{-3}_{water\ treated}$, which is comparable or lower than the consumption reported for well-established desalination technologies, such as membrane processes (1-12 and 2-12 kWh m^{-3} for electrodialysis and reverse osmosis, respectively) or thermal processes (14-25 and 7-25 kWh m^{-3} for multi-stage flash desalination and multi-effect evaporation/distillation, respectively) (Al-Amshawee et al., 2020). Furthermore, it is important to consider that these processes exploit established technologies that operate on a pilot or full scale, while the system in this study, although already showing competitive

results, represents a proof-of-concept with significant scope for improvement in terms of process performance (i.e., removal and desalination rates) and energy consumption.

4.3.3 Chloride recovery and synthesis of disinfectants

During Phase 4, a progressive accumulation of chloride ions in the anolyte solution (i.e., tap water) was observed. The accumulated chloride was partially converted into chlorine (Cl_2) thanks to the anodic potential (+1.49±0.06 V vs SHE), which was close to the minimum required for chlorine production (i.e., +1.4 V vs SHE). After about 15 days, chlorides concentration in the anodic compartment reached a value of 2300 $mgCl^- L^{-1}$, while chlorine concentration stabilized at a value of 26.8±3.4 $mgCl_2 L^{-1}$ from day 6 onward. This concentration is higher than the typical dosage required for disinfection purposes in water treatment plants (0.5–2.0 mg $Cl_2 L^{-1}$). Thus, in the perspective of an on-site application of this technology, the chlorine produced could be slightly dosed for disinfection of the treated water (Ragazzo et al., 2020).

Moreover, the oxidation of chloride to chlorine (ΔG^o=2.72 eV) appears to be particularly convenient also from an energy point of view, since it is 45% less energy-consuming than water electrolysis (ΔG^o=4.92 eV), which is the reaction mainly used at the anode in BES systems for denitrification (Batlle-Vilanova et al., 2019).

Therefore, the production of chlorine compounds in the anodic compartment, which could be used for water disinfection in water treatment plants, shows both economic value and application potential. Currently, chlorine-based disinfectant products are priced at 2.20 € kg^{-1} (averaged from different providers).

From a sanitary and environmental point of view, the production of chlorine in the anodic compartment of the BES has considerable advantages over conventional technologies (i.e., the chlor-alkali process). In fact, BES do not require toxic chemicals and do not produce highly concentrated brines. It also offers advantages from a management point of view, considerably reducing energy costs, which are high in the chlor-alkali process, and disposal costs of the brine.

Based on these considerations, the possibility of producing chlorine spontaneously from a groundwater treatment process, which does not involve the production of intermediates or

waste products and with reduced energy consumption, is of particular interest to develop increasingly sustainable processes.

4.3.4 Comparison with state of the art and perspectives

To the authors' best knowledge, this is the first study addressing simultaneous nitrate removal, desalination, and chlorine synthesis in a bioelectrochemical system. The results achieved in this study were compared with those reported in the literature concerning groundwater denitrification and/or desalination by BES and other technologies (Table 4.3).

Previous studies showed that high nitrate removal rates can be achieved, working under both potentiostatic (Ceballos-Escalera et al., 2021; Liu et al., 2019; Pous et al., 2015) and galvanostatic conditions (Zhou et al., 2007). In particular, Pous et al. (2015) showed that denitrification rates increased as the energy input increased. It must be considered that denitrification rates were achieved under very different operating conditions, and direct comparisons may be difficult. For example, Ceballos-Escalera et al. (2021) reported removal rates of 519±53 $mgNO_3^-$-N L^{-1} d^{-1}, much higher than those reported in our study (39±1 $mgNO_3^-$-N L^{-1} d^{-1}). However, if nitrate removal rates are normalized considering the electrode surface area of the cathode, an average of 600 $mgNO_3^-$-N m^{-2} d^{-1} was obtained in our study, about twice the value achieved by Ceballos-Escalera et al. (2021) (i.e., 300 $mgNO_3^-$-N m^{-2} d^{-1}). This means that by increasing the electrode surface area available, it will be possible to develop a greater amount of biomass, thus optimizing denitrification performance.

The simultaneous denitrification and desalination of groundwater was investigated only by Zhang et al. (2013), using a submerged microbial desalination denitrification cell. The oxidation of organic matter at the anode was used to generate the electrons required to drive electro-migration (i.e., desalination), and much lower nitrate removal rates were achieved compared to other studies (Table 4.3).

Regarding groundwater desalination, previous studies focused mainly on nitrate removal using technologies such as electrodialysis and reverse osmosis. Some of these technologies require the addition of chemicals, and none of them is oriented towards the recovery of value-added products (Table 4.3).

Although the addition of hydrochloric acid was necessary in the present study during Phase 4 for active pH control, a significant part of chloride was recovered as free chlorine, which is a value-added chemical and may contribute to reducing management costs. As for energy requirements, the proof-of-concept 3-compartment BES investigated in our study already showed SEC comparable with those reported in the literature (Pirsaheb et al., 2015; Bi et al., 2011). In this sense, there is still considerable room for improvement in SEC reduction since the process can be further optimized in terms of operating conditions (e.g., by lowering the HRT), geometrical configuration (e.g., the distances between electrodes and membranes), and materials. In this respect, reducing the HRT may lead to better denitrification performance in terms of nitrate removal rates and specific energy consumption. Pous et al. (2017) reported that lowering the HRT (i.e., increasing the influent flow rate) plays an important role in modulating the denitrifying performance of BES, likely due to a combination of better hydrodynamics and enhanced biomass activity. As for the geometrical configuration, the inter-membrane distance used in our proof-of-concept configuration (i.e., 0.5 cm) was higher than that usually adopted in conventional electrodialysis systems (0.02-0.3 cm). A further decrease in inter-membrane distance may lead to lower internal resistance (Kim et al., 2013), and consequently better desalination performances.

Table 4.3. Comparison of operating conditions and main results with previous studies.

Reference	Type of reactor or process	Influent type	Fixed parameter	Nitrate removal efficiency [%]	Nitrate removal rates [$mgNO_3\text{-}N^{-}\,L^{-1}\,d^{-1}$]	Desalination efficiency [%]	Energy consumption [$kWh\,m^{-3}$]	Addition of chemicals	Recovery/ Production of value-added substances
This study (Phase 4)	3-compartment BES (bioelectrochemical system)	synthetic groundwater	current	69±2	39±1	63± 5	3.48 ± 0.13	Yes, hydrochloric acid	Yes, Cl_2
Ceballos-Escalera, 2021	Tubular BES (bioelectrochemical system)	synthetic groundwater	potential	90 ±6	519±53	-	-	No	No
Pous et al., 2015	2-compartment BES (bioelectrochemical system)	real groundwater	potential	96±2	98.2	-	0.20	No	No
Zhou et al., 2007	3D BER (Biofilm Electrode Reactor)	real groundwater	current	97	n.m.	-	0.44	Yes, ethanol and sulphuric acid	No
Zhang et al., 2013	SMDDC (Submerged Microbial Desalination Denitrification Cell)	synthetic groundwater	-	91	17	94	n.m.	Yes, sodium acetate	No
Liu et al., 2019	a combined SMFC (Sediment Microbial Fuel Cell)	real groundwater	potential	n.m	93	-	n.m.	No	No
El Midaoui et al., 2002	Electrodialysis	real groundwater	potential	93	n.m.	77	0.08	No	No
Bi et al., 2011	Electrodialysis	synthetic groundwater	potential	99	n.m.	n.m.	1.7	No	No
Pirsaheb et al., 2015	Electrodialysis	real groundwater	current	47	n.m.	72	2	Yes, hydrochloric acid	No
Pirsaheb et al., 2015	Reverse osmosis	real groundwater	current	91	n.m.	73	1.2	Yes, hydrochloric acid and antiscalant	No

4.4 Conclusions

A proof-of-concept based on a 3-compartment bioelectrochemical cell configuration was designed and tested in this study to treat saline groundwater contaminated by nitrates. As a novelty, the proposed system successfully combined simultaneous nitrate reduction, desalination, and production of a value-added chemical in a single reactor, within a circular economy-based approach. Several operating conditions were tested, and the galvanostatic mode (applied current: 10 mA) with pH control in the bio-cathodic compartment allowed to achieve high nitrogen and salinity removal and significant recovery of free chlorine (i.e., a disinfectant commonly used in the water treatment sector), with much-improved process stability and low power consumption. The contribution of bioelectrochemical and electrochemical denitrification and ion migration across membranes to nitrate removal was assessed, and electroactive biomass was proved to enhance BES performance significantly. Standard quality requirements for drinking water in terms of nitrate concentration (91/767/EU) and electrical conductivity (98/83/CE) were successfully met with this cell configuration, paving the ground for the development of a sustainable technology to tackle an urgent environmental issue such as water scarcity.

Acknowledgements

This study was funded by Fondo di Sviluppo e Coesione 2014-2020, Patto per lo sviluppo della Regione Sardegna - Area Tematica 3 - Linea d' Azione 3.1, "Interventi di sostegno alla ricerca". Project SARdNAF "Advanced Systems for the Removal of Nitrates from Groundwater", ID: RASSR53158.

The Centre for Research University Services (CeSAR) of the University of Cagliari (Italy) is to be thanked for the SEM analysis.

Thanks to Dr Martina Piredda for the support with the ICP-OES analyses.

References

Al-Amshawee, S., Yunus, M.Y.B.M., Azoddein, A.A.M., Hassell, D.G., Dakhil, I.H., Hasan, H.A., 2020. Electrodialysis desalination for water and wastewater: A review. Chem. Eng. J. 380, 122231. https://doi.org/10.1016/j.cej.2019.122231

Alfarrah, N., Walraevens, K., 2018. Groundwater Overexploitation and Seawater Intrusion in Coastal Areas of Arid and Semi-Arid Regions. Water 10, 143. https://doi.org/10.3390/w10020143

Aliaskari, M., Schäfer, A.I., 2021. Nitrate, arsenic and fluoride removal by electrodialysis from brackish groundwater. Water Res. 190, 116683. https://doi.org/10.1016/j.watres.2020.116683

Bamforth, S.M., Singleton, I., 2005. Bioremediation of polycyclic aromatic hydrocarbons: current knowledge and future directions. J. Chem. Technol. Biotechnol. 80, 723–736. https://doi.org/10.1002/jctb.1276

Batlle-Vilanova, P., Rovira-Alsina, L., Puig, S., Balaguer, M.D., Icaran, P., Monsalvo, V.M., Rogalla, F., Colprim, J., 2019. Biogas upgrading, CO2 valorisation and economic revaluation of bioelectrochemical systems through anodic chlorine production in the framework of wastewater treatment plants. Sci. Total Environ. 690, 352–360. https://doi.org/10.1016/j.scitotenv.2019.06.361

Ben Sik Ali, M., Hamrouni, B., Dhahbi, M., 2010. Electrodialytic Defluoridation of Brackish Water: Effect of Process Parameters and Water Characteristics. CLEAN - Soil Air Water n/a-n/a. https://doi.org/10.1002/clen.200900301

Bi, J., Peng, C., Xu, H., Ahmed, A.-S., 2011. Removal of nitrate from groundwater using the technology of electrodialysis and electrodeionization. Desalination Water Treat. 34, 394–401. https://doi.org/10.5004/dwt.2011.2891

Burri, N.M., Weatherl, R., Moeck, C., Schirmer, M., 2019. A review of threats to groundwater quality in the anthropocene. Sci. Total Environ. 684, 136–154. https://doi.org/10.1016/j.scitotenv.2019.05.236

Cao, X., Huang, X., Liang, P., Xiao, K., Zhou, Y., Zhang, X., Logan, B.E., 2009. A New Method for Water Desalination Using Microbial Desalination Cells. Environ. Sci. Technol. 43, 7148–7152. https://doi.org/10.1021/es901950j

Carrey, R., Ballesté, E., Blanch, A.R., Lucena, F., Pons, P., López, J.M., Rull, M., Solà, J., Micola, N., Fraile, J., Garrido, T., Munné, A., Soler, A., Otero, N., 2021. Combining multi-isotopic and molecular source tracking methods to identify nitrate pollution sources in surface and groundwater. Water Res. 188, 116537. https://doi.org/10.1016/j.watres.2020.116537

Ceballos-Escalera, A., Pous, N., Chiluiza-Ramos, P., Korth, B., Harnisch, F., Bañeras, L., Balaguer, M.D., Puig, S., 2021. Electro-bioremediation of nitrate and arsenite polluted groundwater. Water Res. 190, 116748. https://doi.org/10.1016/j.watres.2020.116748

Coss, A., 2004. Pancreatic Cancer and Drinking Water and Dietary Sources of Nitrate and Nitrite. Am. J. Epidemiol. 159, 693–701. https://doi.org/10.1093/aje/kwh081

Della Rocca, C., Belgiorno, V., Meriç, S., 2007. Overview of in-situ applicable nitrate removal processes. Desalination 204, 46–62. https://doi.org/10.1016/j.desal.2006.04.023

Desloover, J., Puig, S., Virdis, B., Clauwaert, P., Boeckx, P., Verstraete, W., Boon, N., 2011. Biocathodic Nitrous Oxide Removal in Bioelectrochemical Systems. Environ. Sci. Technol. 45, 10557–10566. https://doi.org/10.1021/es202047x

Djouadi Belkada, F., Kitous, O., Drouiche, N., Aoudj, S., Bouchelaghem, O., Abdi, N., Grib, H., Mameri, N., 2018. Electrodialysis for fluoride and nitrate removal from synthesized photovoltaic industry wastewater. Sep. Purif. Technol. 204, 108–115. https://doi.org/10.1016/j.seppur.2018.04.068

Dykstra, J.E., Heijne, A. ter, Puig, S., Biesheuvel, P.M., 2021. Theory of transport and recovery in microbial electrosynthesis of acetate from CO 2. Electrochimica Acta 379, 138029. https://doi.org/10.1016/j.electacta.2021.138029

El Midaoui, A., Elhannouni, F., Taky, M., Chay, L., Menkouchi Sahli, M.A., Echihabi, L., Hafsi, M., 2002. Optimization of nitrate removal operation from ground water by electrodialysis. Sep. Purif. Technol. 29, 235–244. https://doi.org/10.1016/S1383-5866(02)00092-8

Epsztein, R., Nir, O., Lahav, O., Green, M., 2015. Selective nitrate removal from groundwater using a hybrid nanofiltration–reverse osmosis filtration scheme. Chem. Eng. J. 279, 372–378. https://doi.org/10.1016/j.cej.2015.05.010

Gounari, C., Skordas, K., Gounaris, A., Kosmidis, D., Karyoti, A., 2014. Seawater Intrusion and Nitrate Pollution in Coastal Aquifer of Almyros – Nea Anchialos Basin, Central Greece 10, 13.

Hu, K., Huang, Y., Li, H., Li, B., Chen, D., White, R.E., 2005. Spatial variability of shallow groundwater level, electrical conductivity and nitrate concentration, and risk assessment of nitrate contamination in North China Plain. Environ. Int., Soil Contamination and Environmental Health 31, 896–903. https://doi.org/10.1016/j.envint.2005.05.028

Kim, J., Park, K., Yang, D.R., Hong, S., 2019. A comprehensive review of energy consumption of seawater reverse osmosis desalination plants. Appl. Energy 254, 113652. https://doi.org/10.1016/j.apenergy.2019.113652

Kim, Y., Logan, B.E., 2013. Microbial desalination cells for energy production and desalination. Desalination 308, 122–130. https://doi.org/10.1016/j.desal.2012.07.022

Koter, S., Chojnowska, P., Szynkiewicz, K., Koter, I., 2015. Batch electrodialysis of ammonium nitrate and sulfate solutions. J. Membr. Sci. 496, 219–228. https://doi.org/10.1016/j.memsci.2015.08.064

Li, Chen, Xie, Liu, Xiong, 2019. Bioelectrochemical Systems for Groundwater Remediation: The Development Trend and Research Front Revealed by Bibliometric Analysis. Water 11, 1532. https://doi.org/10.3390/w11081532

Liu, J., Gao, Z., Wang, Z., Xu, X., Su, Q., Wang, S., Qu, W., Xing, T., 2020. Hydrogeochemical processes and suitability assessment of groundwater in the Jiaodong Peninsula, China. Environ. Monit. Assess. 192, 384. https://doi.org/10.1007/s10661-020-08356-5

Liu, R., Zheng, X., Li, M., Han, L., Liu, X., Zhang, F., Hou, X., 2019. A three chamber bioelectrochemical system appropriate for in-situ remediation of nitrate-contaminated groundwater and its reaction mechanisms. Water Res. 158, 401–410. https://doi.org/10.1016/j.watres.2019.04.047

Logan, B.E., Hamelers, B., Rozendal, R., Schröder, U., Keller, J., Freguia, S., Aelterman, P., Verstraete, W., Rabaey, K., 2006. Microbial Fuel Cells: Methodology and Technology †. Environ. Sci. Technol. 40, 5181–5192. https://doi.org/10.1021/es0605016

Menció, A., Mas-Pla, J., Otero, N., Regàs, O., Boy-Roura, M., Puig, R., Bach, J., Domènech, C., Zamorano, M., Brusi, D., Folch, A., 2016. Nitrate pollution of groundwater; all right..., but nothing else? Sci. Total Environ. 539, 241–251. https://doi.org/10.1016/j.scitotenv.2015.08.151

Naser, A.M., Rahman, M., Unicomb, L., Doza, S., Ahmed, K.M., Uddin, M.N., Selim, S., Gribble, M.O., Anand, S., Clasen, T.F., Luby, S.P., 2017. Drinking water salinity and kidney health in southwest coastal Bangladesh: baseline findings of a community-based stepped-wedge randomised trial. The Lancet, Inaugural Planetary Health/GeoHealth Annual Meeting 389, S15. https://doi.org/10.1016/S0140-6736(17)31127-3

Nguyen, V.K., Hong, S., Park, Y., Jo, K., Lee, T., 2015. Autotrophic denitrification performance and bacterial community at biocathodes of bioelectrochemical systems with either abiotic or biotic anodes. J. Biosci. Bioeng. 119, 180–187. https://doi.org/10.1016/j.jbiosc.2014.06.016

Nguyen, V.K., Park, Y., Yang, H., Yu, J., Lee, T., 2016. Effect of the cathode potential and sulfate ions on nitrate reduction in a microbial electrochemical denitrification system. J. Ind. Microbiol. Biotechnol. 43, 783–793. https://doi.org/10.1007/s10295-016-1762-6

Patil, S., Harnisch, F., Schröder, U., 2010. Toxicity Response of Electroactive Microbial Biofilms - A Decisive Feature for Potential Biosensor and Power Source Applications. ChemPhysChem 11, 2834–2837. https://doi.org/10.1002/cphc.201000218

Pirsaheb, M., n.d. Comparing operational cost and performance evaluation of electrodialysis and reverse osmosis systems in nitrate removal from drinking water in Golshahr, -->Mashhad. Desalination Water Treat. 9.

Pous, N., Balaguer, M.D., Colprim, J., Puig, S., 2018. Opportunities for groundwater microbial electro-remediation. Microb. Biotechnol. 11, 119–135. https://doi.org/10.1111/1751-7915.12866

Pous, N., Puig, S., Balaguer, M.D., Colprim, J., 2017. Effect of hydraulic retention time and substrate availability in denitrifying bioelectrochemical systems. Environ. Sci. Water Res. Technol. 3, 922–929. https://doi.org/10.1039/C7EW00145B

Pous, N., Puig, S., Dolors Balaguer, M., Colprim, J., 2015. Cathode potential and anode electron donor evaluation for a suitable treatment of nitrate-contaminated groundwater in bioelectrochemical systems. Chem. Eng. J. 263, 151–159. https://doi.org/10.1016/j.cej.2014.11.002

Puig, S., Coma, M., Desloover, J., Boon, N., Colprim, J., Balaguer, M.D., 2012. Autotrophic Denitrification in Microbial Fuel Cells Treating Low Ionic Strength Waters. Environ. Sci. Technol. 46, 2309–2315. https://doi.org/10.1021/es2030609

Puig, S., Serra, M., Vilar-Sanz, A., Cabré, M., Bañeras, L., Colprim, J., Balaguer, M.D., 2011. Autotrophic nitrite removal in the cathode of microbial fuel cells. Bioresour. Technol. 102, 4462–4467. https://doi.org/10.1016/j.biortech.2010.12.100

Rabaey, K., 2009. Bioelectrochemical Systems: From Extracellular Electron Transfer to Biotechnological Application. Water Intell. Online 8. https://doi.org/10.2166/9781780401621

Ragazzo, P., Chiucchini, N., Piccolo, V., Spadolini, M., Carrer, S., Zanon, F., Gehr, R., 2020. Wastewater disinfection: long-term laboratory and full-scale studies on performic acid in comparison with peracetic acid and chlorine. Water Res. 184, 116169. https://doi.org/10.1016/j.watres.2020.116169

Ramírez-Moreno, M., Rodenas, P., Aliaguilla, M., Bosch-Jimenez, P., Borràs, E., Zamora, P., Monsalvo, V., Rogalla, F., Ortiz, J.M., Esteve-Núñez, A., 2019. Comparative Performance of Microbial Desalination Cells Using Air Diffusion and Liquid Cathode Reactions: Study of the Salt Removal and Desalination Efficiency. Front. Energy Res. 7, 135. https://doi.org/10.3389/fenrg.2019.00135

Regan, S., Hynds, P., Flynn, R., 2017. An overview of dissolved organic carbon in groundwater and implications for drinking water safety. Hydrogeol. J. 25, 959–967. https://doi.org/10.1007/s10040-017-1583-3

Rezvani, F., Sarrafzadeh, M.-H., Ebrahimi, S., Oh, H.-M., 2019. Nitrate removal from drinking water with a focus on biological methods: a review. Environ. Sci. Pollut. Res. 26, 1124–1141. https://doi.org/10.1007/s11356-017-9185-0

Sevda, S., Yuan, H., He, Z., Abu-Reesh, I.M., 2015. Microbial desalination cells as a versatile technology: Functions, optimization and prospective. Desalination 371, 9–17. https://doi.org/10.1016/j.desal.2015.05.021

Sleutels, T.H.J.A., Hamelers, H.V.M., Rozendal, R.A., Buisman, C.J.N., 2009. Ion transport resistance in Microbial Electrolysis Cells with anion and cation exchange membranes. Int. J. Hydrog. Energy 34, 3612–3620. https://doi.org/10.1016/j.ijhydene.2009.03.004

Troudi, N., Hamzaoui-Azaza, F., Tzoraki, O., Melki, F., Zammouri, M., 2020. Assessment of groundwater quality for drinking purpose with special emphasis on salinity and nitrate contamination in the shallow aquifer of Guenniche (Northern Tunisia). Environ. Monit. Assess. 192, 641. https://doi.org/10.1007/s10661-020-08584-9

Twomey, K.M., Stillwell, A.S., Webber, M.E., 2010. The unintended energy impacts of increased nitrate contamination from biofuels production. J Env. Monit 12, 218–224. https://doi.org/10.1039/B913137J

Virdis, B., Rabaey, K., Yuan, Z., Keller, J., 2008. Microbial fuel cells for simultaneous carbon and nitrogen removal. Water Res. 42, 3013–3024. https://doi.org/10.1016/j.watres.2008.03.017

Ward, M., Jones, R., Brender, J., de Kok, T., Weyer, P., Nolan, B., Villanueva, C., van Breda, S., 2018. Drinking Water Nitrate and Human Health: An Updated Review. Int. J. Environ. Res. Public. Health 15, 1557. https://doi.org/10.3390/ijerph15071557

Xu, D., Li, Y., Yin, L., Ji, Y., Niu, J., Yu, Y., 2018. Electrochemical removal of nitrate in industrial wastewater. Front. Environ. Sci. Eng. 12, 9. https://doi.org/10.1007/s11783-018-1033-z

Zhang, S., Mao, G., Crittenden, J., Liu, X., Du, H., 2017. Groundwater remediation from the past to the future: A bibliometric analysis. Water Res. 119, 114–125. https://doi.org/10.1016/j.watres.2017.01.029

Zhang, Y., Angelidaki, I., 2013. A new method for in situ nitrate removal from groundwater using submerged microbial desalination–denitrification cell (SMDDC). Water Res. 47, 1827–1836. https://doi.org/10.1016/j.watres.2013.01.005

Zhou, M., Fu, W., Gu, H., Lei, L., 2007. Nitrate removal from groundwater by a novel three-dimensional electrode biofilm reactor. Electrochimica Acta 52, 6052–6059. https://doi.org/10.1016/j.electacta.2007.03.064

Zhou, M., Wang, W., Chi, M., 2009. Enhancement on the simultaneous removal of nitrate and organic pollutants from groundwater by a three-dimensional bio-electrochemical reactor. Bioresour. Technol. 100, 4662–4668. https://doi.org/10.1016/j.biortech.2009.05.002

Appendix II

Additional figures

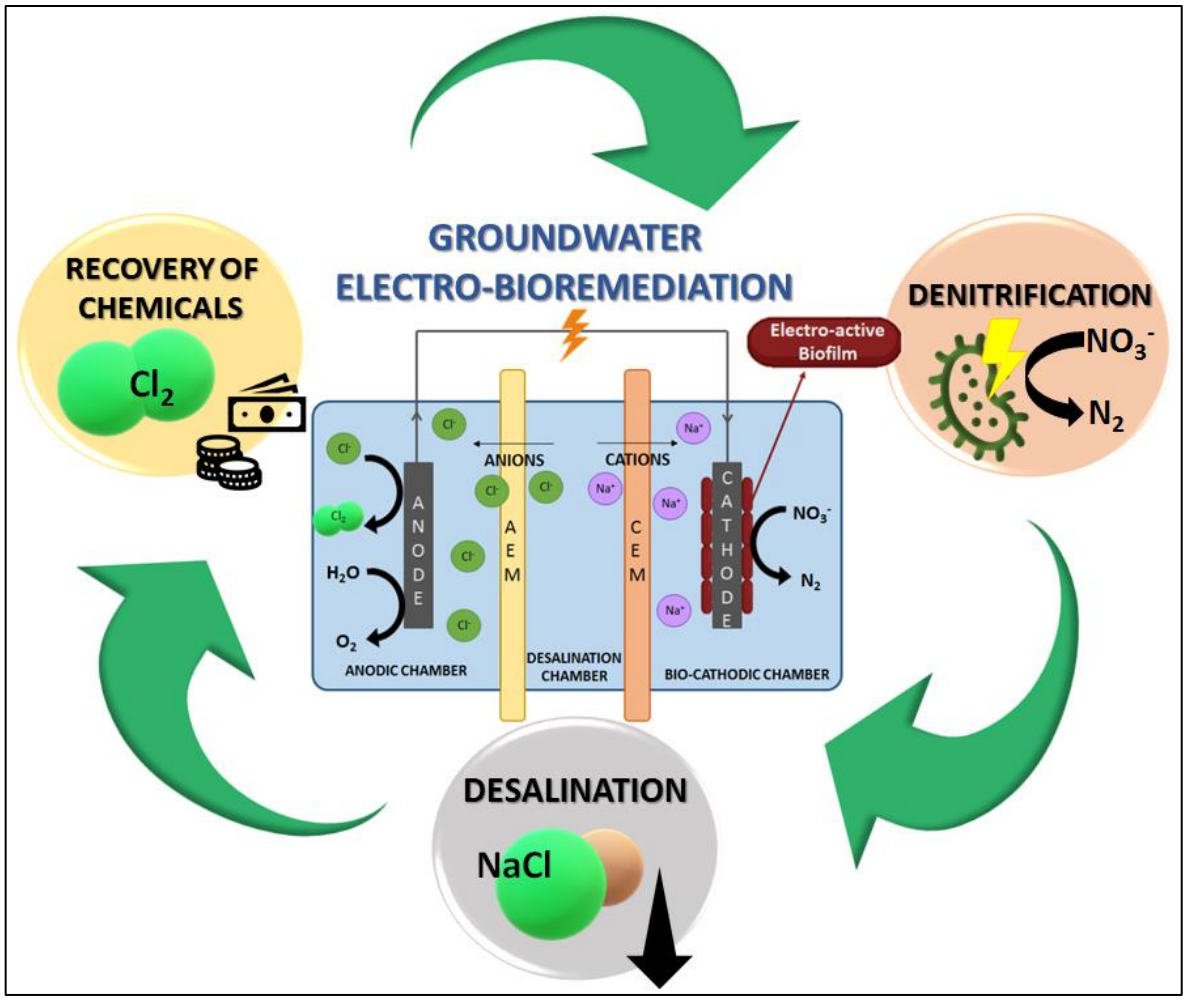

Figure AII-1. Schematic diagram summarising the present study.

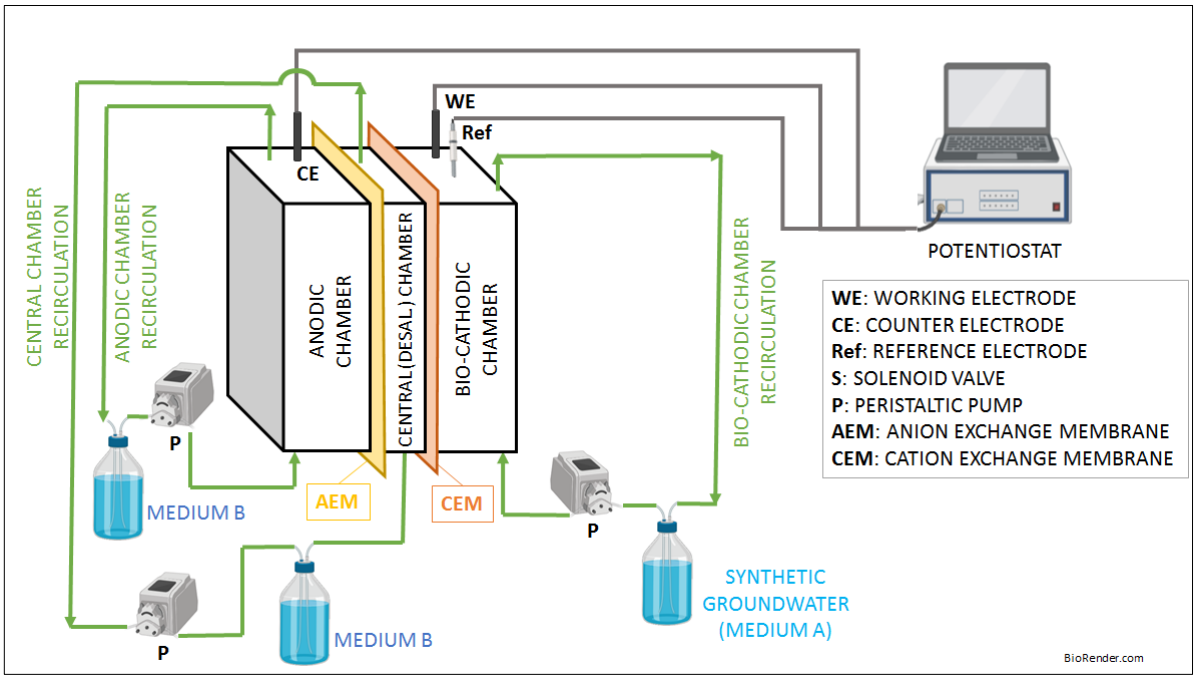

Figure AII-2: Schematic process flow diagram during Phase 1 of experimentation.

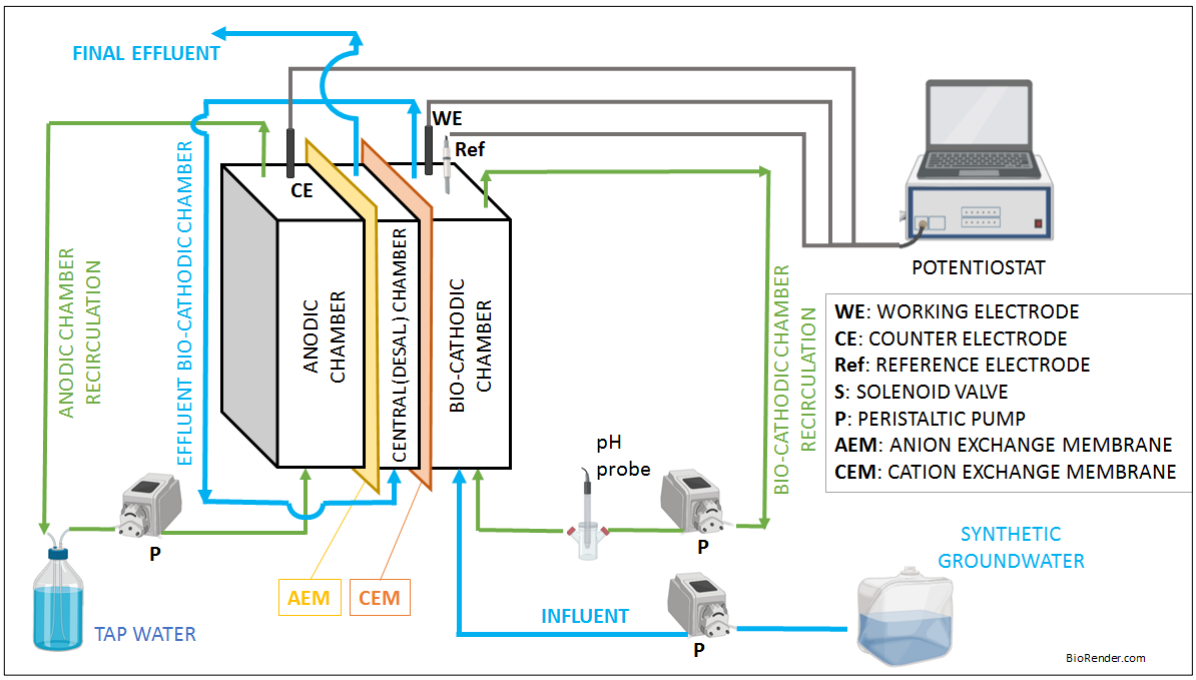

Figure AII-3: Schematic process flow diagram during Phases 2 and 3 of experimentation.

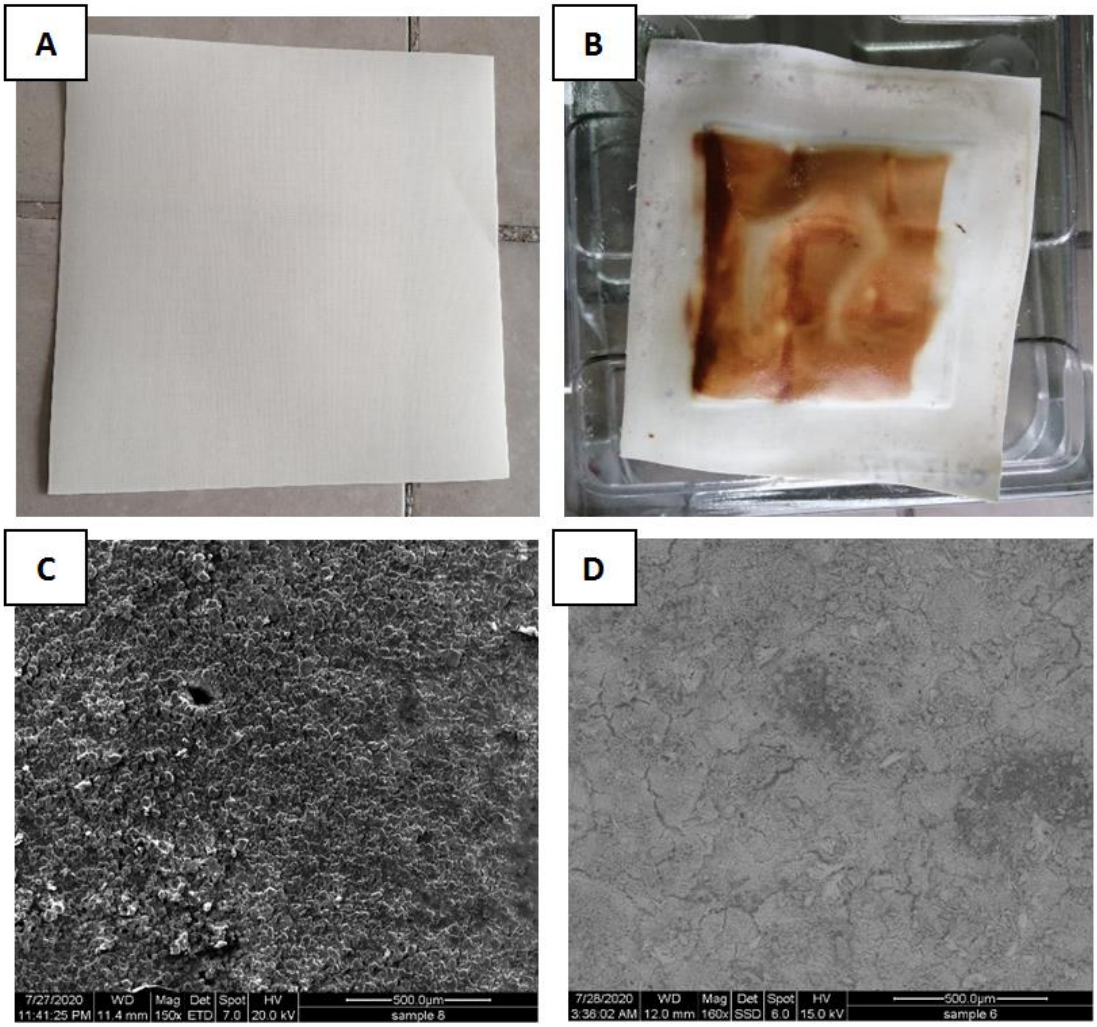

Figure AII-4: Pictures and SEM images of the anion exchange membrane before (A,C) and after (B,D) the sudden increase in pH occurred in the bio-cathodic compartment during Phase 3.

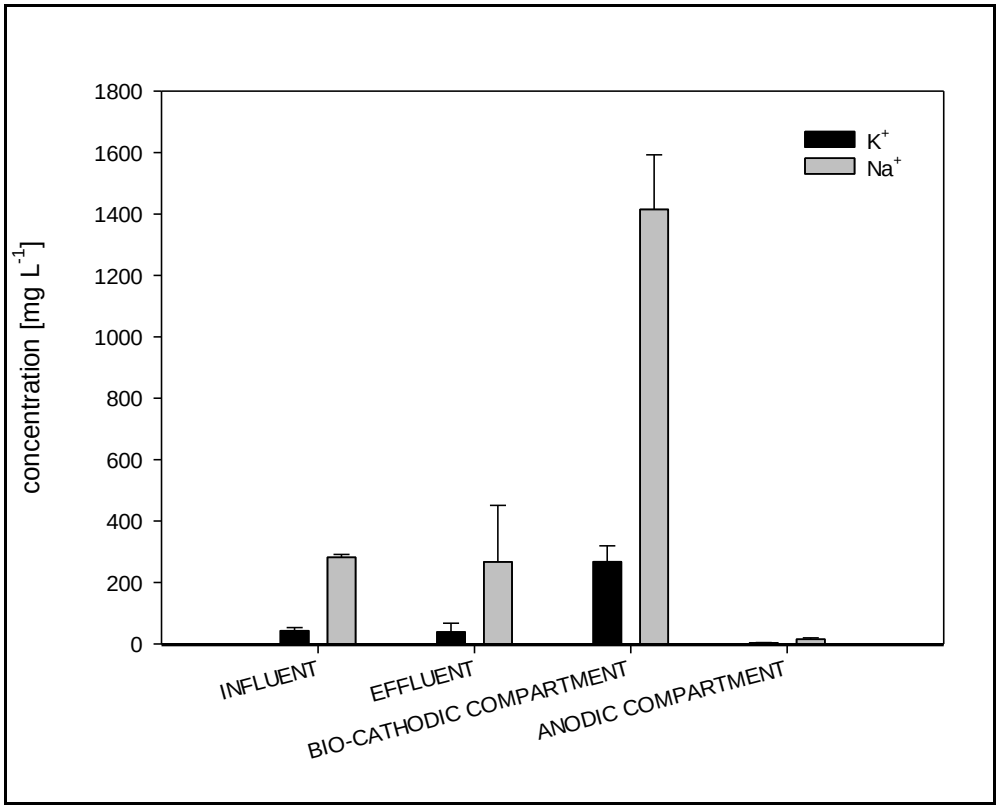

Figure AII-5: Distribution of the main cations in the bio-cathodic and anodic compartments, and in reactors influent and effluent, during Phase 4.

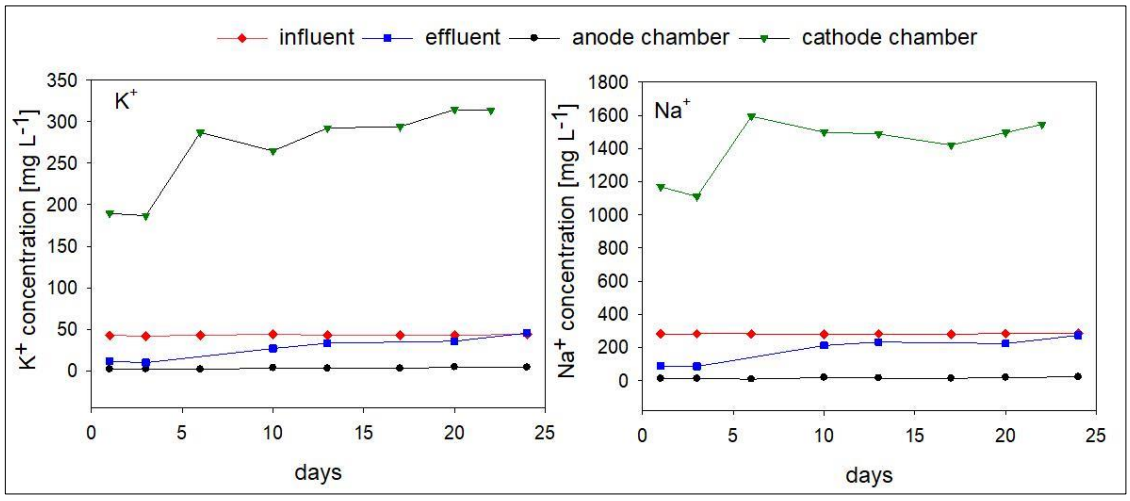

Figure AII-6: Representative trend of potassium and sodium concentrations observed in during Phase 4.

5 EFFECT OF HYDRAULIC RETENTION TIME ON THE ELECTRO-BIOREMEDIATION OF NITRATE IN SALINE GROUNDWATER[1]

Abstract

Bioelectrochemical systems (BES) have proven their capability to treat nitrate-contaminated saline groundwater and simultaneously recover value-added chemicals (such as disinfection products) within a circular economy-based approach. In this study, the effect of the hydraulic retention time (HRT) on nitrate and salinity removals, as well as on free chlorine production, was investigated in a 3-compartment BES working in galvanostatic mode, with the perspective of process intensification and future scale-up. Reducing the HRT from 30.1±2.3 to 2.4±0.2 hours led to a corresponding increase in nitrate removal rates (from 17±1 up to 131±1 $mgNO_3^-$-N $L^{-1}d^{-1}$), although a progressive decrease in desalination efficiency (from 77±13 to 12±2%) was observed. Nitrate concentration and salinity close to threshold limits indicated by the World Health Organization for drinking water, as well as significant chlorine production, were achieved with an optimal HRT of 4.9±0.4 h. At the optimal HRT, specific energy consumption was low ($6.8 \cdot 10^{-2} \pm 0.3 \cdot 10^{-2}$ kWh $g^{-1}NO_3^-N_{removed}$), considering that the supplied energy supports three processes simultaneously. A logarithmic equation correlated well with nitrate removal rates at the applied HRTs and may be used to predict BES behaviour with different HRTs. The results provide useful information for the scale-up of BES treating multi-contaminated groundwater.

[1]The work described in this chapter will be submitted to a peer-review international ISI Journal for its possible publication.

5.1 Introduction

Groundwater is a critical freshwater reservoir, and it is fundamental for global water and food security. The spread of contaminants in groundwater can limit its use as drinking water, so actions must be taken to ensure a safe drinking water supply (Janža, 2022). Bioelectrochemical systems are emerging as sustainable alternatives for the treatment of contaminated groundwater. Such systems are based on the ability of electroactive microorganisms to perform oxidation and reduction reactions by exchanging electrons with an electrode (Pous et al., 2018). Therefore, they are particularly suitable for groundwater treatment, as they promote bioremediation without the supply of chemicals as electron acceptors/donors.

Most of the studies focus on the removal of one type of contaminant at a time (e.g., nitrate, organics, heavy metals, calcium, etc.), which is useful for a deep understanding and optimisation of the processes involved (Beretta et al., 2020; Ceballos-Escalera et al., 2022, 2021; Palma et al., 2018; Sevda et al., 2018; Verdini et al., 2015). However, groundwater matrices are highly complex and heterogeneous influencing the behaviour of BES and representing a key aspect of process development and scale-up. One of the most intriguing challenges that researchers are currently facing is thus the application of BES to the bioremediation of multi-contaminated groundwater.

Among contaminants, nitrate is often found in groundwater at high concentrations co-existing with other pollutants. Nitrate contamination in groundwater is frequently due to inefficient farming practices and careless management of livestock activities (Kwon et al., 2021; Serio et al., 2018). The Nitrates Directive (91/767/EU) sets a nitrate concentration limit of 50 $mgNO_3^- L^{-1}$ (11.3 $mgNO_3^-$-N L^{-1}) in drinking water for human health, safety, and environmental protection. In this framework, the possibility of simultaneously removing nitrates and other contaminants from groundwater is of particular interest.

The presence of co-contaminants associated with nitrate can result from natural sources (e.g., arsenic derived from the reductive dissolution of arsenic-rich minerals) and anthropogenic activities (e.g., perchlorate derived from the production of car airbags, fireworks and fertilisers, Lian et al., 2016). Ceballos-Escalera et al. (2021) successfully removed nitrate and arsenic from groundwater using a tubular BES. The treatment combined nitrate reduction to dinitrogen gas and arsenite oxidation to arsenate (which shows less toxicity, solubility and mobility) within

the same reactor. In this way, the ability of BES to denitrify without being affected by arsenite and under low electrical conductivity conditions (about 1 mS cm^{-1}) was demonstrated.

Wang et al., 2021 investigated the simultaneous removal of nitrate and perchlorate from groundwater with cathodic potential regulation. Results demonstrated that the mechanism of nitrate and perchlorate reduction in the BES was the direct electron transfer from the cathode to the bacteria, and the dominant bacterial community on the cathode was proven to have the ability to reduce nitrate and perchlorate. However, regardless of the potential applied to the cathode or not, nitrate inhibited the reduction of perchlorate.

The occurrence of high nitrate (30.0 mgNO_3^--N L^{-1}) and salinity levels (3.3±0.3 mS cm^{-1}) in groundwater was recently dealt with by Puggioni et al. (2021) (Chapter 4). In this study, in contrast to the previous studies where co-contaminants required removal by oxidation/reduction, the treatment coupled reduction with a separation of co-contaminants. A proof-of-concept based on a 3-compartment BES allowed the simultaneous removal of nitrate (39±1 mgNO_3^--N L^{-1} d^{-1}) and salinity (chloride removal rate of 13±2 gCl^- L^{-1} d^{-1}) from groundwater but also the production of value-added chemicals (i.e., free chlorine). The electroactive biomass attached to the cathode carried out the denitrification in the bio-cathodic compartment, while desalination took place in the central compartment thanks to electrochemically driven migration of ions across the two ion exchange membranes. In the anodic compartment, anions, mainly chloride, accumulated. Part of the accumulated chloride was converted into chlorine, which represents a value-added product that could also be used for disinfection in water treatment plants. The galvanostatic operation (applied current: 0.16 mA $cm^{-2}_{membrane}$) with pH control (< 9) in the bio-cathodic compartment resulted in high nitrogen and salinity removal efficiencies (69±2% and 63±5% respectively) and significant recovery of free chlorine (26.8±3.4 mgCl_2 L^{-1}). Standard quality requirements for drinking water in terms of nitrate concentration (91/767/EU) and electrical conductivity (98/83/CE) were successfully met with this cell configuration. However, considering the high capital costs required to implement BES-based technologies (Zhang and Angelidaki, 2013), and the need to promote the scale-up of these systems, the process needs to be further optimised by increasing nitrate removal rates, reducing energy consumption. The performance of such systems could be limited by the hydrodynamics and the corresponding substrate distribution (Vilà-Rovira et al., 2015). Hydrodynamics are reinforced at higher flowrates (lower HRTs). This strategy was confirmed by Ceballos-

Escalera et al., 2021 and Pous et al., 2017, reaching higher denitrifying capacities in denitrifying BES. However, the role of the HRT may be different in more complex groundwater and BES configurations like the one described by Puggioni et al. (2021) (Chapter 4), where biotic (e.g., nitrate removal) and abiotic (i.e., desalination, chloride removal and chlorine production) processes co-exist in the same reactor. In the present work, the effects of increasing influent flowrates on simultaneous denitrification and desalination of groundwater in a 3-compartment cell were investigated, providing helpful information for its optimisation with a view to a future application at pilot scale. Moreover, the bacterial communities of biomass established under the galvanostatic mode, used in the present study, and potentiostatic mode, previously tested by Puggioni et al. (2021) (Chapter 4), were characterised and compared.

5.3 Materials and methods

5.3.1 Reactor set-up

Two identical 3-compartment cells made of polycarbonate were used (Puggioni et al., 2021 - Chapter 4). The bio-cathode compartment contained the graphite felt cathode electrode (64 cm^2, degree of purity 99.9%, AlfaAesar, Germany), and it was physically separated from the central compartment by a cation exchange membrane (CEM 7000, Membrane International Inc., USA). The anode compartment, containing the anode electrode consisting of a titanium mesh coated with mixed metals oxide (Ti-MMO, 15 cm^2, NMT-Electrodes, South Africa), was physically separated from the central compartment by an anion exchange membrane (AEM 7001, Membranes International Inc., USA). A reference electrode (Ag/AgCl, +0.197 V vs SHE, mod. MF2052, BioAnalytical Systems, USA) was placed in the bio-cathode compartment. Cathode, anode, and reference electrodes were connected to a multichannel potentiostat (Ivium technologies, IviumNstat, NL). The system was thermostatically controlled at 25±1 °C.

5.3.2 Groundwater composition

A synthetic medium mimicking nitrate concentration and salinity of groundwater from the nitrate vulnerable zone of Arborea (Sardinia, Italy) was fed to the bio-cathode compartment. This medium contained 216.6 mg L^{-1} KNO_3 (corresponding to 30.0 mgNO_3^--N L^{-1}); 10 mg L^{-1} NH_4Cl (corresponding to 2.6 mgNH_4^+-N L^{-1}), 4.64 mg L^{-1} KH_2PO_4; 11.52 mg L^{-1} K_2HPO_4; 350 mg

L^{-1} $NaHCO_3$; 2000 mg L^{-1} NaCl and 100 µL L^{-1} of trace elements solution (Patil et al., 2010). The media was prepared using distilled water and pre-flushed with N_2 gas for 15 minutes to avoid any presence of oxygen. The medium's electrical conductivity and pH were 3.06±0.5 mS cm^{-1} and 8.2±0.3, respectively.

5.3.3 Experimental procedure

The cells were started-up and tested as described by Puggioni et al. (2021). The bio-cathode compartment was continuously fed with groundwater, and the effluent was sent into the central compartment to achieve desalination. Tap water was recirculated in the anode compartment and replaced periodically (about every 10 days). The potentiostat was set in galvanostatic mode at current of 10 mA (0.16 mA $cm^{-2}_{membrane}$). A pH control (< 9) was implemented to avoid excessive pH increases in the bio-cathode compartment by dosing HCl (1 M) in the bio-cathode recirculation line. The probe for continuous pH measurement (Mettler Toledo, mod. InPro 3253i/SG/225, USA) was connected to a transmitter (Mettler Toledo, mod. M300, USA), which recorded data every 10 minutes.

The enhancement of electro-bioremediation systems must be linked to the treatment capacity. In this sense, hydraulic retention time (HRT) was used as the operational parameter as presented in Table 5.1.

Different HRTs were tested, from the previous proof-of-concept (Puggioni et al. 2021) value 30.1±2.3 (Test 1) to 2.4±0.2 h (Test 6), by increasing the influent flowrate. During Test 7, the same HRT of Test 5 (4.9±0.4 h) was applied to confirm the stability of the system. Each HRT was maintained for about one month. The nitrate concentration in the influent was also maintained at 29.3±3.5 mgNO_3^--N L^{-1}.

Table 5.1. Experimental procedure.

Tests	Influent flow rate	HRT Bio-cathode + central compartment	HRT' central compartment	NO_3^--N loading rate
	[L d^{-1}]	[h]	[h]	[mg L^{-1} d^{-1}]
1	0.11	30.1±2.3	6.7±0.3	23.57±1.84
2	0.17	20.3±1.5	4.5±0.2	35.14±2.39
3	0.31	10.9±0.8	2.4±0.1	62.61±3.90
4	0.46	7.3±0.6	1.6±0.1	82.21±3.07
5	0.68	4.9±0.4	1.1±0.05	125.48±2.98
6	1.42	2.4±0.2	0.5±0.02	261.05±16.07
7	0.68	4.9±0.4	1.1±0.05	130.92±11.27

5.3.4 Analytical methods

Samples were periodically drawn from influent (once per week), effluent (three times per week), bio-cathode and anode compartments (three times per week) in order to evaluate overall cell performances. The same samples from the duplicate cell were taken once a week to confirm the process progress of the main cell. Liquid samples were analysed for quantification of anions, i.e., chloride (Cl^-), nitrite (NO_2^--N), nitrate (NO_3^--N), phosphate (PO_4^{3-}), and sulphate (SO_4^{2-}), using an ion chromatograph (ICS-90, Dionex-Thermofisher, USA) equipped with an AS14A Ion-PAC 5 µm column. Samples were filtered (acetate membrane filter, 0.45 µm porosity) and properly diluted with grade II water. The concentrations of the main cations, i.e., potassium (K^+) and sodium (Na^+), were determined using an ICP/OES (Varian 710-ES, Agilent Technologies, USA): samples were filtered (acetate membrane filter, 0.45 µm porosity), acidified (nitric acid, 1% v:v) and diluted with grade I water.

Electrical conductivity and pH were measured using a benchtop meter (HI5522, Hanna Instruments, Italy).

The concentration of free chlorine was analysed using spectrophotometric techniques (DR1900, Hach Lange, Germany) and the DPD (N,N-diethyl-p-phenylenediamine) free chlorine method (DPD free chlorine reagent powder pillows Cat. 2105569, Hach Lange, Germany).

Nitrous oxide (N_2O) was measured using an N_2O liquid-phase microsensor (Unisense, Denmark) located in the effluent line of the reactors, thanks to a dedicated glass measuring cell.

The resulting bio-cathode potentials were recorded every five minutes through potentiostat (Ivium technologies, IviumNstat, NL). Cell potential was periodically checked using a multimeter (K2M, mod. KDM-600C, Italy).

The bacterial community composition of the bio-catalytic biomass was characterised (full details of the analyses carried out and the results are shown in Appendix III).

5.3.5 Calculations

Nitrate Removal Efficiency (N-RE) and Nitrate Removal Rate (N-RR) were calculated according to equations 1 and 2, respectively:

$$\mathrm{N-RE\ [\%]} = \frac{C_{NO_3^- - N(inf)} - C_{NO_3^- - N(eff)}}{C_{NO_3^- - N(inf)}} \times 100 \quad \textbf{(1)}$$

$$\mathrm{N-RR\ [mg\ N\ L^{-1}\ d^{-1}]} = \frac{C_{NO_3^- - N(inf)} - C_{NO_3^- - N(eff)}}{HRT} \quad \textbf{(2)}$$

Where $C_{NO_3^-N(inf)}$ and $C_{NO_3^-N(eff)}$ [mg L^{-1}] are nitrate concentrations in the influent and the effluent, respectively, while HRT [d] is the hydraulic retention time considering the cathodic and central compartments volumes.

The desalination performance was evaluated by calculating the electrical conductivity removal efficiency (EC-RE, equation 3), the chloride removal efficiency (Cl^--RE, equation 4), and the chloride removal rate (Cl^--RR, equation 5).

$$\mathrm{EC-RE\ [\%]} = \frac{EC_{(inf)} - EC_{(eff)}}{EC_{(inf)}} \times 100 \quad \textbf{(3)}$$

$$\mathrm{Cl^- - RE\ [\%]} = \frac{C_{Cl^-(inf)} - C_{Cl^-(eff)}}{C_{Cl^-(inf)}} \times 100 \quad \textbf{(4)}$$

$$\mathrm{Cl^- - RR\ [mg\ L^{-1}\ d^{-1}]} = \frac{C_{Cl^-(inf)} - C_{Cl^-(eff)}}{HRT'} \quad \textbf{(5)}$$

where $EC_{(eff)}$ [mS cm^{-1}] and $C_{Cl-(eff)}$ [mg L^{-1}] represent the effluent electrical conductivity and chloride concentration, respectively. $EC_{(inf)}$ and $C_{Cl-(inf)}$ correspond to the electrical conductivity and chloride concentration of the solution in the bio-cathodic compartment (i.e., the influent to the central compartment), respectively, to consider the chloride input due to the acid dosage in this compartment. HRT' [d] is the hydraulic retention time of the central compartment.

The coulombic efficiency for nitrate reduction (εNO_x) was calculated according to equation 6 (Virdis et al., 2008):

$$\varepsilon NO_x[\%] = \frac{I}{n\,\Delta C_{NO_x} Q_{in} F} \times 100 \quad \textbf{(6)}$$

where I is the fixed current [A]; n is the number of electrons that can be accepted by 1 mol of oxidised nitrogen compound present in the bio-cathodic compartment assuming N_2 is the final product; ΔC_{NOx} is the difference between the nitrate concentration in the cathodic influent and effluent [molNO_3^--N L^{-1}]; Q_{in} is the influent flow rate [L s^{-1}]; F is Faraday's constant [96485 Ce^-mol^{-1}].

The current efficiency (CE) was expressed as the percentage of the charge associated with the chloride removed from the central compartment to the amount of electric charge transferred (ECT) across the membranes (Ramírez-Moreno et al., 2019). CE [%] and ECT [C m^{-3}] were calculated using equations 7 and 8, respectively:

$$CE\ [\%] = \frac{v\,z\,F\left(C_{Cl^-(inf)} - C_{Cl^-(eff)}\right)}{ECT} \times 100 \quad \textbf{(7)}$$

$$ECT\ [C\ m^{-3}] = \frac{\int I\,dt}{V} \quad \textbf{(8)}$$

where v and z represent the stoichiometric coefficient and the valence of the chloride ion, respectively; V [m^{-3}] is the volume of water treated; dt is the time [s].

The specific energy consumption (SEC) was calculated according to equation 9 (Djouadi Belkada et al., 2018):

$$SEC\ [kWh\ m^{-3}] = \frac{I \int E\,dt}{V} \textbf{(9)}$$

where E is the cell potential [V].

5.4 Results and discussion

5.4.1 Effect of the HRTs on the denitrification and desalination performances

The system's enhancement was tested by increasing the influent flowrate and, thus, reducing the HRT. Figure 5.1 shows the average NO_3^--N loading and removal rates at different influent flowrates. The loading rate changed from 23.6±1.8 $mgNO_3^-$-N $L^{-1}d^{-1}$ in Test 1 to 261±16 $mgNO_3^-$-N $L^{-1}d^{-1}$ in Test 6. Nitrogen Removal Rate also increased (from 16.9±1.3 $mgNO_3^-$-N $L^{-1}d^{-1}$ in Test 1 to 130.8±14.7 $mgNO_3^-$-N $L^{-1}d^{-1}$ in Test 6) but did not follow the same trend as the NLR, since a gradual deviation was observed.

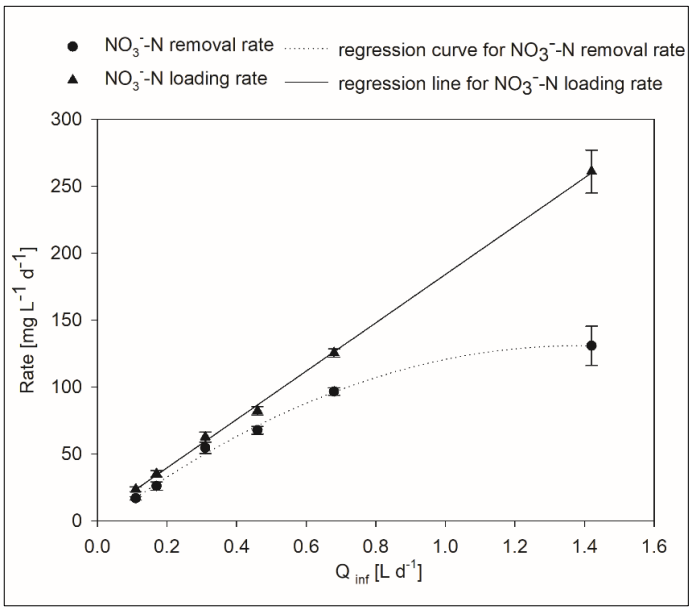

Figure 5.1. Average trend in nitrate-nitrogen loading into the system and nitrate-nitrogen removal rate as influent flowrate (Q_{inf}) increases.

The increase in the NRR with the influent flowrate could be explained by an increase in the denitrification activity of the autotrophic biomass due to the proper supply of nitrate and its improved distribution (Pous et al., 2017).

Despite the increasing NRR, nitrate concentration in the effluent started to increase from Test 4 onward (Figure 5.2). The nitrate effluent concentration remained below the threshold limits (<11.3 $mgNO_3^-$-N L^{-1} according to the Nitrate Directive 91/767/EU) throughout the experiment

except during Test 6 (flowrate 1.42 L d^{-1} and HRT of 2.4±0.2 h) (13.5±2.8 mgNO_3^--N L^{-1}, corresponding to a N-RE of 50±8 %).

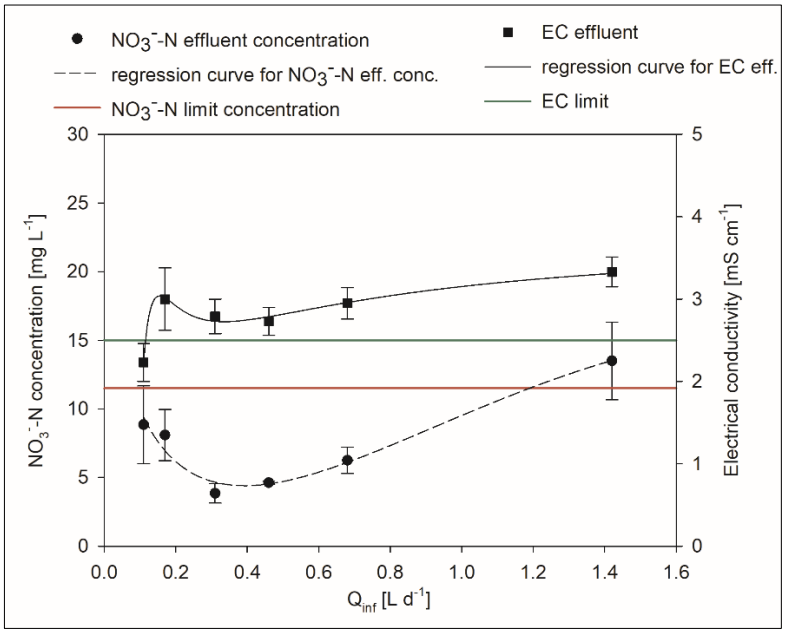

Figure 5.2. Average trend of nitrate concentration and electrical conductivity (EC) in the effluent as influent flowrate increased.

During Test 6, low concentrations of nitrite and nitrous oxide were detected in the effluent (0.22±0.08 mgNO_2^--N L^{-1} and up to 0.5 mgN_2O-N L^{-1}, respectively). Therefore, it is evident that during Test 6 (influent flowrate of 1.42 L d^{-1}), limiting operating conditions were reached for the system regarding nitrate removal.

Interestingly, the increase in nitrate removal rate as HRT decreased was also observed in previous studies. Figure 5.3 compares the trend in nitrate removal rate versus the HRT for the current study and those reported by Pous et al. (2017) and Ceballos-Escalera et al. (2021), exploiting tubular systems with hydraulically connected anode and cathode compartments. Although the systems were highly heterogeneous in terms of configuration (3-chamber plate cell vs tubular cells), materials (graphite felt vs granular graphite), and operating conditions (galvanostatic vs potentiostatic modes), the same mathematical model was able to fit the observed NRR vs HRT relationship.

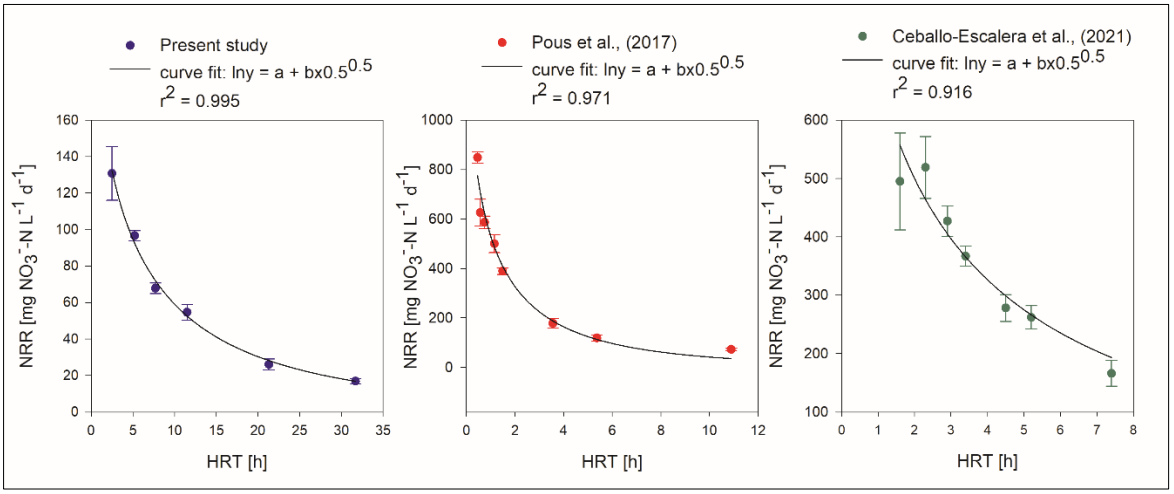

Figure 5.3. Comparison of nitrate removal rate (NRR) trends versus the HRT for the present study with that reported by Pous et al. (2017) and Ceballos-Escalera et al. (2021) and modelling of results.

This result is interesting, as it confirms that increasing the influent flowrate (and thus reducing the HRT) can positively influence denitrification activity. Therefore, regardless of the type of configuration or operating conditions used, that process behaviour with different HRTs may be reasonably predicted, providing useful information in the perspective of reactor scale-up.

A final test (Test 7) was carried out by bringing the HRT value back to that corresponding to Test 5 (i.e., 4.9±0.4 h) to restore the denitrifying process and verify microbial activity. The performance in terms of nitrate removal observed during Test 5 (N-RE = 77±3%, and N-RR = 96.7±2.8 mgNO_3^--N $L^{-1}d^{-1}$) was immediately restored during Test 7, resulting in an average N-RE of 89±4% and N-RR of 112±7.5 mgNO_3^--N $L^{-1}d^{-1}$. In addition, while in Test 6 (HRT of 1.4 h), the effluent concentration of nitrate exceeded the legal limits (13.5±3 mgNO_3^--N L^{-1}), the concentration was below the limits in Tests 5 and 7 (6±1 and 3±1 mgNO_3^--N L^{-1}, respectively). No nitrite or nitrous oxide were detected in the outlet during Test 7. The slight increase in performance observed between Test 5 and Test 7 demonstrates that biomass growth may have contributed a small part to the increase in denitrifying performance. This result confirms the limiting conditions for denitrification reached in Test 6, during which a general decline in terms of nitrate removal and production of intermediates were observed. However, this condition turned out to be reversible according to Test 7, demonstrating not a biomass inhibition condition but just an operational limit in Test 6. Since the applied current was initially much higher than that theoretically required to remove the nitrate input (10 mA applied vs approx. 1.4 mA theoretically required in Test 1), the coulombic efficiency for nitrate removal was always

above 100%, decreasing as the HRT decreased, and reaching values close to 100% during Test 6.

An almost opposite trend to that of nitrate removal was observed for the desalination process. The desalination process showed the best performance in Test 1 (with an effluent electrical conductivity of 2.2±0.2 mS cm^{-1}), which met the required limit of 2.5 mS cm^{-1} (98/83/CE Directive) but exceeded this value in Test 2 and gradually worsened in subsequent tests (Figure 5.2). Figure 5.4 shows the trend of electrical conductivity in the influent and effluent of the central desalination compartment and the desalination efficiency. As expected, the overall electrical conductivity removal rate throughout the experiment was 23.4±7.3 mS cm^{-1} d^{-1}, so it did not vary substantially as the HRT decreased. Thus, the desalination trend was limited only by a physico-chemical effect due to insufficient charge replenishment as HRT decreases. This effect could easily be overcome by increasing the applied current in proportion to the increase in influent flowrate.

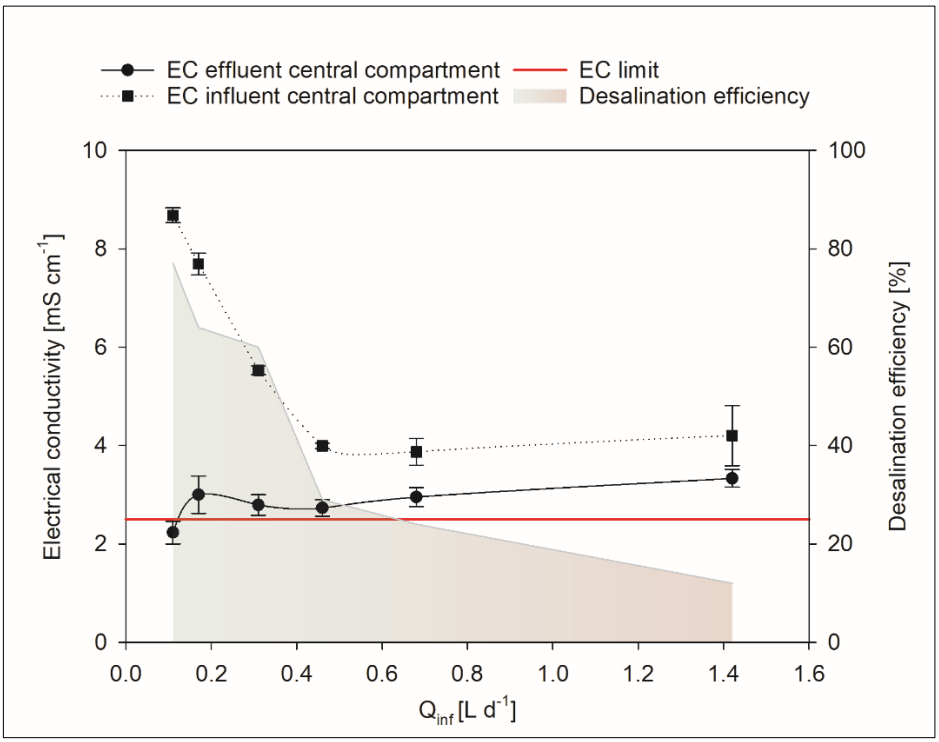

Figure 5.4. Average trend of central compartment influent and effluent electrical conductivity, and desalination efficiency versus the influent flowrate. The red line indicates the electrical conductivity limit for freshwater (2.5 mS cm^{-1}).

The influent electrical conductivity of the central desalination compartment (corresponding to the effluent of the bio-cathode compartment) dropped from 8.7±0.2 mS cm^{-1} in Test 1 to 4.2±0.6 mS cm^{-1} in Test 6, likely as a result of the increased influent flowrate which probably

led to a faster turnover of the solution in the bio-cathodic compartment, reducing the accumulation of both Cl^- ions due to the acid dosage, and cations migrating from the central compartment through the CEM. The average chloride concentration measured in the cathode compartment (and thus including the influent and acid dosage) decreased from 3622±443 in Test 1 to 1385±56 $mgCl^- L^{-1}$ in Test 6, while the sodium concentration decreased from 2355±370 to 1040±182 $mgNa^+ L^{-1}$, respectively, for Test 1 and Test 6.

On the other hand, the effluent electrical conductivity increased slightly to 3.3 mS cm^{-1}. The electrical conductivity trend in the bio-cathode compartment and effluent trend resulted in a reduction of the overall desalination efficiency, which dropped to 12±2% in the last test (from 77±13% in Test 1). Coherently, the current efficiency related to the removal of chloride in the central compartment decreased during the experiment from 89±14% in Test 1 to 59±15% in Test 6. This performance could be related to the variation of the influent flowrate and may be explained by insufficient HRT (passing from 6.7±0.3 h in Test 1 to 0.5±0.02 h in Test 6) in the central desalination compartment. Calculating the theoretical quantity of chloride ions that can be transferred through the membranes by applying a current of 10 mA to the varying HRT gives 2.8 g L^{-1} for Test 1 and 0.22 g L^{-1} for Test 6. These values are very close to those actually obtained and correspond to 2.5±0.4 and 0.13±0.03 $gCl^-_{removed} L^{-1}$, respectively, for Test 1 and Test 6, confirming the above results. Thus, the HRT decrease did not allow sufficient ions to migrate through the membranes to observe a significant reduction in effluent electrical conductivity. The adverse effect of low HRT on desalination performance was already demonstrated for the technology closest to the present study, i.e., MDCs (microbial desalination cells). Indeed, Jingyu et al. (2017) reported that HRT influences the removal of total dissolved solutes (TDS), increasing with the HRT, resulting in a higher current generation in MDC.

Chlorine production in the anodic compartment was monitored throughout the whole experimentation, and an average chlorine concentration of 14±3 $mgCl_2 L^{-1}$ was observed. An essential aspect of monitoring is the durability of materials in contact with chlorine, as it is a powerful oxidant, and it tends to attack and damage them. For this reason, it was decided to replace the solution in the anodic compartment periodically (about every 10 days, producing an average concentration of 16±1 $mgCl_2 L^{-1}$) to avoid system damage. As described in Chapter 4, higher values of chlorine concentration (approx. 30 $mgCl_2 L^{-1}$) were obtained by Puggioni et al.

(2021) in the same system at the highest HRT tested, but without the periodic replacement of the solution.

5.4.2 Considerations on pH development during the process

Increasing the influent flow rate also had an effect on pH trend in the different compartments. pH control plays a significant role in ensuring optimal denitrifying microbial activity, as a neutral pH is strictly necessary for this biological process (Clauwaert et al., 2009). Such control has become essential to optimise water desalination performance. Several studies demonstrated that the pH gradient between the anode and cathode compartments could lead to potential losses (of approximately 0.095 V) that adversely affect the desalination efficiencies of MDCs (Jingyu et al., 2017).

During the experiment, the periodic dosage of acid to control the pH in the bio-cathodic compartment remained constant all over the experimental period. This occurrence resulted in a difference mainly in the effluent pH as a function of the influent flowrate. Figure 5.5 shows that while the influent pH mainly remained constant, the effluent pH increased from near-acidic (4.1±1.2) in Test 1 to slightly alkaline (7.8±0.3) in Test 6.

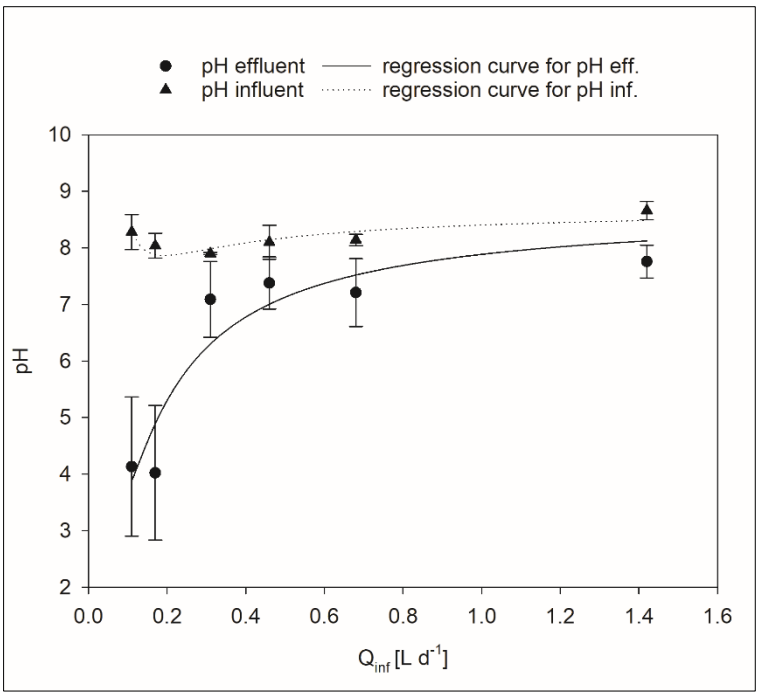

Figure 5.5. Average influent and effluent pH trend versus the influent flowrate.

Acidic pH values in the effluent corresponding to the first tests may be due to the higher HRT in the central desalination compartment (6.7±0.3 h in Test 1) that allowed protons produced at the anode (pH 2.0±0.7) to pass through the AEM, because of their small size. By reducing the HRT (to 0.5±0.02 h in Test 6) as the influent flowrate increased, the solution replacement led to a slowing down of the pH increase in the bio-cathode compartment and a lower passage of protons through the AEM into the effluent. In addition, the acid dosage per m^3 of treated water was reduced as the influent flowrate increased, which means lower operating costs for pH balancing.

5.4.3 Sustainability perspective on the application of BES for simultaneous denitrification and desalination

In order to move towards scaling-up of the technology for groundwater treatment, the system must be both technically and economically feasible. For this reason, a preliminary cost-benefit analysis was carried out comparing the main operational costs associated with the technology and the potential benefits obtained according to experimental data.

The operating costs of a technology depend significantly on the energy consumption of the process. Figure 5.6 presents the profiles of the specific energy consumption (SEC) per gram of NO_3^--N removed and SEC per volume of water treated as a function of influent flowrate and compared with the trend in nitrate removal rate.

During the experiment, an optimisation was observed not only in the removal of nitrate but also in energy consumption, which was significantly reduced to values of $5.1 \cdot 10^{-2} \pm 0.7 \cdot 10^{-2}$ kWh $g^{-1}NO_3^-\text{-}N_{removed}$ and 0.5±0.03 kWh $m^{-3}_{water\ treated}$ (starting from $35.2 \cdot 10^{-2} \pm 3.6 \cdot 10^{-2}$ kWh $g^{-1}NO_3^-\text{-}N_{removed}$ and 6.1±0.4 kWh $m^{-3}_{water\ treated}$, respectively).

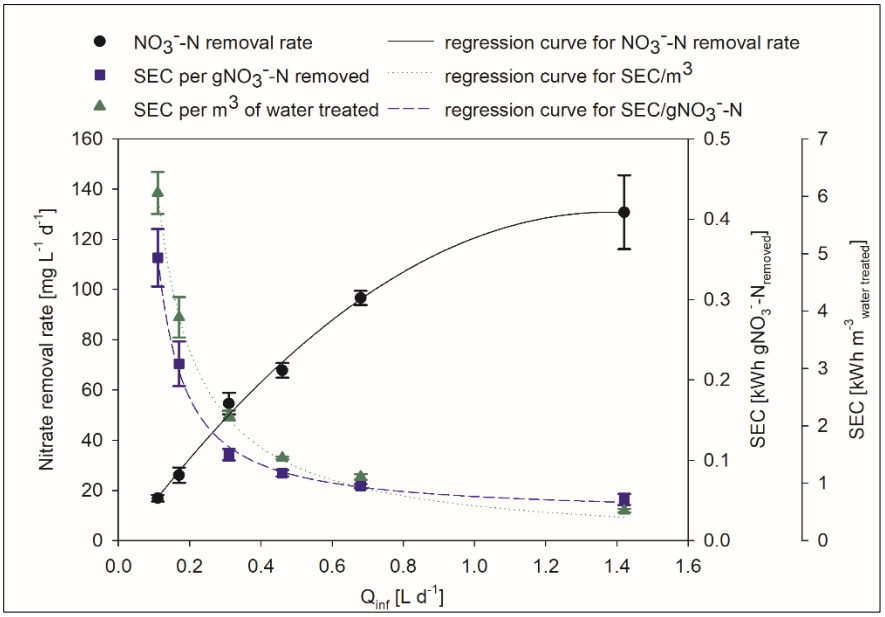

Figure 5.6. Average trends in specific energy consumed (SEC) per gram of nitrate-nitrogen removed and per volume of water treated, and nitrate removal rate as the inlet flow rate changes.

Pous et al. (2015) reported a list of specific energy consumptions for various technologies such as bioelectrochemical systems (BES), biofilm electrode reactor (BER), membrane bioreactor (MBR), electrodialysis (ED) and reverse osmosis (RO) (Zhao et al., 2011; Twomey et al., 2010; McAdam and Judd, 2008; Ortiz et al., 2008). Compared to the reported values, the energy consumption per m^3 of treated water was within the consumption range reported for desalination technologies, i.e., electrodialysis and reverse osmosis (between 0.04 and 2.09 kWh $m^{-3}_{treated\ water}$). The energy consumption per gram of nitrate removed obtained in the present study was in line with those of the technologies reported for nitrate removal only (BES and BER mainly), thus between $0.16 \cdot 10^{-2}$ and $7 \cdot 10^{-2}$ kWh $g^{-1}NO_3^-$-$N_{removed}$. Specifically, the values obtained in this study are closer to those of BER ($7 \cdot 10^{-2}$ kWh $g^{-1}NO_3^-$-$N_{removed}$), which applies a potential difference between the electrodes, in contrast to BES where the potential of the cathode electrode is fixed. This type of catalytical operation produces hydrogen in the cathode compartment, which is then used by bacteria to reduce nitrate. In the present study, the current was fixed, and the potential established at the cathode (approximately -1.3 V vs Ag/AgCl) was suitable for hydrogen production. According to Pous et al. (2015), fixing the cathode potential makes it possible to control the reduction of nitrate in the end products and implies less energy consumption. In the present study, however, the aim is not only to remove nitrate, but also to reduce the electrical conductivity of water, as well as the production of value-

added products (chlorine). In fact, during the process, part of the chloride accumulated in the solution of the anodic compartment is converted into free chlorine (Puggioni et al., 2021). Thus, the energy applied is used to carry out three processes simultaneously with consumption comparable to systems carrying out a single process (i.e., only denitrification or desalination). Under optimal operating conditions (HRT = 4.9±0.4 h), the total cost of energy consumption is 0.23 € m^{-3}, assuming an energy cost of 0.21 € kWh^{-1} (Eurostat, 2021). This value is competitive, considering that Ceballos-Escalera et al. (2022) estimated an operating cost of 0.14 € m^{-3} only for the bio-electrochemical nitrate removal.

From an economic point of view, the production of chlorine also plays an important role. Chlorine is a disinfectant agent that is highly used in water treatment plants, and its market value is growing significantly due to the rising demand from the agrochemical and pharmaceutical industries. Moreover, the rising demand for water treatment applications combined with increased awareness of better hygiene practices resulting from the impact of the Sars-CoV-2 pandemic will drive the need for chlorine among industrialists. Greaves et al. (2022) demonstrated that Sars-CoV-2 is successfully eliminated by disinfection with free chlorine in both deionised water and wastewater. Web-based chlorine market data show a forecast growth of the chlorine value at a CAGR (compound annual growth rate) between 3.5 and 4.5% for the period 2021-2027.

In the present study, up to 0.17 gCl_2 per $gCl^-_{removed}$ was produced, and this production can easily be increased by switching to a continuous mode in the anodic compartment or by stripping the chlorine produced. In fact, Puggioni et al. (2021) showed higher production rates at the start of the batch that gradually decreased to a plateau over long periods of operation. Therefore, switching to continuous mode would increase production rates while avoiding chlorine accumulation and excessive concentrations in the anode compartment. Optimising the chlorine capture system seems essential to maximise its production and reduce the contact time with the materials in the bioelectrochemical cell.

5.5 Conclusions

At higher flowrates (and lower HRT, between 7.3±0.6 and 2.4±0.2 h), an increase in nitrate removal was found, reaching removal rates of 131 $mgNO_3^-$-N $L^{-1}d^{-1}$. The operating limit for denitrification was reached at an HRT of 2.4±0.2 h, during which an effluent nitrate concentration above legal limits (91/767/EU) and the presence of intermediates were observed. Desalination performance was reduced (from 77±13% in Test 1 to 12±2% in Test 6), but the effluent electrical conductivity remained close to the legal limits (98/83/CE).

The tests carried out in the present study demonstrate the economic potential of the proposed technology thanks to the possibility of considerably reducing energy consumption while simultaneously increasing denitrification performance. Such result was achieved simply by acting on the treated flowrate (by reducing hydraulic retention times) and not on the reactor volumes, which would imply additional costs in terms of materials and space. Finally, chlorine production represents an enormous potential for possible real application as it would reduce the costs of any on-site disinfection or, in general, an economic return if it were to be resold.

Acknowledgements

This study was funded by Fondo di Sviluppo e Coesione 2014-2020, Patto per lo sviluppo della Regione Sardegna - Area Tematica 3 - Linea d' Azione 3.1, "Interventi di sostegno alla ricerca". Project SARdNAF "Advanced Systems for the Removal of Nitrates from Groundwater", ID: RASSR53158.

Thanks to Ms. Orietta Masala (CNR-IGAG) for her support with the ICP/OES analysis.

An acknowledgement is due to Prof. Elena Tamburini and Mr Riccardo Ardu (Department of Biomedical Sciences, University of Cagliari) for their support with the NGS analysis.

References

Batlle-Vilanova, P., 2019. Biogas upgrading, CO2 valorisation and economic revaluation of bioelectrochemical systems through anodic chlorine production in the framework of wastewater treatment plants. Sci. Total Environ. 9.

Beretta, G., Daghio, M., Espinoza Tofalos, A., Franzetti, A., Mastorgio, A.F., Saponaro, S., Sezenna, E., 2020. Microbial Assisted Hexavalent Chromium Removal in Bioelectrochemical Systems. Water 12, 466. https://doi.org/10.3390/w12020466

Ceballos-Escalera, A., Pous, N., Balaguer, M.D., Puig, S., 2022. Electrochemical water softening as pretreatment for nitrate electro bioremediation. Sci. Total Environ. 806, 150433. https://doi.org/10.1016/j.scitotenv.2021.150433

Ceballos-Escalera, A., Pous, N., Chiluiza-Ramos, P., Korth, B., Harnisch, F., Bañeras, L., Balaguer, M.D., Puig, S., 2021. Electro-bioremediation of nitrate and arsenite polluted groundwater. Water Res. 190, 116748. https://doi.org/10.1016/j.watres.2020.116748

Clauwaert, P., Desloover, J., Shea, C., Nerenberg, R., Boon, N., Verstraete, W., 2009. Enhanced nitrogen removal in bioelectrochemical systems by pH control. Biotechnol. Lett. 31, 1537–1543. https://doi.org/10.1007/s10529-009-0048-8

Djouadi Belkada, F., Kitous, O., Drouiche, N., Aoudj, S., Bouchelaghem, O., Abdi, N., Grib, H., Mameri, N., 2018. Electrodialysis for fluoride and nitrate removal from synthesised photovoltaic industry wastewater. Sep. Purif. Technol. 204, 108–115. https://doi.org/10.1016/j.seppur.2018.04.068

Electricity price statistics [WWW Document], n.d. URL https://ec.europa.eu/eurostat/statistics-explained/index.php?title=Electricity_price_statistics (accessed 11.29.21).

Greaves, J., Fischer, R.J., Shaffer, M., Bivins, A., Holbrook, M.G., Munster, V.J., Bibby, K., 2022. Sodium hypochlorite disinfection of SARS-CoV-2 spiked in water and municipal wastewater. Sci. Total Environ. 807, 150766. https://doi.org/10.1016/j.scitotenv.2021.150766

Janža, M., 2022. Optimisation of well field management to mitigate groundwater contamination using a simulation model and evolutionary algorithm. Sci. Total Environ. 807, 150811. https://doi.org/10.1016/j.scitotenv.2021.150811

Jingyu, H., Ewusi-Mensah, D., Norgbey, E., 2017. Microbial desalination cells technology: a review of the factors affecting the process, performance and efficiency. DESALINATION WATER Treat. 87, 140–159. https://doi.org/10.5004/dwt.2017.21302

Kwon, E., Park, J., Park, W.-B., Kang, B.-R., Woo, N.C., 2021. Nitrate contamination of coastal groundwater: Sources and transport mechanisms along a volcanic aquifer. Sci. Total Environ. 768, 145204. https://doi.org/10.1016/j.scitotenv.2021.145204

Lian, J., Tian, X., Guo, J., Guo, Y., Song, Y., Yue, L., Wang, Y., Liang, X., 2016. Effects of resazurin on perchlorate reduction and bioelectricity generation in microbial fuel cells and its catalysing mechanism. Biochem. Eng. J. 114, 164–172. https://doi.org/10.1016/j.bej.2016.06.028

McAdam, E.J., Judd, S.J., 2008. Immersed membrane bioreactors for nitrate removal from drinking water: Cost and feasibility. Desalination 231, 52–60. https://doi.org/10.1016/j.desal.2007.11.038

Ortiz, J., Exposito, E., Gallud, F., Garciagarcia, V., Montiel, V., Aldaz, A., 2008. Desalination of underground brackish waters using an electrodialysis system powered directly by photovoltaic energy. Sol. Energy Mater. Sol. Cells 92, 1677–1688. https://doi.org/10.1016/j.solmat.2008.07.020

Palma, E., Daghio, M., Franzetti, A., Petrangeli Papini, M., Aulenta, F., 2018. The bioelectric well: a novel approach for *in situ* treatment of hydrocarbon-contaminated groundwater. Microb. Biotechnol. 11, 112–118. https://doi.org/10.1111/1751-7915.12760

Patil, S., Harnisch, F., Schröder, U., 2010. Toxicity Response of Electroactive Microbial Biofilms-A Decisive Feature for Potential Biosensor and Power Source Applications. ChemPhysChem 11, 2834–2837. https://doi.org/10.1002/cphc.201000218

Pous, N., Balaguer, M.D., Colprim, J., Puig, S., 2018. Opportunities for groundwater microbial electro-remediation. Microb. Biotechnol. 11, 119–135. https://doi.org/10.1111/1751-7915.12866

Pous, N., Puig, S., Balaguer, M.D., Colprim, J., 2017. Effect of hydraulic retention time and substrate availability in denitrifying bioelectrochemical systems. Environ. Sci. Water Res. Technol. 3, 922–929. https://doi.org/10.1039/C7EW00145B

Pous, N., Puig, S., Dolors Balaguer, M., Colprim, J., 2015. Cathode potential and anode electron donor evaluation for a suitable treatment of nitrate-contaminated groundwater in bioelectrochemical systems. Chem. Eng. J. 263, 151–159. https://doi.org/10.1016/j.cej.2014.11.002

Puggioni, G., Milia, S., Dessì, E., Unali, V., Pous, N., Balaguer, M.D., Puig, S., Carucci, A., 2021. Combining electro-bioremediation of nitrate in saline groundwater with concomitant chlorine production. Water Res. 206, 117736. https://doi.org/10.1016/j.watres.2021.117736

Ramírez-Moreno, M., Rodenas, P., Aliaguilla, M., Bosch-Jimenez, P., Borràs, E., Zamora, P., Monsalvo, V., Rogalla, F., Ortiz, J.M., Esteve-Núñez, A., 2019. Comparative Performance of Microbial Desalination Cells Using Air Diffusion and Liquid Cathode Reactions: Study of the Salt Removal and Desalination Efficiency. Front. Energy Res. 7, 135. https://doi.org/10.3389/fenrg.2019.00135

Serio, F., Miglietta, P.P., Lamastra, L., Ficocelli, S., Intini, F., De Leo, F., De Donno, A., 2018. Groundwater nitrate contamination and agricultural land use: A grey water footprint perspective in Southern Apulia Region (Italy). Sci. Total Environ. 645, 1425–1431. https://doi.org/10.1016/j.scitotenv.2018.07.241

Sevda, S., Sreekishnan, T.R., Pous, N., Puig, S., Pant, D., 2018. Bioelectroremediation of perchlorate and nitrate contaminated water: A review. Bioresour. Technol. 255, 331–339. https://doi.org/10.1016/j.biortech.2018.02.005

Twomey, K.M., Stillwell, A.S., Webber, M.E., 2010. The unintended energy impacts of increased nitrate contamination from biofuels production. J Env. Monit 12, 218–224. https://doi.org/10.1039/B913137J

Verdini, R., Aulenta, F., de Tora, F., Lai, A., Majone, M., 2015. Relative contribution of set cathode potential and external mass transport on TCE dechlorination in a continuous-flow bioelectrochemical reactor. Chemosphere 136, 72–78. https://doi.org/10.1016/j.chemosphere.2015.03.092

Vilà-Rovira, A., Puig, S., Balaguer, M.D., Colprim, J., 2015. Anode hydrodynamics in Bioelectrochemical Systems 9. RSC Advances. https://pubs.rsc.org/en/Content/ArticleLanding/2015/RA/c5ra11995b

Virdis, B., Rabaey, K., Yuan, Z., Keller, J., 2008. Microbial fuel cells for simultaneous carbon and nitrogen removal. Water Res. 42, 3013–3024. https://doi.org/10.1016/j.watres.2008.03.017

Wang, C., Dong, J., Hu, W., Li, Y., 2021. Enhanced simultaneous removal of nitrate and perchlorate from groundwater by bioelectrochemical systems (BESs) with cathodic potential regulation. Biochem. Eng. J. 173, 108068. https://doi.org/10.1016/j.bej.2021.108068

Wang, X., Aulenta, F., Puig, S., Esteve-Núñez, A., He, Y., Mu, Y., Rabaey, K., 2020. Microbial electrochemistry for bioremediation. Environ. Sci. Ecotechnology 1, 100013. https://doi.org/10.1016/j.ese.2020.100013

Zhang, Y., Angelidaki, I., 2013. A new method for in situ nitrate removal from groundwater using submerged microbial desalination–denitrification cell (SMDDC). Water Res. 47, 1827–1836. https://doi.org/10.1016/j.watres.2013.01.005

Zhao, Y., Feng, C., Wang, Q., Yang, Y., Zhang, Z., Sugiura, N., 2011. Nitrate removal from groundwater by cooperating heterotrophic with autotrophic denitrification in a biofilm–electrode reactor. J. Hazard. Mater. 192, 1033–1039. https://doi.org/10.1016/j.jhazmat.2011.06.008

Appendix III

Analysis of bacterial communities by NGS of 16S rRNA gene

The composition of the bacterial communities from bio-cathodic biomass was characterised. Samples of the biofilms formed on the bio-cathode were axenically collected at the end of Test 5 (Table 5.1). Five cathode points were sampled, and the biomass was pooled into a composite sample to mitigate the effects of microscale heterogeneity on the bio-cathode. Biomass samples were stored at -20°C before DNA extraction. Genomic DNA was extracted from biomass samples (250 mg wet weight) using the DNeasy PowerSoil Pro Kit (QIAGEN) and DNA was subsequently purified using the DNeasy PowerClean Cleanup Kit (QIAGEN). The DNA quality and concentration were determined on agarose gel using a DNA quantitation standard. DNA samples were submitted to Bio-Fab Research srl (Rome, Italy) for sequencing of the V3-V4 region of the bacterial 16S rRNA gene on an Illumina Miseq platform (Illumina, San Diego, CA) using 2 × 300 bp paired-end reads.

For data processing, raw sequences were demultiplexed by the sequencing facility. Reads were trimmed to remove primer sequences using the CutAdapt version 3.5. Sequences were imported into Quantitative Insights into Microbial Ecology (QIIME 2) version 2020-11 (Bolyen et al., 2019). Using the DADA2 pipeline (Callahan et al., 2016), reads with ambiguous and poor-quality bases were discarded, good quality reads dereplicated and denoised, and the paired reads merged. Chimeras and singletons were identified and removed from the dataset. DADA2 was used to produce alternative sequence variants (ASVs), thus obtaining a filtered ASV-abundance table. For each ASV, a representative sequence was used for taxonomy assignment against the Silva database release 138 (Quast et al., 2013). The indices of diversity (richness as the number of observed ASV, Shannon with an e log base) and evenness (Pielou's) were used to assess the alpha-diversity by using the vegan R package (Oksanen et al., 2019). Read count data were normalised by Cumulative Sum Scaling (CSS) transformation, using the metagenomeSeq package (Paulson et al., 2013). The Bray-Curtis similarity index between samples was calculated.

Bacterial community diversity on the bio-cathode of the 3-compartment BES

Cathodic biomass was collected at the end of Test 5. The bacterial community composition of the biomass is shown in Figure AIII-1. The most abundant phyla of Bacteria in the biomass were Proteobacteria (44.0%) followed by Actinobacteriota (16.0%), Firmicutes (11.8%), Bacteroidota (10.8%), Planctomycetota (5.1%) and Chloroflexi (4.8%). The other less abundant phyla were all below the 3%, while the unassigned sequences accounted for 1.1% in the composition of bacterial community. At order level, the most abundant taxa were Rhizobiales (17.0%), Corynebacteriales (7.4%), and Burkholderiales (6.6%), followed by Xanthomonadales (4.5%), Alteromonadales (4.3%), and Thermomicrobiales (4.2%). At genus level, seven most abundant taxa accounted for more than 20% of the total community, including the genera *Rhizobium* (3.9%) and *Bosea* (3.1%) in Rhizobiales, *Mycobacterium* (3.2%) and *Gordonia* (2.4%) in Corynebacteriales, *Fontibacter* (2.6%) in Cytophagales, *Clostridium sensu strictu* (2.4%) in Firmicutes as well as the uncultured JG30-KF-CM45 in Thermomicrobiales (3.2%).

In order to compare the biomass established under the galvanostatic mode (GM), used in the present study, and potentiostatic mode, previously tested by Puggioni et al. (2021), a sample of the biofilm formed on the bio-cathode of the cell working in potentiostatic mode (PM) was also analysed and the difference in the bacterial communities between the GM and PM biomass investigated in terms of alpha-diversity and community composition.

The community in GM biomass was characterised by a minor bacterial alpha-diversity as highlighted by a lower number of ASVs (i.e., reduced richness) and a higher community dominance (i.e., reduced evenness) in comparison to the PM biomass (Table AIII-1). A marked difference in the bacterial community composition was also evident at the different taxonomic ranks. As compared to the PM biomass, the GM bio-cathodic community is characterised by the increase in the relative abundances (RAs) of Proteobacteria (+11.2%) and Firmicutes (+6.4%), and the decrease in RAs of Planctomycetota (-8.9%) and Chloroflexi (-7.3%). At order level, the more pronounced changes in RAs were the enrichment in Rhizobiales (+7.9%), Corynebacteriales (+5.3%), Alteromonadales (+3.5%), and Xanthomonadales (+3.4%). The comparison between PM and GM also showed the reduction in Pirellulales (-3.1%). Moreover, Caldilineales and Anaerolineales were not detected in the GM cathodic biofilm, while they accounted for 3.4% and 2.6% in the PM biomass, respectively. At genus level, the highest differences were

found for the taxa *Rhizobium, Bosea, Fontibacter, Gordonia,* which were all below the 0.5% in PM biomass, while they predominated the composition of GM bacterial community (Figure AIII-1,B). Out of the 646 ASVs found in the PM biomass, 88 ASVs were shared between the two communities, while 11 and 558 ASVs were unique of GM and PM biomass, respectively (Figure AIII-1,C). Among the ASVs unique of the GM biomass, ASV01 affiliated to an uncultured lineage of Burkholderiales was also the most abundant ASV, accounting for 2.5% of the GM bacterial community (Table AIII-2). Other ASVs exclusively found in the GM biomass were ASV026 (1.1%) and ASV027 (1.1%) affiliated to the genera *Fontibacter* and *Nocardia*, respectively.

Table AIII-1. Diversity (S: richness as number of observed ASVs, H': Shannon with an e log base) and evenness (J': Pielou's) indices of bacterial communities of the biofilms formed on the bio-cathode of the 3-compartment bioelectrochemical cells.

Sample	S	J'	H'(lodge)
PM	646	0.998	6.34
GM	99	0.988	4.51

Overall, biodiversity was severely restricted under galvanostatic mode. Presented results suggested that test conditions exerted a selective pressure on the bacterial community of the cathodic biofilm influencing its organization and enriching few dominant populations. Moreover, an active role in denitrifying biomass has been previously proposed for several bacteria dominating the GM bio-cathodic biomass. More specifically, isolates affiliated to Rhizobiales have been proved to denitrify under autotrophic and heterotrophic conditions (Vilar-Sanz et al., 2108), and the genus *Rhizobium* has been implied in denitrification in MFC system for treating saline wastewater (Xu et al., 2019). *Clostridium sensu strictu* has been detected at a high amount in MEC biomass and suggested to be responsible for autotrophic denitrification in a bioelectrochemically-assisted constructed wetland system (Sotres et al., 2015; Xu et al., 2017). Recently, the genus *Fontibacter* has been found to be enriched after long term adaptation in a BES for nitrate removal from coke wastewater effluent (Tang et al., 2017) and a species of the genus, isolated from an MFC, has been proved to couple oxidation of organic matter to Fe(III) reduction (Zhang et al., 2013). On the contrary, other dominant populations in the

GM biomass, such as Corynebacteriales, have been less extensively described, and their metabolic role in bioelectrochemical systems is far to be undiscovered.

Figure AIII-1. Bacterial communities of the biofilms formed on the bio-cathode of the 3-compartment bio-electrochemical cells **A:** Bar plot showing the contribution at phylum level in cathodic biomass under galvanostatic mode (GM). **B:** twenty most abundant genera in GM biomass and comparison with biomass established under potentiostatic mode (PM). **C:** Venn chart showing the overlap of ASVs in bacterial communities of cathodic GM and PM biomasses.

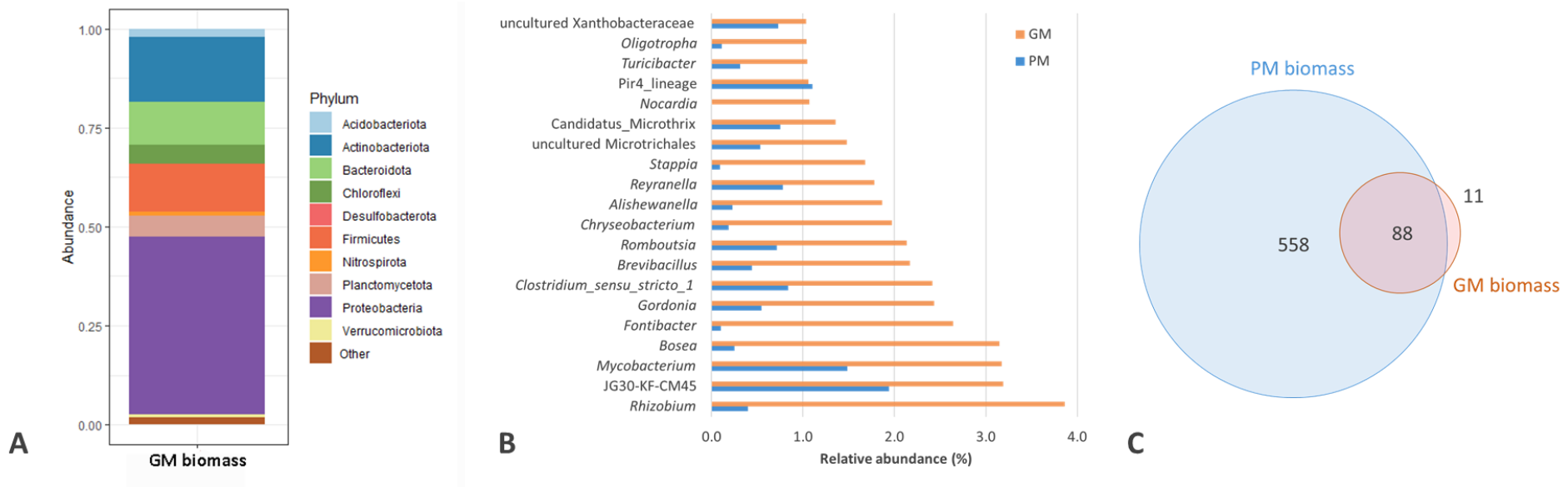

Table AIII-2. Relative abundances (RA%) and taxonomic affiliation of the ASVs exclusively found in the community of the GM biomass.

ID	Domain	Phylum	Class	Order	Family	Genus	RA
ASV001	Bacteria	Proteobacteria	Betaproteobacteria	Burkholderiales			2.5%
ASV026	Bacteria	Bacteroidota	Bacteroidia	Cytophagales	Cyclobacteriaceae	Fontibacter	1.1%
ASV027	Bacteria	Actinobacteriota	Actinobacteria	Corynebacteriales	Nocardiaceae	Nocardia	1.1%
ASV049	Bacteria	Actinobacteriota	Actinobacteria	Micrococcales	Microbacteriaceae		0.9%
ASV056	Bacteria	Proteobacteria	Gammaproteobacteria	Pasteurellales	Pasteurellaceae	Haemophilus	0.9%
ASV074	Bacteria	Actinobacteriota	Actinobacteria	Corynebacteriales	Nocardiaceae	Rhodococcus	0.7%
ASV077	Bacteria	Acidobacteriota	Blastocatellia	Blastocatellales	Blastocatellaceae	Blastocatella	0.7%
ASV083	Bacteria	Firmicutes	Bacilli	Lactobacillales	Carnobacteriaceae	Dolosigranulum	0.6%
ASV087	Bacteria	Actinobacteriota	Thermoleophilia	Solirubrobacterales	67-14	67-14	0.6%
ASV091	Bacteria	Chloroflexi	OLB14	OLB14	OLB14	OLB14	0.6%
ASV092	Bacteria	Proteobacteria	Alphaproteobacteria	Defluviicoccales	Defluviicoccaceae	Defluviicoccus	0.6%

References – Appenix III

Bolyen, E., Rideout, J. R., Dillon, M. R., Bokulich, N. A., Abnet, C. C., Al-Ghalith, G. A., et al.. (2019). Reproducible, interactive, scalable and extensible microbiome data science using QIIME 2. Nature Biotechnology, 37(8), 852–857. https://doi.org/10.1038/s41587-019-0209-9

Callahan, B. J., McMurdie, P. J., Rosen, M. J., Han, A. W., Johnson, A. J. A., & Holmes, S. P. (2016). DADA2: High-resolution sample inference from Illumina amplicon data. Nature Methods, 13(7), 581–583. https://doi.org/10.1038/nmeth.3869

Oksanen, J., Blanchet, F. G., Friendly, M., Kindt, R., Legendre, P.,McGlinn, D., et al. (2019). Vegan. Community Ecology Package.

Paulson, J. N., Colin Stine, O., Bravo, H. C., & Pop, M. (2013). Differential abundance analysis for microbial marker-gene surveys. Nature Methods, 10(12), 1200–1202. https://doi.org/10.1038/nmeth.2658

Quast, C., Pruesse, E., Yilmaz, P., Gerken, J., Schweer, T., Yarza, P., et al. (2013). The SILVA ribosomal RNA gene database project: improved data processing and web-based tools. Nucleic Acids Res. 41, 590–596. doi: 10.1093/nar/gks1219

Sotres, A., Cerrillo, M., Viñas, M., & Bonmatí, A. (2015). Nitrogen recovery from pig slurry in a two-chambered bioelectrochemical system. Bioresource Technology, 194, 373–382. https://doi.org/10.1016/j.biortech.2015.07.036

Tang, R., Wu, D., Chen, W., Feng, C., & Wei, C. (2017). Biocathode denitrification of coke wastewater effluent from an industrial aeration tank: Effect of long-term adaptation. Biochemical Engineering Journal, 125, 151–160. https://doi.org/10.1016/j.bej.2017.05.022

Vilar-Sanz, A., Pous, N., Puig, S., Balaguer, M. D., Colprim, J., & Bañeras, L. (2018). Denitrifying nirK-containing alphaproteobacteria exhibit different electrode driven nitrite reduction capacities. Bioelectrochemistry, 121, 74–83. https://doi.org/10.1016/j.bioelechem.2018.01.007

Xu, D., Xiao, E., Xu, P., Zhou, Y., He, F., Zhou, Q., … Wu, Z. (2017). Performance and microbial communities of completely autotrophic denitrification in a bioelectrochemically-assisted constructed wetland system for nitrate removal. Bioresource Technology, 228, 39–46. https://doi.org/10.1016/j.biortech.2016.12.065

Xu, F., Ouyang, D. long, Rene, E. R., Ng, H. Y., Guo, L. ling, Zhu, Y. jie, Kong, Q. (2019). Electricity production enhancement in a constructed wetland-microbial fuel cell system for treating saline wastewater. Bioresource Technology, 288(May), 121462. https://doi.org/10.1016/j.biortech.2019.121462

Zhang, J., Yang, G. Q., Zhou, S., Wang, Y., Yuan, Y., & Zhuang, L. (2013). *Fontibacter ferrireducens* sp. nov., an Fe(III)-reducing bacterium isolated from a microbial fuel cell. International Journal of Systematic and Evolutionary Microbiology, 63(PART3), 925–929. https://doi.org/10.1099/ijs.0.040998-0

6 IMPLICATIONS AND OUTLOOK

This research aimed to study the applicability of BES to the treatment of nitrate-contaminated saline groundwater in combination with other contaminants (Figure 6.1). This objective was pursued using dedicated bioelectrochemical reactors and monitoring their performances with different configurations and operating conditions.

Besides enhancing the knowledge base concerning the applicability of BES to treat multi-contaminated groundwater, the study also aimed to obtain helpful information for scaling up the technology.

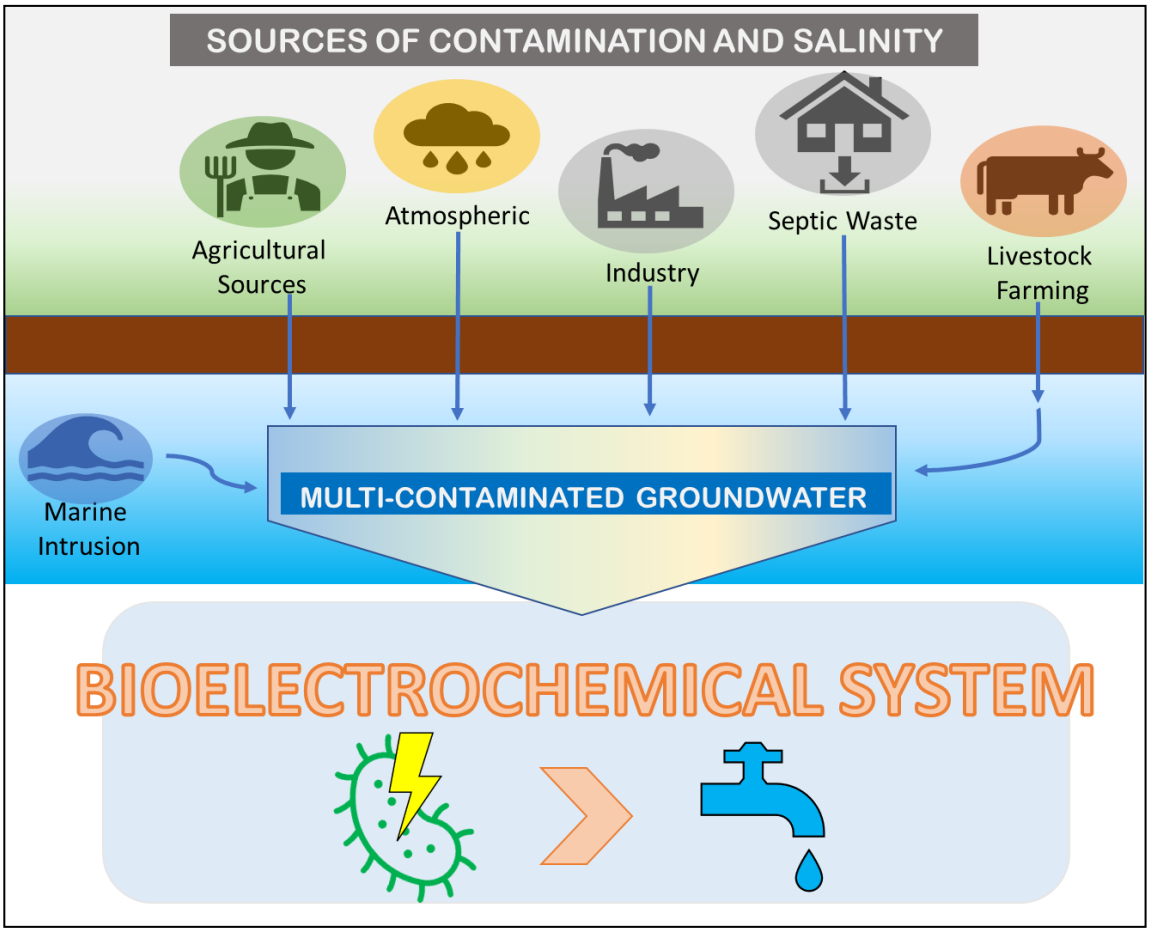

Figure 6.1. Summary image of the general objective of the present PhD thesis.

6.1 Implications of the PhD thesis

Among the contaminants present in groundwater, nitrate is one of the most common and, therefore, one of the most studied for bioelectrochemical treatment. If operational conditions are well chosen, BES proved to be an alternative for the bioremediation of nitrate also in combination with other pollutants like arsenic (Ceballos-Escalera et al., 2021), perchlorate (C. Wang et al., 2021), and sulphate (Lai et al., 2015).

From the results discussed in previous chapters, BES proved to be a sustainable alternative for the treatment of groundwater contaminated by nitrate and affected by high salinity, as well as by the presence of calcium (Ca^{2+}) and manganese (Mn^{2+}). The following considerations may be drawn:

- The presence of Ca^{2+} and Mn^{2+} influenced BES performance significantly in terms of nitrate removal. High calcium concentrations negatively affected the durability of bioelectrochemical cell materials, in particular membranes and electrodes, likely due to its progressive deposition on their surface, thus reducing the denitrifying capacity. As for manganese, possible removal due to microbial activity was observed, but further studies are needed to identify the process(es) involved. The general community structure of the biomass attached to the bio-cathode was only slightly influenced by the high concentrations of Ca^{2+} and Mn^{2+}.
- The configuration of the bioelectrochemical system is one of the critical factors in the electro-bioremediation of saline multi-contaminated groundwater. This PhD thesis proposed a proof-of-concept based on a **3-compartment configuration** that allows the simultaneous biotic removal of nitrate and abiotic desalination, and the production of value-added chemicals. An important characteristic of the configuration used was the low width of the central compartment (0.5 cm), which allowed to minimise the distance between membranes, thereby reducing the internal resistance of the system and consequently promoting the migration of ions, i.e., the desalination process.
- The operating conditions are crucial in reaching the treatment targets at reasonable costs. The operation in galvanostatic mode, instead of potentiostatic mode, allowed better performance in terms of **denitrification and desalination,** and to produce

value-added products, such as **chlorine**. In this case, a Ti-MMO anode electrode was needed, which was demonstrated to be a catalyst for the production of free chlorine (Batlle-Vilanova et al., 2019). The standards for drinking water were met in terms of nitrate and nitrite concentrations, and electrical conductivity. The implementation of **pH control** in the recirculation line of the bio-cathodic compartment allows avoiding excessive pH increase (> 10) during galvanostatic operation, and thus consequent membrane damage, as well as inhibition of electroactive biofilm.

- The operation at low **HRT** (2.5 h) enhanced nitrate removal rates and reduced energy consumption. This could be linked to an improvement in the hydrodynamics of the system, and accordingly, in the nitrate diffusion towards the working electrode. However, reducing HRT led to a decrease in desalination efficiency. Too low HRT did not allow sufficient ions to migrate through the membranes to observe a significant reduction in effluent electrical conductivity.

Table 6.1 summarises the results obtained in this PhD thesis compared with some of the recent studies on BES applied to treating water contaminated by nitrates, with or without other contaminants.

Table 6.1. Comparison of the main results obtained in this PhD thesis with previous studies. (n.m. – not mentioned)

Reference	BES reactor type	Influent type	Fixed parameter	Nitrate removal efficiency [%]	Nitrate removal rates [$mgNO_3^-$-N L^{-1} d^{-1}]	Energy consumption [kWh g^{-1} $NO_3^-N_{removed}$]	Presence/treatmer of other contaminants	Addition of chemicals	Recovery/ Production of value-added substances
This study (Chapter 5)	3-compartment BES	synthetic groundwater	current	89±2	112±8	$6.4\cdot10^{-2}\pm0.3\cdot10^{-2}$	Salinity	hydrochloric acid	Yes, Cl_2
This study (Chapter 4)	3-compartment BES	synthetic groundwater	current	69±2	39±1	0.13±0.01	Salinity	hydrochloric acid	Yes, Cl_2
This study (Chapter 2)	2-compartment BES	synthetic groundwater	potential	46±2	22±6	$0.9\cdot10^{-2}\pm0.09\cdot10^{-2}$	Calcium and Magnanese	No	No
Ceballos-Escalera et al., 2022	Tubular BES	softened groundwater	potential	97%	1269±30	$6.3\cdot10^{-2}\pm0.3\cdot10^{-2}$	No		
Ceballos-Escalera et al., 2021	Tubular BES	synthetic groundwater	potential	90 ±6	519±53	n.m.	Arsenic	No	No
Wang et al., 2021	2-compartment BES	synthetic groundwater	potential	99	16±1	n.m.	Perchlorate	No	No
X. Wang et al., 2021	2-compartment BES	synthetic groundwater	periodic potential	86	205	$1.5\cdot10^{-2}\pm0.05\cdot10^{-2}$	No		No
Pous et al., 2017	Tubular BES	synthetic groundwater	potential	50	849	$1.5\cdot10^{-2}\pm0.03\cdot10^{-2}$	No	No	No
Lai et al., 2015	2-compartment BES	modified real groundwater	potential	n.m.	n.m.	n.m.	cis-dichloroethylene and sulfate	cis-dichloroethylene $NaHCO_3$	No
Zhang et al., 2013	SMDDC (Submerged Microbial Desalination Deni-trification Cell)	synthetic groundwater	-	91	17	n.m.	Salinity	sodium acetate	No

6.2 Outlook (Future perspectives)

Despite the recent interest in studying bioelectrochemical systems applied to multi-contaminated groundwater treatment, many aspects should be explored further. Future research directions in this area can have different perspectives.

In terms of fundamental knowledge, the interactions between the different contaminants and each contaminant's effect on the microbiological composition should be investigated. In the specific case of nitrate reduction in the presence of other pollutants, it is important to identify the reactor microbiome and what kind of effect each contaminant may have on the denitrifying activity of the cathodic biofilm.

From an engineering perspective, the clear objective in the next years should be scaling up the technology and evaluating *in-situ* applicability. The reproducibility of lab-scale results in pilot-scale plants is a key step for the successful future of denitrifying bioelectrochemical systems. Furthermore, while it is important to continue developing and optimising on-site treatment systems that allow several processes to be managed simultaneously in a more easily controllable manner, it is also necessary to consider the development of systems that can be applied directly *in-situ*. BES are, in fact, a suitable option for *in-situ* groundwater treatment due to their cost-effectiveness, sustainability and flexibility. They are also characterised by the possibility of exploiting different redox environments at both anode and cathode, working at different set potentials, and operating as a flexible technology (Cecconet et al., 2020; Wang et al., 2020; Modin and Aulenta, 2017). Systems developed for *in-situ* treatment are generally simpler and less efficient. Still, they can be very useful especially considering the many drawbacks that can make a conventional *in-situ* remediation process relatively complex, e.g., limited presence of electron acceptors/donors, insufficient intra-aquifer mixing, slow metabolism and growth rates of microorganisms. For this reason, some technologies developed so far often involve adding chemicals, nutrients, and oxygen or the introduction of microbial communities adapted to the selective degradation of target contaminants; they can require post-treatment or are only efficient on a range of pollutants (Cecconet et al., 2020).

BES application could overcome most of these challenges and therefore appears particularly interesting.

In this sense, the work presented in this PhD thesis is proceeding with the construction and evaluation of a simple reactor, i.e., a tubular bioelectrochemical system, for *in-situ* saline groundwater denitrification. The system is designed for direct installation in existing wells and meets the "ideal" *in-situ* bioelectrochemical treatment requirements outlined in a recent study by Cecconet et al. (2020), such as the absence of membranes to reduce costs and maintenance, the use of a potentiostat to set the desired working potential, and easy scalability.

The focus was on an extremely simple system characterised by the absence of membranes to reduce costs and maintenance, the presence of internal recirculation to allow intensive contact between biomass and substrate, electrodes with a large surface area to allow extensive biofilm growth, and the use of a potentiostat to set the desired working potential.

The system consists of two concentric tubes. The cathode electrode, consisting of a stainless steel mesh, is placed between the two tubes. Stainless steel was chosen as the cathode material, instead of carbon-based material, because of its cost-effectiveness, and it is easy to clean in the event of calcium deposits on its surface. The anode electrode (granular graphite) is located inside the central tube. The two compartments (cathodic and anodic) are hydraulically connected. The influent flow comes from the bottom of the cathode compartment and then passes (thanks to holes at the top of the central tube) into the anode compartment. The water is extracted from the anodic compartment by a pump, and another pump is dedicated to the cathodic solution's recirculation. The potentiostat controls the cathode potential, thanks to the presence of the reference electrode inside the cathode compartment. Figure 6.2 shows some details of the system under study, while Figure 6.3 shows a schematic diagram flow.

The cell is currently in the start-up phase and is fed with synthetic groundwater with a nitrate concentration of approximately 30mgNO_3^--N L^{-1}.

Besides process optimisation, the next step will be to evaluate such systems to treat real multi-contaminated groundwater (e.g., nitrate with manganese, sulphate or hydrocarbons).

Figure 6.2. Details of the system for *in-situ* groundwater treatment, currently under study.

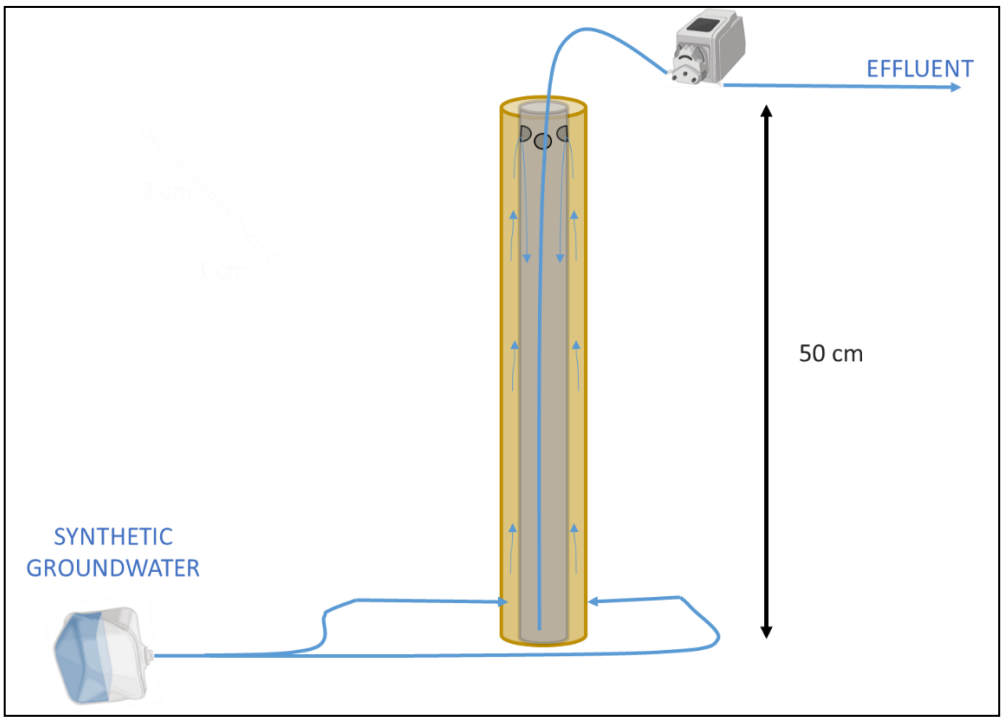

Figure 6.3. Schematic diagram flow of the tubular cell for *in-situ* groundwater treatment.

References

Batlle-Vilanova, P., 2019. Biogas upgrading, CO2 valorisation and economic revaluation of bioelectrochemical systems through anodic chlorine production in the framework of wastewater treatment plants. Sci. Total Environ. 9.

Ceballos-Escalera, A., Pous, N., Balaguer, M.D., Puig, S., 2022. Electrochemical water softening as pretreatment for nitrate electro bioremediation. Sci. Total Environ. 806, 150433. https://doi.org/10.1016/j.scitotenv.2021.150433

Ceballos-Escalera, A., Pous, N., Chiluiza-Ramos, P., Korth, B., Harnisch, F., Bañeras, L., Balaguer, M.D., Puig, S., 2021. Electro-bioremediation of nitrate and arsenite polluted groundwater. Water Res. 190, 116748. https://doi.org/10.1016/j.watres.2020.116748

Cecconet, D., Sabba, F., Devecseri, M., Callegari, A., Capodaglio, A.G., 2020. In situ groundwater remediation with bioelectrochemical systems: A critical review and future perspectives. Environ. Int. 137, 105550. https://doi.org/10.1016/j.envint.2020.105550

Lai, A., Verdini, R., Aulenta, F., Majone, M., 2015. Influence of nitrate and sulfate reduction in the bioelectrochemically assisted dechlorination of cis-DCE. Chemosphere 125, 147–154. https://doi.org/10.1016/j.chemosphere.2014.12.023

Modin, O., Aulenta, F., 2017. Three promising applications of microbial electrochemistry for the water sector. Environ. Sci. Water Res. Technol. 3, 391–402. https://doi.org/10.1039/C6EW00325G

Pous, N., Puig, S., Balaguer, M.D., Colprim, J., 2017. Effect of hydraulic retention time and substrate availability in denitrifying bioelectrochemical systems. Environ. Sci. Water Res. Technol. 3, 922–929. https://doi.org/10.1039/C7EW00145B

Wang, C., Dong, J., Hu, W., Li, Y., 2021. Enhanced simultaneous removal of nitrate and perchlorate from groundwater by bioelectrochemical systems (BESs) with cathodic potential regulation. Biochem. Eng. J. 173, 108068. https://doi.org/10.1016/j.bej.2021.108068

Wang, X., Aulenta, F., Puig, S., Esteve-Núñez, A., He, Y., Mu, Y., Rabaey, K., 2020. Microbial electrochemistry for bioremediation. Environ. Sci. Ecotechnology 1, 100013. https://doi.org/10.1016/j.ese.2020.100013

Wang, X., Prévoteau, A., Rabaey, K., 2021. Impact of Periodic Polarisation on Groundwater Denitrification in Bioelectrochemical Systems. Environ. Sci. Technol. 55, 15371–15379. https://doi.org/10.1021/acs.est.1c03586

Zhang, Y., Angelidaki, I., 2013. A new method for in situ nitrate removal from groundwater using submerged microbial desalination–denitrification cell (SMDDC). Water Res. 47, 1827–1836. https://doi.org/10.1016/j.watres.2013.01.005

LIST OF PUBLICATIONS

Journal articles and Conference proceedings

- Puggioni, G., Milia, S., Dessì, E., Unali, V., Pous, N., Balaguer, M.D., Puig, S., Carucci, A., 2021. *Combining electro-bioremediation of nitrate in saline groundwater with concomitant chlorine production*. Water Research. 206, 117736. https://doi.org/10.1016/j.watres.2021.117736

- Puggioni, G., Milia, S., Dessì, E., Unali, V., Pous, N., Balaguer, M.D., Puig, S., Carucci, A., 2021. *Electro-bioremediation of nitrate from saline groundwater and concomitant chlorine production*. 5th European Meeting of the International Society for Microbial Electrochemistry and Technology (EU-ISMET2021). Girona (Spain) - Hybrid event. September 13-15, 2021.

- Puggioni, G., Carucci, A., Dessì, E., Pous, N., Puig, S., Unali, V., Milia, S., 2021. *Electro-bioremediation of nitrate contaminated saline groundwater.* 17th International Conference on Environmental Science and Technology (CEST 2021). Athens (Greece) – Hybrid event. September 01-04, 2021.

- Carucci, A., Milia, S., Pous, N., Puggioni, G., Puig, S., Unali, V., 2021. *Bio-electricity driven treatment of high salinity groundwater contaminated with nitrates*. XI International symposium on environmental engineering (SIDISA 2021). Turin (Italy). June 29th – July 2nd, 2021.

- Puggioni, G., Milia, S., Dessì, E., Unali, V., Pous, N., Puig, S., Carucci, A., 2020. *Simultaneous denitrification and desalination of groundwater in 3-chamber BES configuration.* 1st Virtual ISMET Meeting. Portugal – Online event. October 07-09, 2020

ACKNOWLEDGEMENTS

Special thanks to my supervisors, Professor Carucci, Professor Puig, and Dr Milia, for sharing their knowledge and experience with me, for their valuable advice, and great support. They have all contributed enormously to my professional and personal growth during my PhD, and I am very grateful to them. A further thank you to Stefano (Dr Milia), undoubtedly the most important person for the success of this thesis, thank you for your trust and for enabling me to give my best!

I would like to thank the whole group of professors, technicians and researchers of the environmental engineering laboratory at DICAAR (Department of Environmental Civil Engineering and Architecture, University of Cagliari). In particular, I would like to thank the group of PhD students and friends with whom I shared most of my PhD, making it full of wonderful experiences and making the inconveniences less disagreeable. I would like to thank Valentina and Emma for helping me with the experimentation and for putting up with me in the bad times. But a huge thank you to everyone else: Giangi, Anna, Fabiano, Marco, Martina, Stefano, Matteo, Giaime, Claudia.

A huge thank you also to the whole LEQUiA team. My stay in the LEQUiA laboratories at the University of Girona allowed me to meet fantastic people with whom I shared intense days of work, study and professional and cultural exchange. Bioelectrochemical systems have become much more enjoyable thanks to all of them. I thank Marilos and Narcís so much for their valuable contribution to my activities and writing, they have been fundamental people throughout my PhD. Thanks to the powerful LEQUiA girls, my friends Alba, Silvia, Laura, and Meritxell. But also, Albert M., Gaetan, Ramiro, Miguel, Albert G., and really the whole LEQUiA family.

Ringrazio la mia splendida famiglia, per aver condiviso con me tutti gli aspetti positivi e negativi del mio percorso di dottorato. Ringrazio i miei genitori per il loro costante sostegno e conforto, sempre pronti a tendermi una mano e sempre capaci di tirarmi su. Ringrazio Tizi, Michi, Albi e la mia Lucrezia per esserci sempre e in ogni modo, anche se un grazie non sarà mai abbastanza per esprimervi la mia gratitudine. Grazie anche ad Anna e Giorgio per il loro prezioso sostegno e affetto.

Infine, ringrazio Riccardo, nessuno più di te sa quanto sono stati intensi questi tre anni e tu sei stato la persona migliore che potessi avere al mio fianco. Grazie per ogni cosa!

Hoping I haven't forgotten anyone, **thanks again to everyone**!